SISSA, Trieste
June 6, 2007

Sub-Riemannian geometry and contact structures in the functional architecture of the primary visual cortex

Jean Petitot

EHESS & CREA

petitot@shs.polytechnique.fr

Introduction

- Neurogeometry concerns the neural implementation of the geometric structures of visual perception.
- These structures are very different from the Euclidean 3D structure of the objective external space which is the ouput of a very sophisticated cognitive construction.
- Many non trivial mathematical structures have been introduced recently to explain the neural implementation of natural low level vision.

- I will focus on two of them:
  - Receptive fields of neural cells and wavelet analysis.
  - Differential geometry and neurogeometry of the functional architecture of area V1.
- We will see how contact, symplectic and sub-Riemannian geometry arise naturally in modeling V1 functional architecture.
- In relation with wavelet analysis this leads to harmonic analysis on Heisenberg type groups.

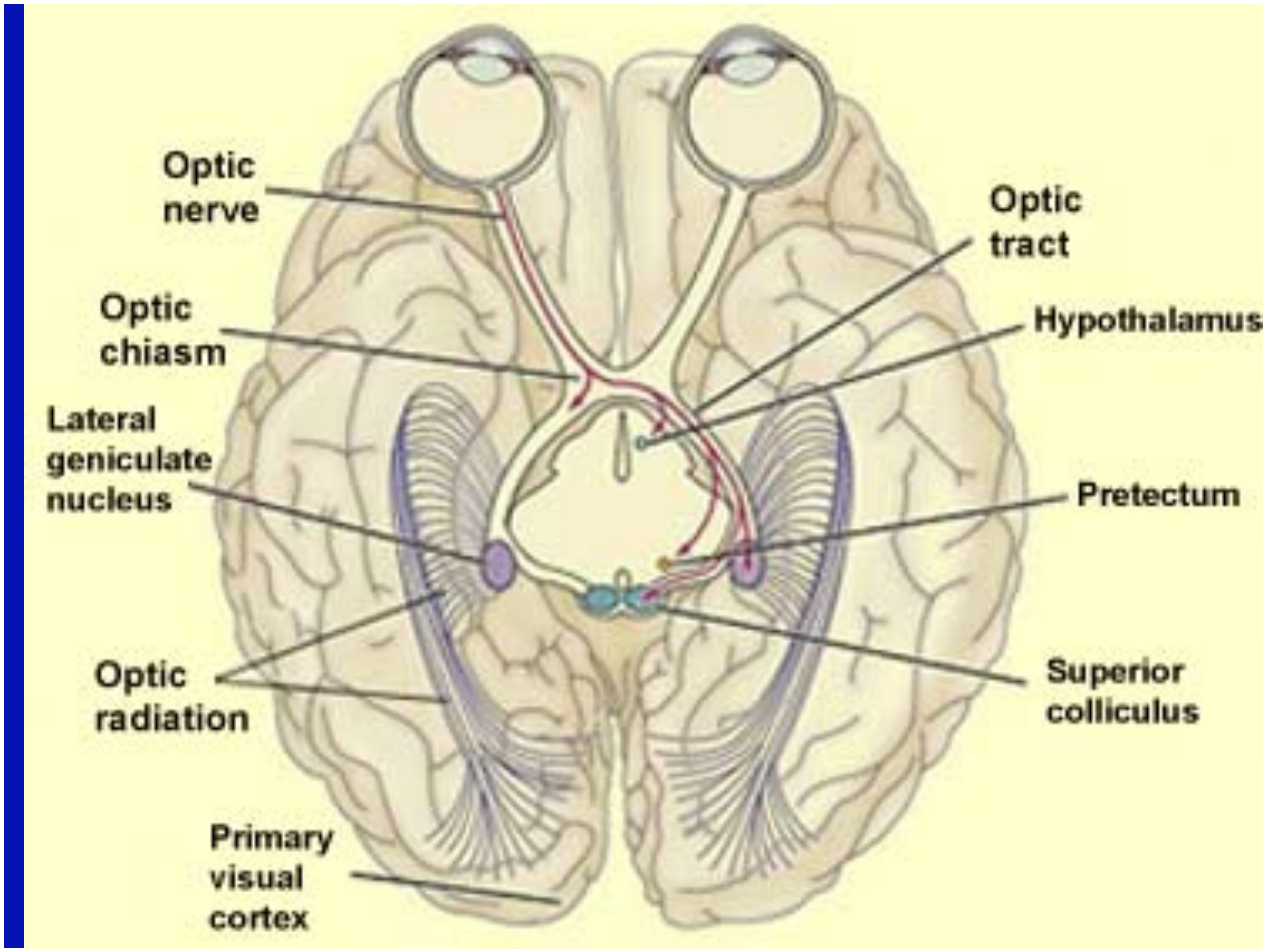
Optic nerve
Optic tract
Optic chiasm
Hypothalamus
Lateral geniculate nucleus
Pretectum
Optic radiation
Superior colliculus
Primary visual cortex

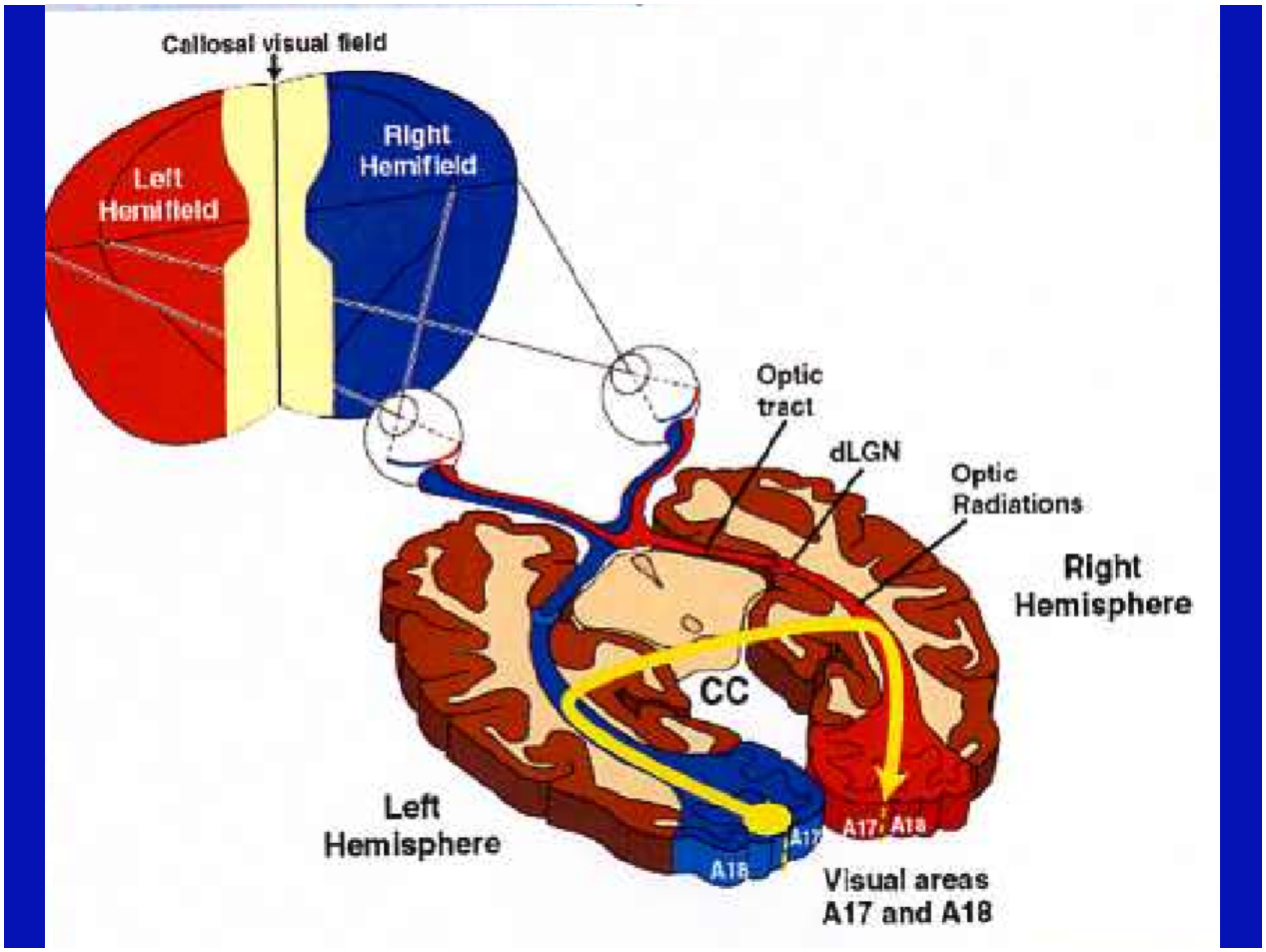
Callosal visual field
Left Hemifield
Right Hemifield
Optic tract
dLGN
Optic Radiations
Right Hemisphere
CC
Left Hemisphere
A17
A18
A18
Visual areas A17 and A18

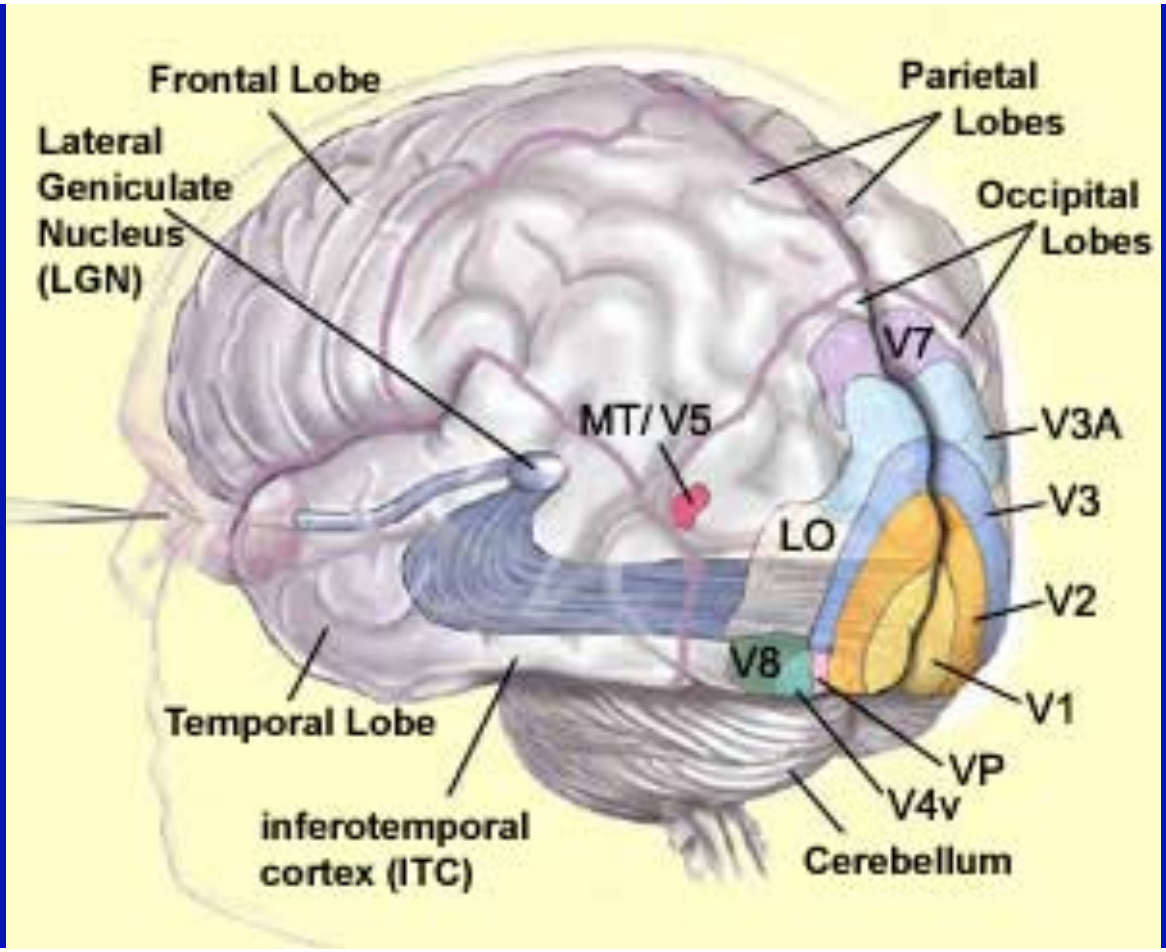

- V1 has a thickness of ≈ 1.8mm with 6 layers. The input layer is the layer 4C.
- New experimental devices allow to observe the activity of the neural micro-modules involved in visual processing.
- But they are extremely difficult to interpret because the underlying connectivity is extremely complex ("local" means hundreds or even thousands neurons each with hundreds or even thousands synapses).

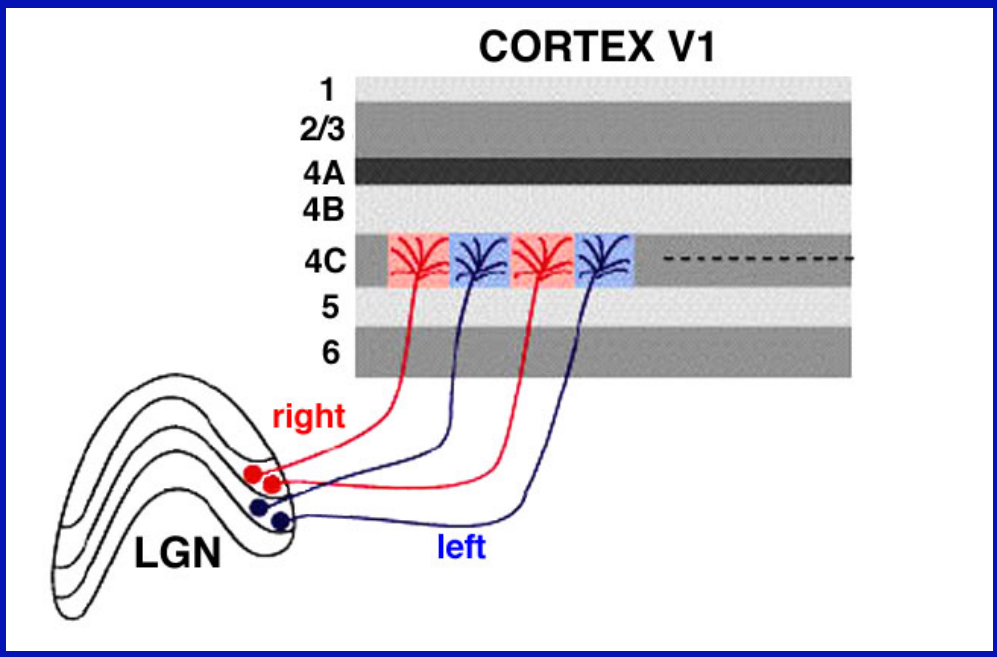

LGN input

Parvo

Magno

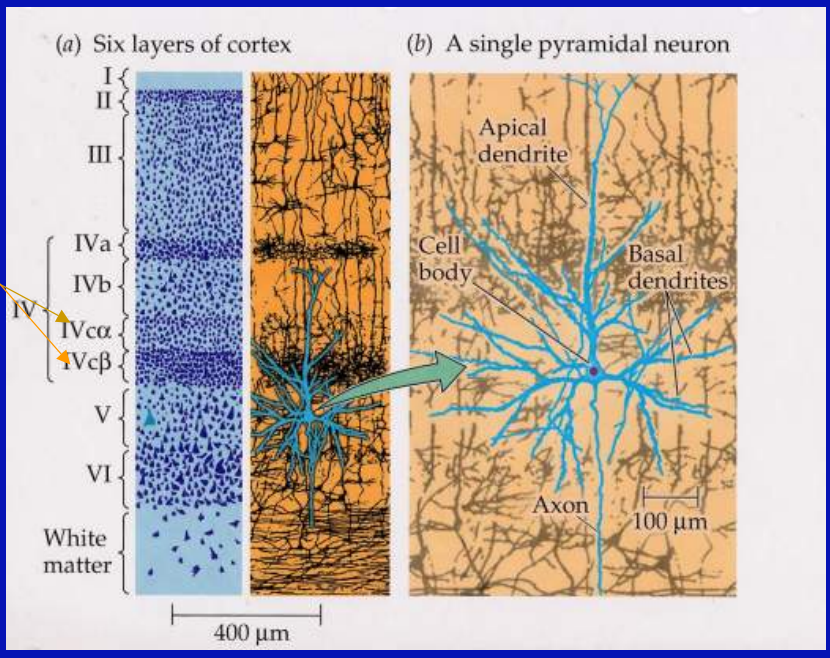

Receptive fields

- The classical receptive field (RF) of a visual neuron is the domain of the retina to which it is connected through the neural connections of the retino-geniculo-cortical pathways, and whose stimulation elicitates a spike response.

- This concept of “minimal discharge field” (MDF) has to be refined to take into account all the complexity of the subthreshold activity of neurons (membrane potential and “synaptic integration field”).
- For simplicity reasons, we will consider only the MDF (spiking responses) of simple neurons.
- The RF is decomposed into ON (excitatory) and OFF (inhibitory) zones.

- Sophisticated techniques enable to record the level curves of their receptive profile (RP) or transfert function as linear filters.
- Level curves of the receptive profiles of the ganglionary cells and of the LGN (G. De Angelis) can be modeled by Laplacians of Gaussians.

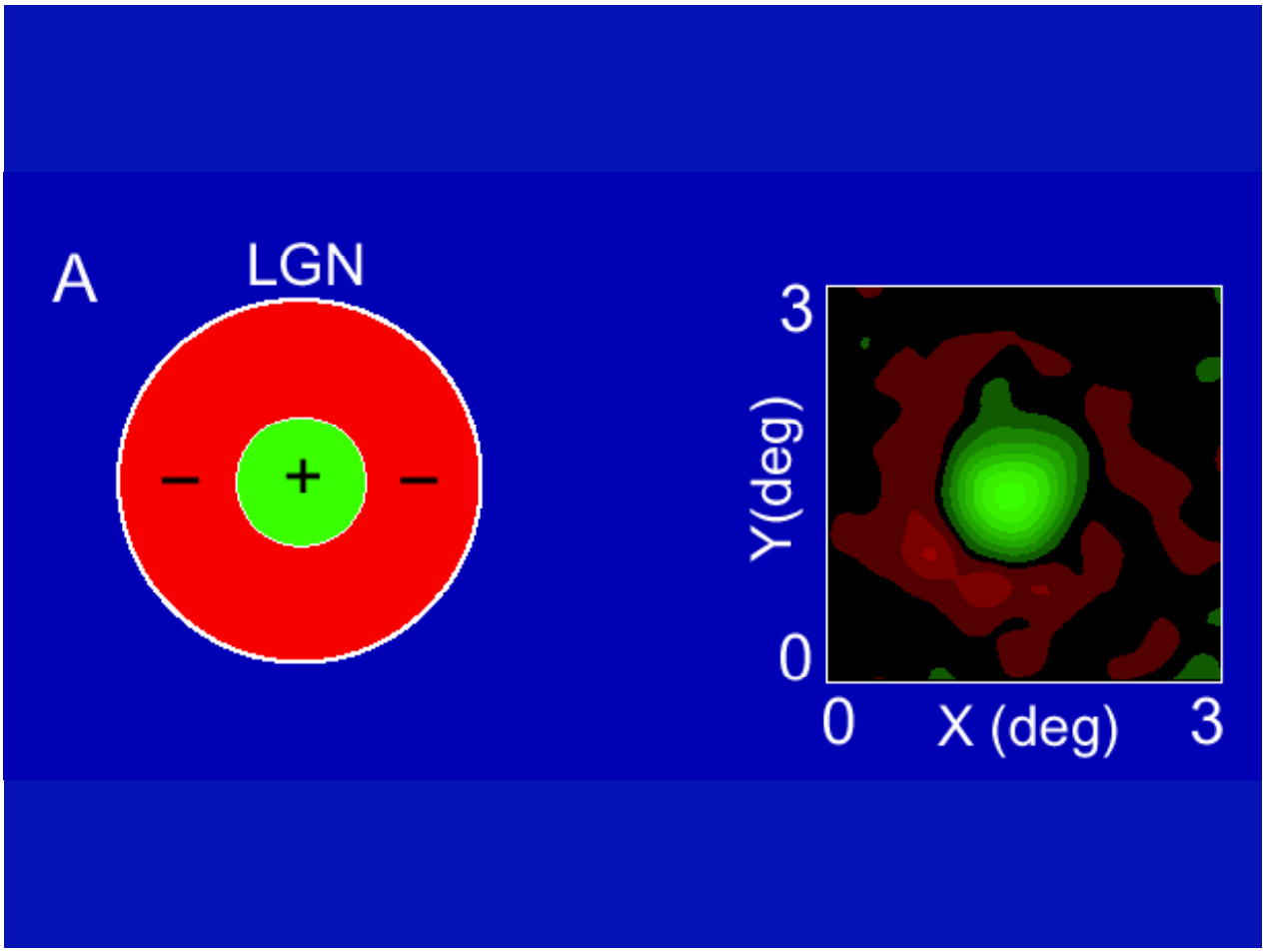

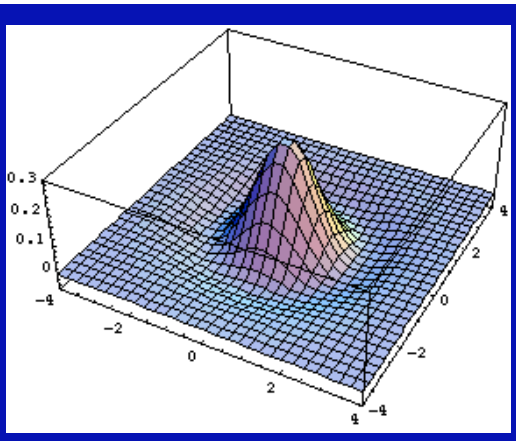

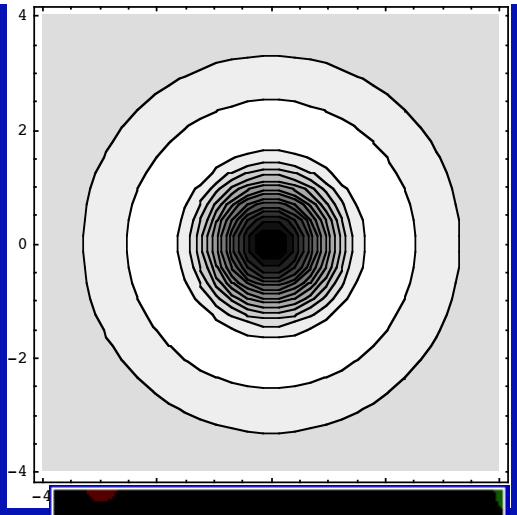

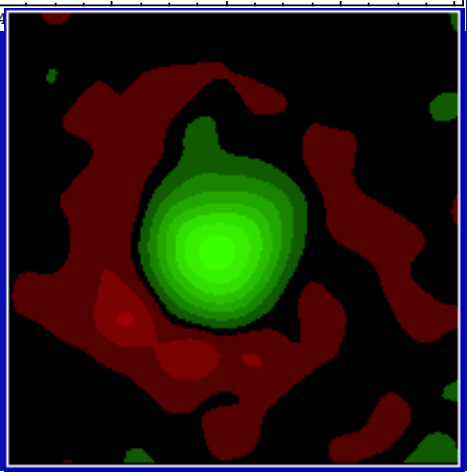

- Level curves of the receptive profiles of some simple cells of V1 can be modeled
  - by second order derivatives of Gaussians,
  - by Gabor wavelets

$$\exp(i2x)\exp\left(-\left(x^2+y^2\right)\right)$$

(real part).

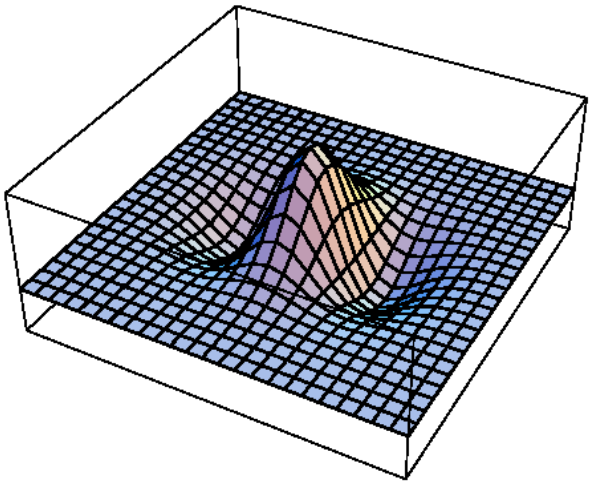

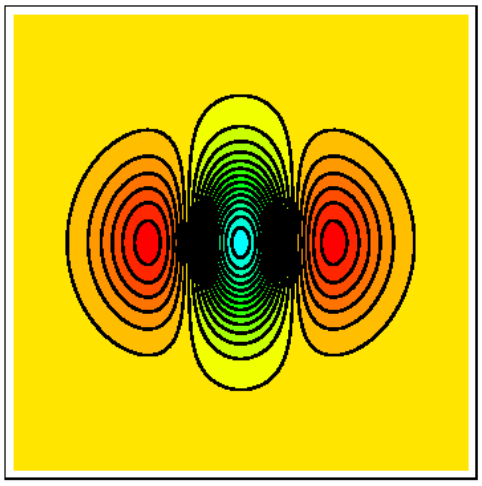

- There exist also RP of simple cells which are like third order derivatives of Gaussians (De Angelis).

B SIMPLE

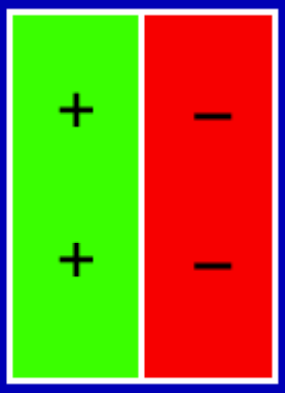

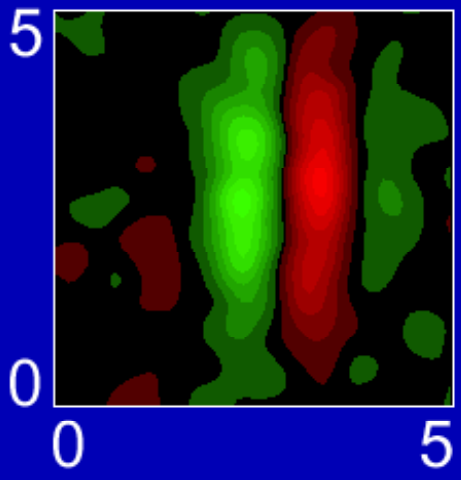

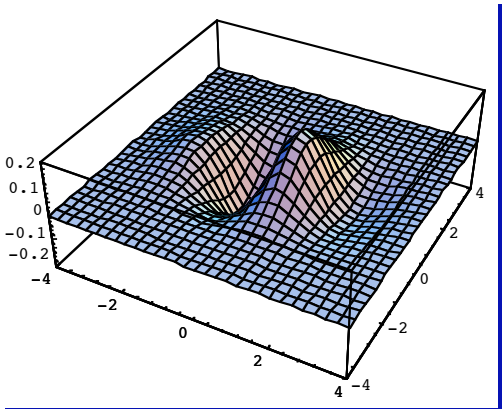

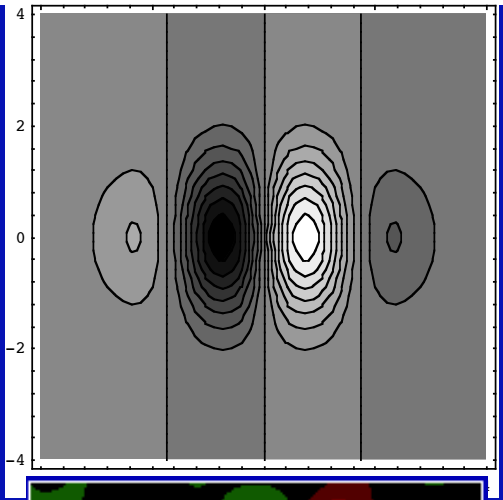

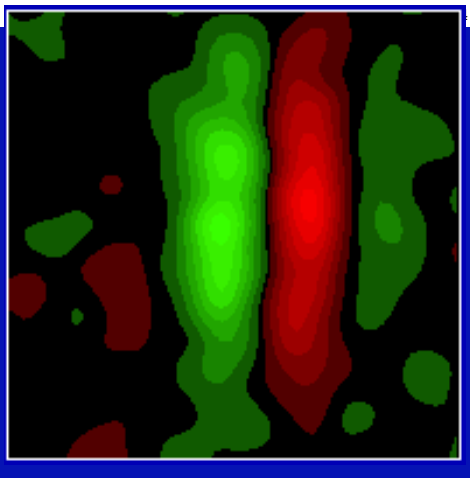

- If we add time (spatio-temporal RPs) we find even fourth order derivatives.
  - White noise method. Correlation between (i) random sequences of flashed bright / dark bars at different positions , and (ii) sequences of spikes. The time is the correlation delay.

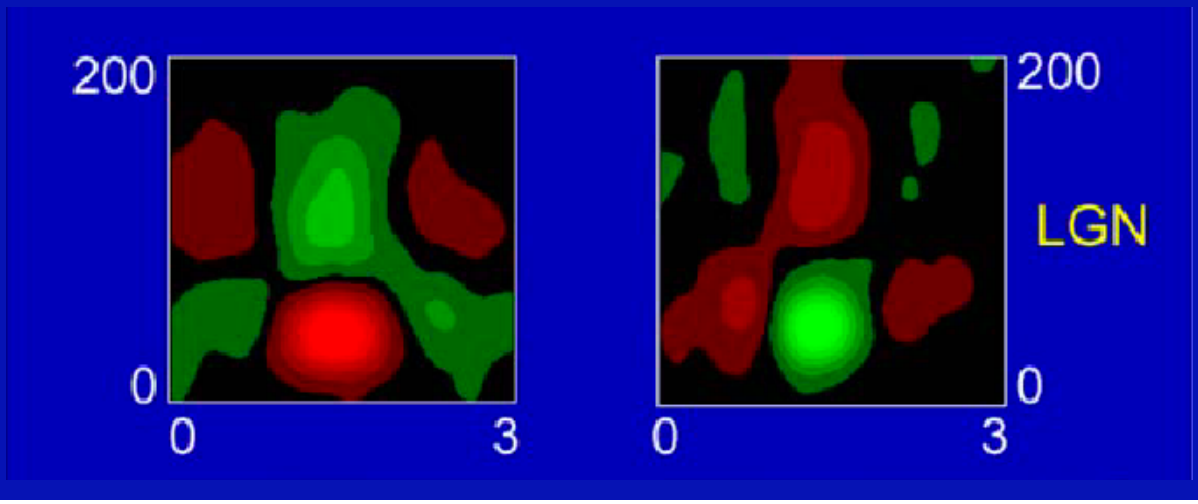

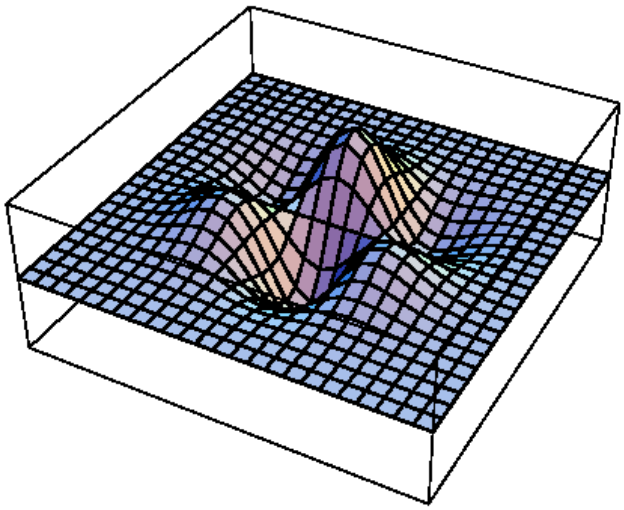

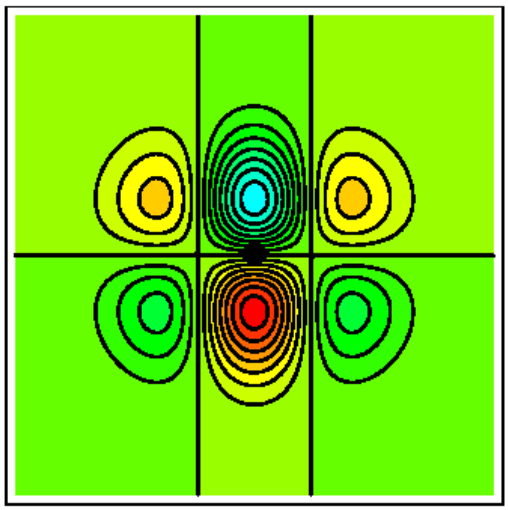

- There is a lot of technical discussions concerning the exact form of RP.
- Richard Young. « The Gaussian Derivative model for spatio-temporal vision », *Spatial Vision*, 14, 3-4, 2001, 261-319.
  - « The initial stage of processing of receptive fields in the visual cortex approximates a 'derivative analyzer' that is capable of estimating the local spatial and temporal directional derivatives of the intensity profile in the visual environment. »
- How ?

- How do the RPs operate on the visual signal?
- Let $I(x,y)$ be the visual signal (x,y are visual coordinates on the retina).
- Let $\varphi(x-x_0,y-y_0)$ be the RP of a neuron N whose receptive field is defined on a domain D of the retina centered on (x_0,y_0).

- *N* acts on the signal *I* as a filter :

$$I_\varphi(x_0, y_0) = \int_D I(x', y')\varphi(x' - x_0, y' - y_0)dx'dy'$$

- A field of such neurons act therefore by convolution on the signal (wavelet analysis)

$$I_\varphi(x, y) = \int_D I(x', y')\varphi(x' - x, y' - y)dx'dy' = (I * \varphi)(x, y)$$

- But from the classical formula

$$I*DG = D(I*G)$$

for *G* a Gaussian and *D* a differential operator, the convolution of the signal *I* with a *DG*-shaped RF amounts to apply *D* to the smoothing (the regularization) $I*G$ of the signal *I* at the scale defined by the width of *G*.

- Hence a wavelet analysis which is a multiscale differential geometry.

Wavelets and group action

- A « mother » profile φ_0 is transformed under the Lie group G of tanslations of positions, rotations of positions, rotations of orientations θ, and scaling σ.
- For a given position $a = (x_0, y_0)$, the filters with variable orientations θ constitute an hypercolumn in the sense of Hubel and Wiesel.

- For a typical Gabor RP, given a curve C, the RP centered at a point $a = (x, y)$ which gives the maximum response has
  - θ = orientation of C,
  - σ codes $dist(a, C)$.

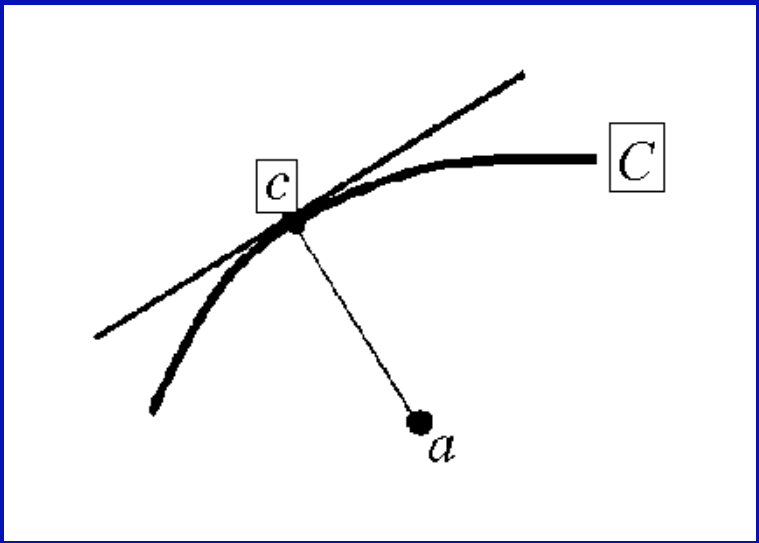

- Mother wavelet

$$\varphi_{(0,\sigma)}(x,y) = \frac{1}{e^{2\sigma}} e^{\frac{-(x^2+y^2)}{e^{2\sigma}}} e^{\frac{2iy}{e^{\sigma}}}$$

- Citti-Sarti :

$$d\left((x,y),c\right) = \frac{1}{\sqrt{2}} e^{\bar{\sigma}}$$

and $\bar{\theta}$ is the direction of *C* at *c*.

- Citti-Sarti : If we look at the maximal responses of the receptive profiles centered at *a*, and if *c* is the nearest point of *C* relative to *a*, then

$$d((x,y),c) = \frac{1}{\sqrt{2}} e^{\bar{\sigma}}$$

and $\bar{\theta}$ is the direction of *C* at *c*.

Engrafting variables : the fibration model

- The simple cells of V1 detect a preferential orientation (static or dynamic : moving gratings).
- They measure, at a certain scale, pairs (*a, p*) of a spatial position *a* in the visual field and of a local orientation *p* at *a*.
- Pairs (*a*, *p*) are called contact elements in contact geometry. Simple neurons of V1 detect contact elements.

- The hypercolumns associate retinotopically to each position *a* of the retina *R* a full exemplar P_a of the space *P* of orientations *p* at *a*.
- An hypercolumn is ≈ 200-500μ wide.
- This functional architecture implements the fibration $\pi : R \times P \rightarrow R$ with base *R*, fiber *P*, and total space $V = R \times P$.

- The hypercolumnar structure has been discovered in the late 50s by Vernon Mountcastle in the somatosensorial cortex of the cat and in the early 60s in the visual cortex by David Hubel and Torsten Wiesel, and after in the motor cortex and the auditory cortex.
- How a curve *C* in *R* is represented in $V = R \times P$?

- If $p = \mathrm{Tan}(\theta)$, $V = R \times P$ is the space $J^1(\mathbf{R}, \mathbf{R})$ of 1-jets of curves C in R.
- If C is a curve in R (a contour), it can be lifted to V via the jet map

$$j : C \rightarrow V = R \times P$$

$a \in C \rightarrow (a, p_a)$ where p_a is the orientation of the tangent of C at a.

- Γ represents C as the enveloppe of its tangents (projective duality).

- The structure of fibration formalizes Hubel 's concept of "engrafting" "secundary" variables (orientation, ocular dominance, color, direction of movement, etc.) on the basic retinal variables (x,y) :
  - « What the cortex does is map not just two but many variables on its two-dimensional surface. It does so by selecting as the basic parameters the two variables that specify the visual field coordinates (…), and on this map it engrafts other variables, such as orientation and eye preference, by finer subdivisions. » (Hubel 1988, p. 131)

- It is the functional architecture of cells with a prefered orientation which explains how V1 can perform global tasks such as contour integration.

Pinwheels

- The fibration $\pi : R \times P \to R$ is of dimension 3 but is implemented in neural layers of dimension 2.

- Many experiments have shown that hypercolumns are geometrically organized in pinwheels.
  - The cortical layer is reticulated by a network of singular points which are the centers of the pinwheels.
  - Locally, around these singular points all the orientations are represented by the rays of a "wheel",
  - and the local wheels are glued together in a global structure.

- The method (Bonhöffer & Grinvald, ~ 1990) of "in vivo optical imaging based on activity-dependent intrinsic signals" allows to acquire images of the activity of the superficial cortical layers.
- The experimental challenge is extremely difficult. Millions of neurons are connected with hundreds and even thousands of synapses for each neuron.
- Single cells recordings or post mortem visualization of the cortical activity via 2-deoxyglucose maps are not sufficient.

- In vivo optical imaging methods have a good spatial resolution (50μ) but a bad temporal resolution.
- They can analyze slow intrinsic changes of optical properties of the cortical layer.
- To visualize the cortical dynamic one needs other methods such as voltage-sensitive dyes which stain active cells : dye molecules are bound to cell membranes and act as molecular transducers transforming changes in membrane potential into optical signals.
- Temporal resolution < 1ms.

- A piece of cortex is exposed in an oil-filled chamber and illuminated by orange light (605nm).
- The amplitude of orientation maps is very weak w.r.t. the light intensity of recorded cortical images. One substracts the mean intensity for all orientations (cocktail blank).
- One does the summation of the images of V1 ’s activity for the different gratings and constructs differential maps.

- The low frequency noise is eliminated.
- The maps are normalized (by dividing the deviation relative to the mean value at each pixel by the global mean deviation).

- In the following picture the orientations are coded by colors and iso-orientation lines are therefore represented by monocolor lines.
- William Bosking, Ying Zhang, Brett Schofield, David Fitzpatrick (Dpt of Neurobiology, Duke) 1997, « Orientation Selectivity and the Arrangement of Horizontal Connections in Tree Shrew Striate Cortex », *J. of Neuroscience*, 17, 6, 2112-2127.
- Layers 2/3 of a Tree Shrew (Tupaya) :

  LGN $\rightarrow$ layer 4 $\rightarrow$ (strictly feed foorward) $\rightarrow$ layers 2/3.

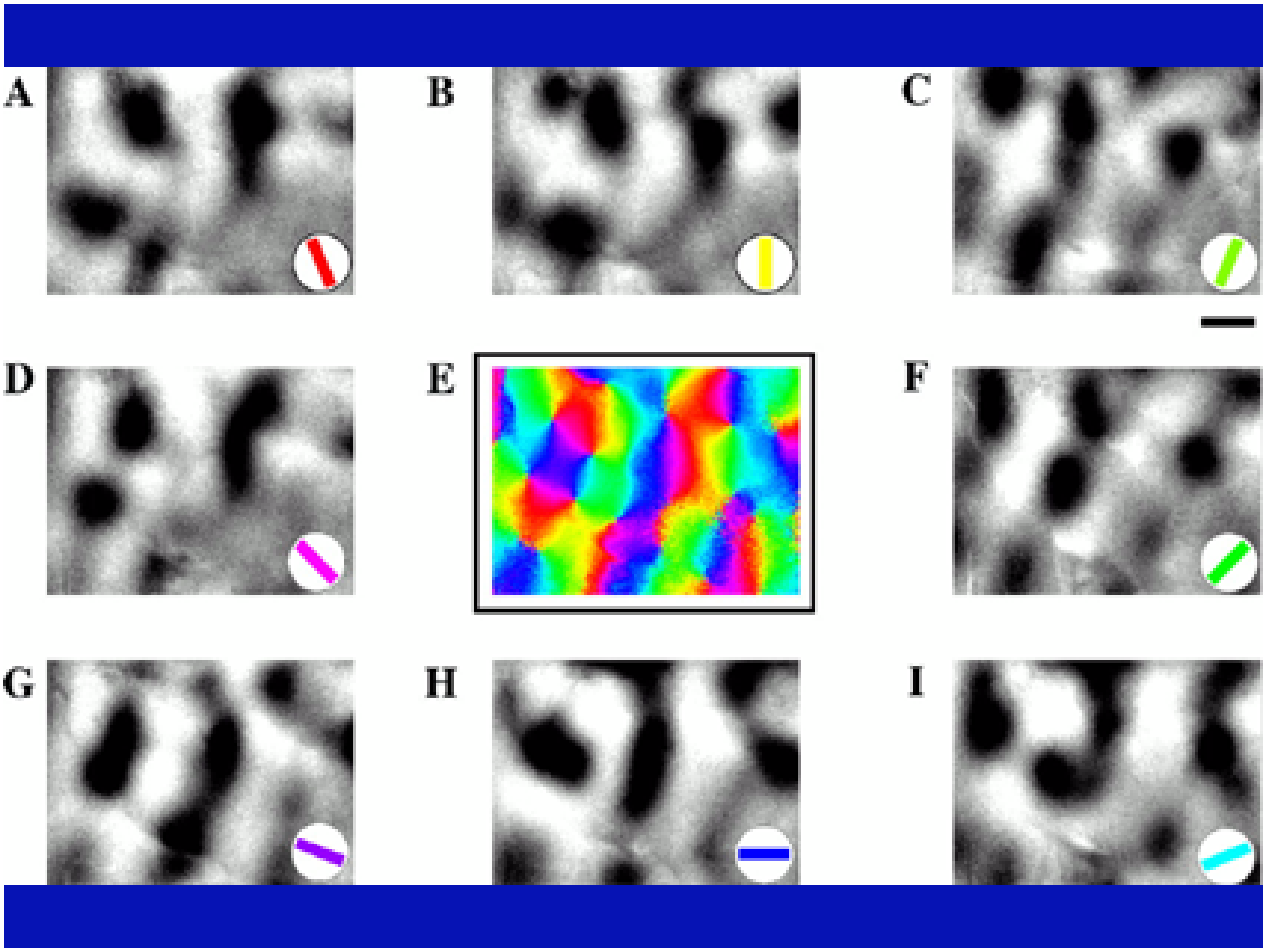
A
B
C
D
E
F
G
H
I

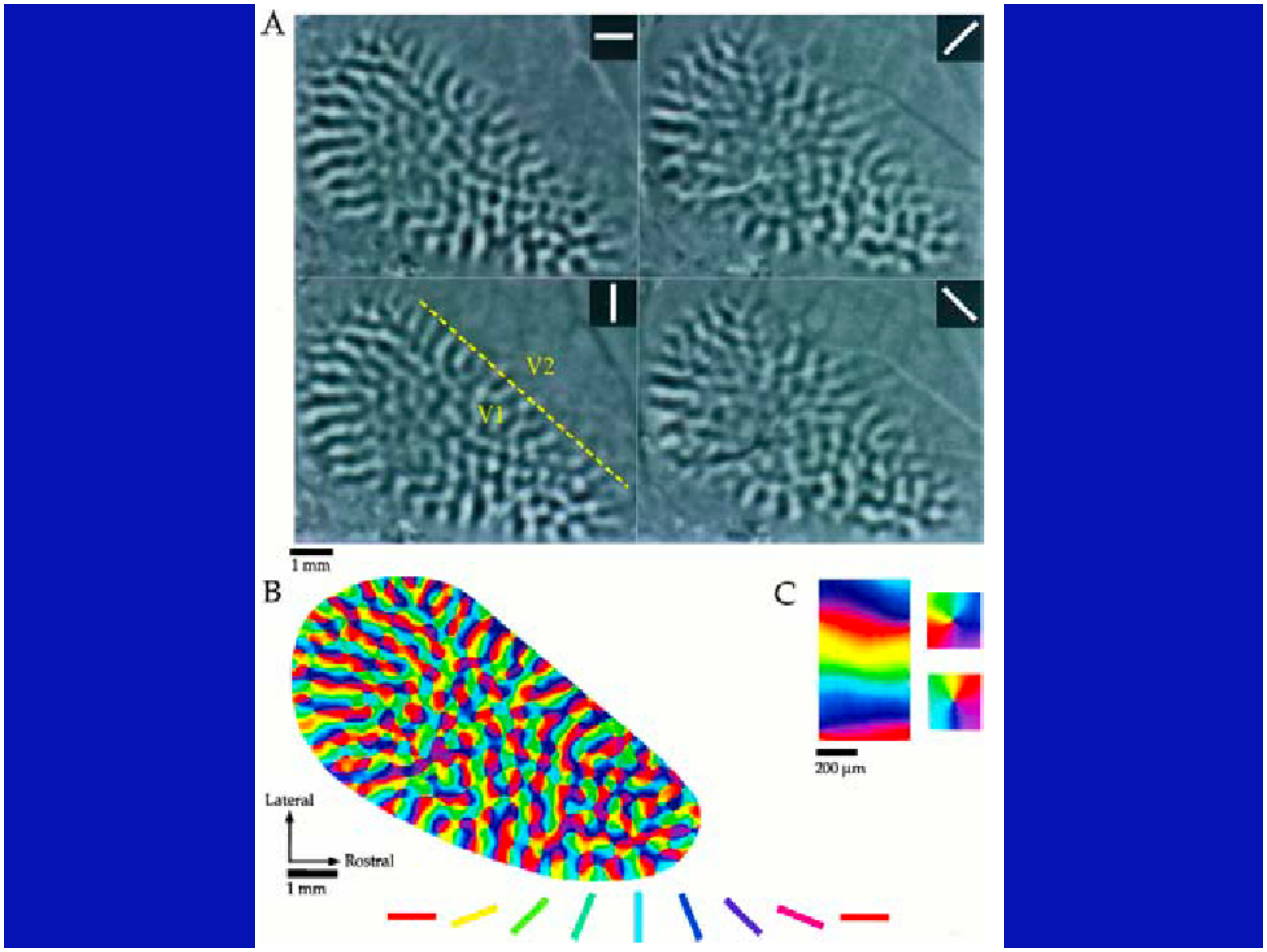
A
V2
V1
1 mm
B
Lateral
Rostral
1 mm
C
200 μm

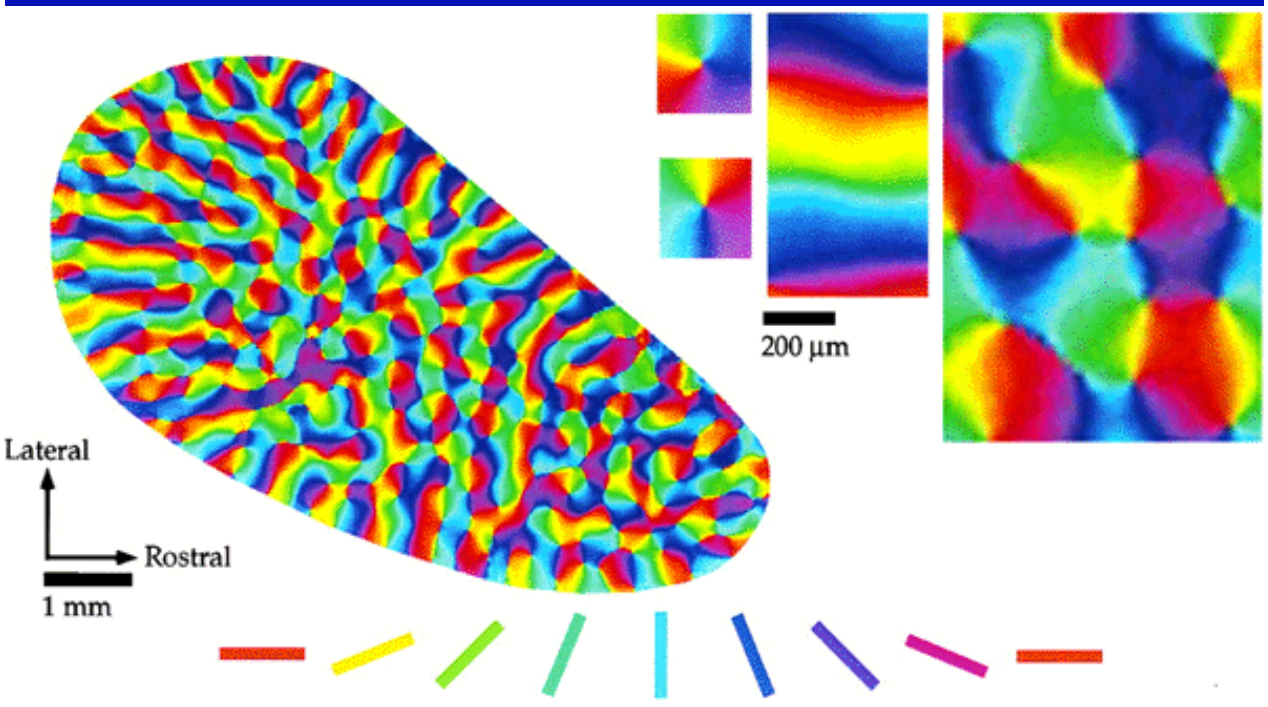
200 μm
Lateral
Rostral
1 mm

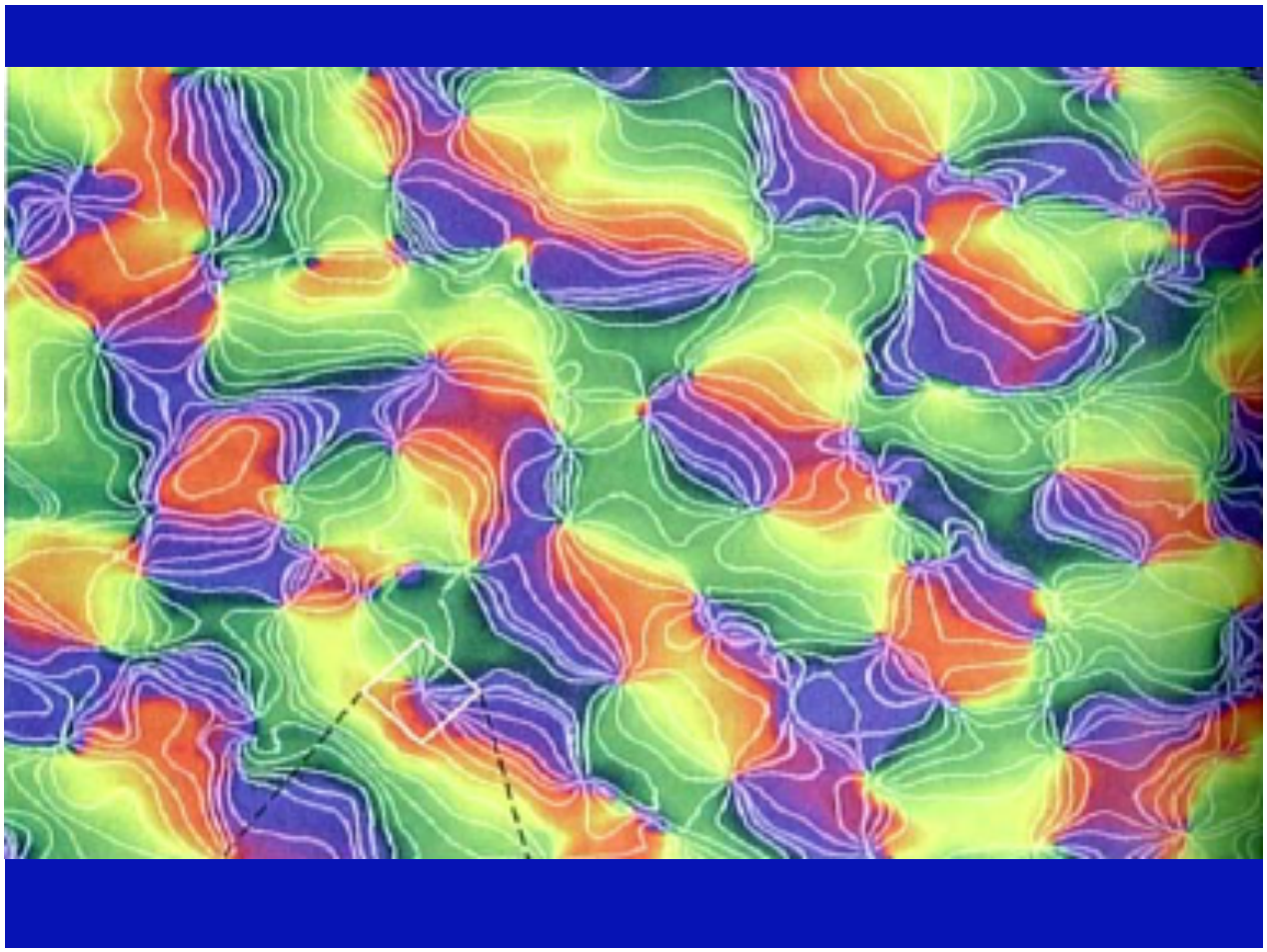

- There are 3 classes of points :
  - regular points where the orientation field is locally trivial;
  - singular points at the center of the pinwheels;
  - saddle-points localized near the centers of the cells of the network.
- Two adjacent singular points are of opposed chiralities (CW and CCW).
- It is like a field in *W* generated by topological charges with « field lines » connecting charges of opposite sign.

- At the boundary between V1 and V2 the configuration is different. Pinwheels of the same chirality are aligned along the boundary (Shigeru Tanaka, Riken Institute).

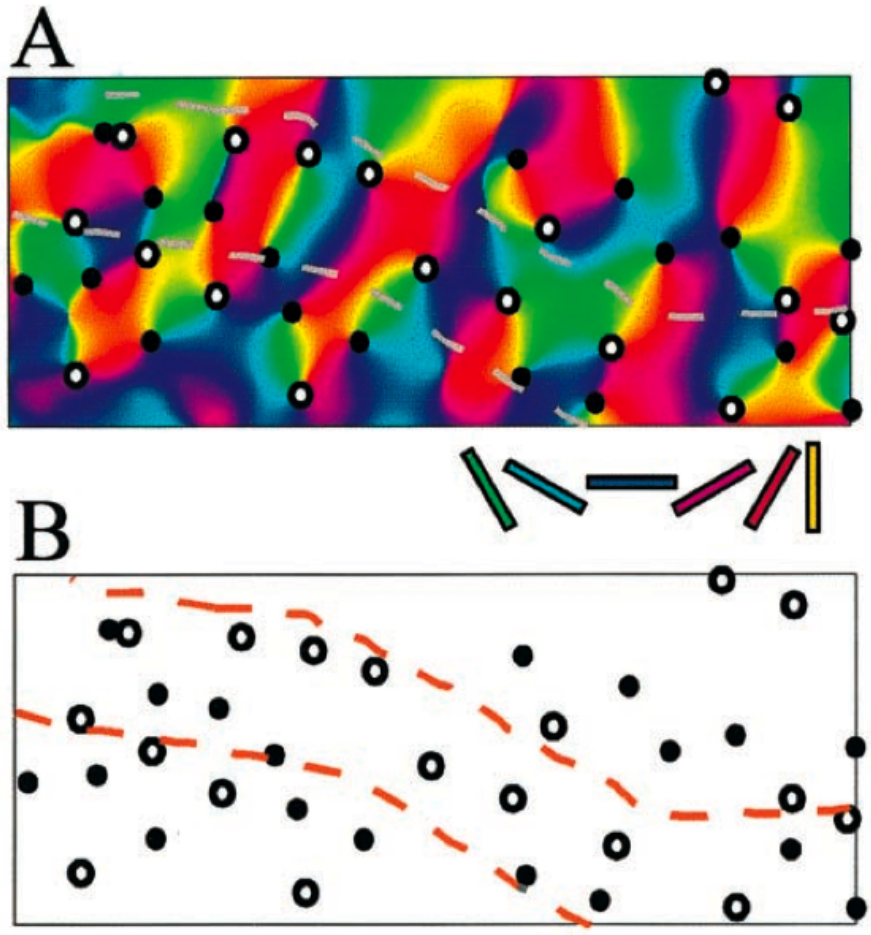

- In the following picture due to Shmuel (cat's area 17), the orientations are coded by colors but are also represented by white segments.
- We observe very well the two types of generic singularities of 1D foliations in the plane.

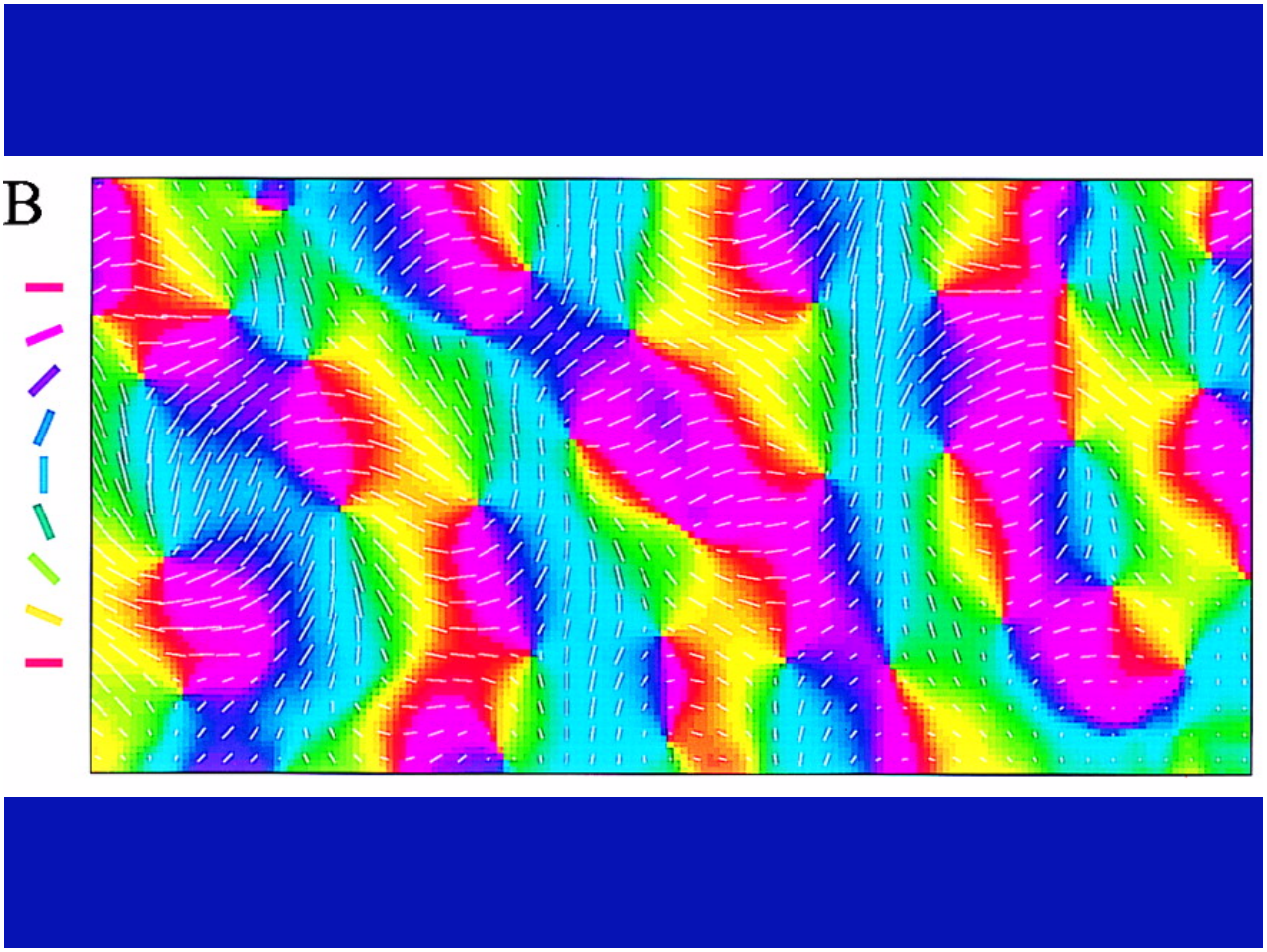
B

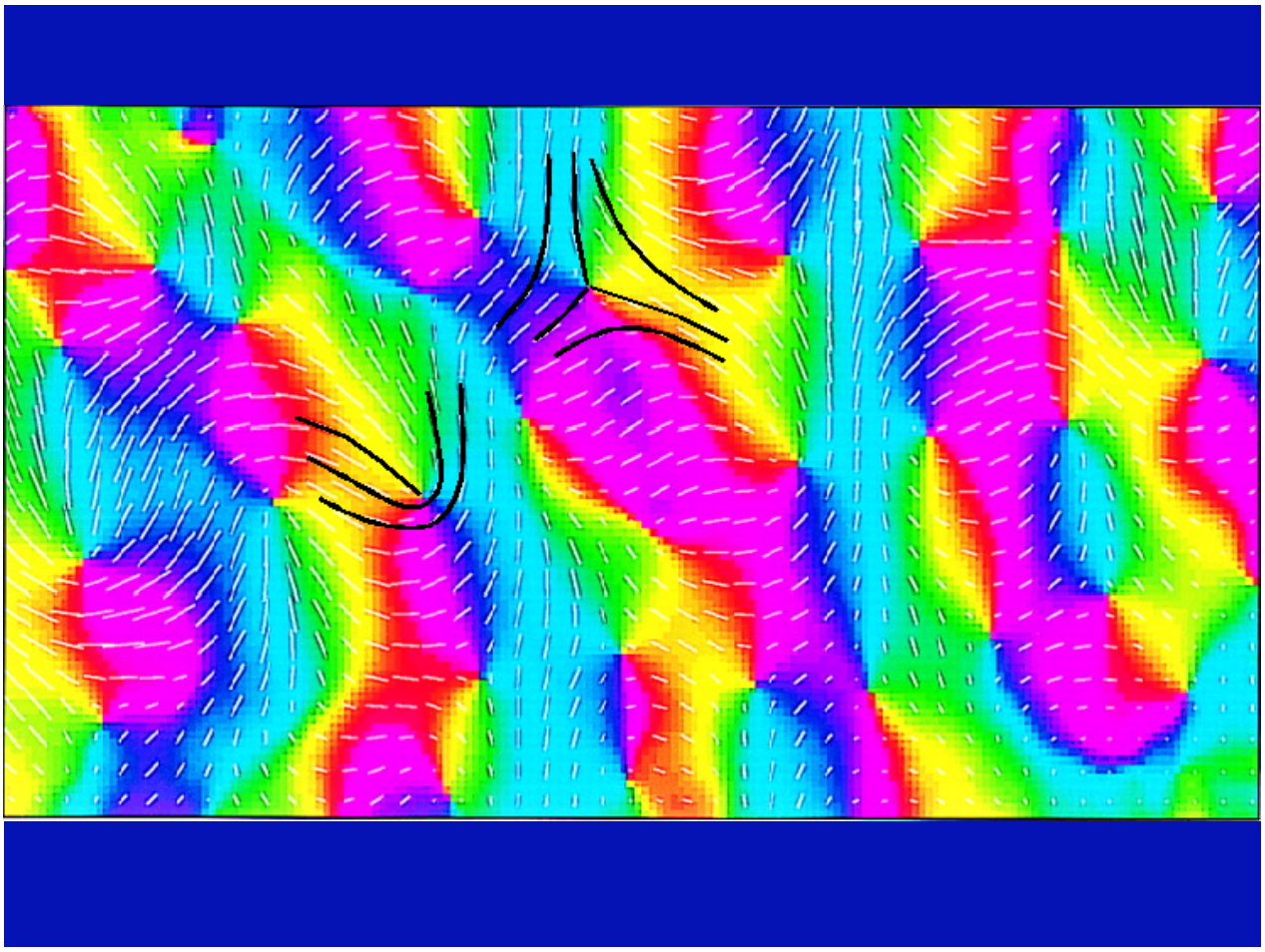

- They arise from the fact that, in general, the direction θ in V1 of a ray of a pinwheel is not the orientation p_θ associated to it in the visual field.
- When the ray spins around the singular point with an angle θ the associated orientation rotates with an angle $\theta/2$. Two diametrally opposed rays correspond to orthogonal orientations.
- There are two cases.

- If the orientation p_θ associated with the ray of angle θ is $p_\theta = \alpha + \theta/2$ (α being the orientation of the ray $\theta = 0$), the two orientations will be the same for

$$p_\theta = \alpha + \theta/2 = \theta$$

  that is for $\theta = 2\alpha$.
- As α is defined modulo π, there is only one solution : end point.

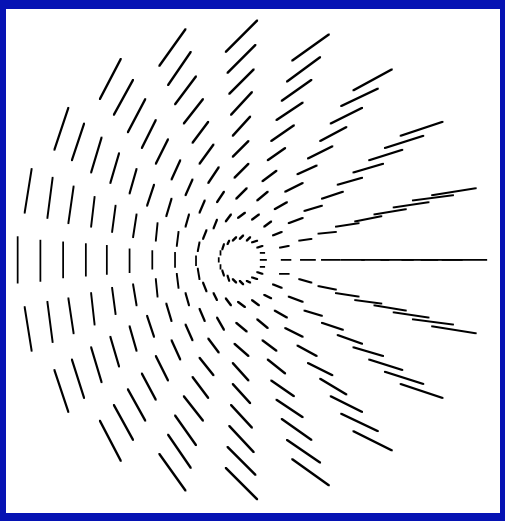

- If the orientation p_θ associated with the ray of angle θ is $p_\theta = \alpha - \theta/2$, the two orientations will be the same for

$$p_\theta = \alpha - \theta/2 = \theta$$

that is for $\theta = 2\alpha/3$.

- As α is defined modulo π, there are three solutions : triple point.

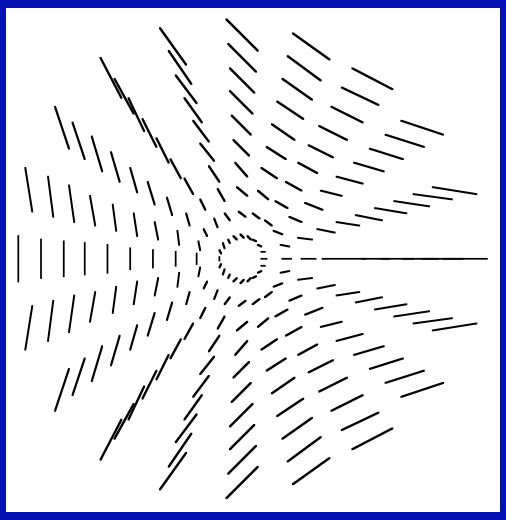

Micro-structure near pinwheel centers

- P. E. Maldonado, I. Gödecke, C. M. Gray, T. Bonhöffer (« Orientation Selectivity in Pinwheel Centers in Cat Striate Cortex », *Science*, 276 (1997) 1551-1555) have analyzed the fine-grained structure of orientation maps at the singularities. They found that

  « orientation columns contain sharply tuned neurons of different orientation preference lying in close proximity ».

- James Schummers « Synaptic integration by V1 neurons depends on location within the orientation map » (*Neuron*, 36, 2002, 969-978) has shown that
  - « neurons near pinwheel centers have subthreshold responses to all stimulus orientations but spike responses to only a narrow range of orientations ».
- Scales.
  - Left (far for from a pinwheel): 8 spikes/s, 10mV, 2s.
  - Right (at a pinwheel): 3 spikes/s, 8mV, 2s.

- Far from a pinwheel cells « show a strong membrane depolarization response only for a limited range of stimulus orientation, and this selectivity is reflected in their spike responses ».
- At a pinwheel center, on the contrary, only the spike response is selective. There is a strong depolarization of the membrane for all orientations.
- The stimuli are moving oriented gratings.

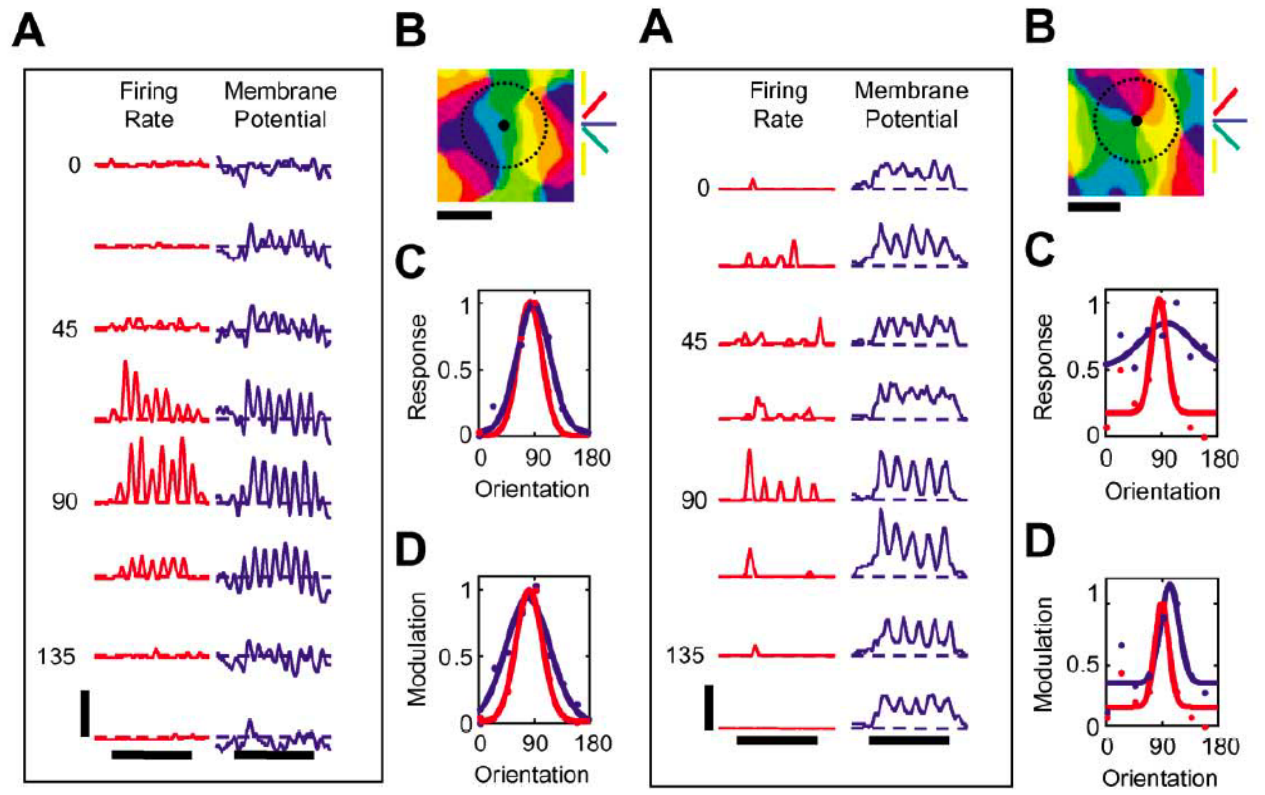

- It is an original solution to the problem of singularities.
- But the spatial (50μ) and depth resolutions of optical imaging is not sufficient.
- One needs single neuron resolution to understand the micro-structure.

- Two-photon calcium imaging *in vivo* provides functional maps at single-cell resolution.
  - Kenichi Ohki, Sooyoung Chung, Prakash Kara, Mark Hübener, Tobias Bonhoeffer and R. Clay Reid,
  - *Highly ordered arrangement of single neurons in orientation pinwheels, Nature* 442, 925-928 (24 August 2006) .

- (In cat) pinwheels are higly ordered at the micro level and « thus pinwheels centres truly represent singularities in the cortical map ».
- Injection of calcium indicator dye (Oregon Green BAPTA-1 acetoxylmethyl esther) which labels few thousands of neurons in a 300-600μ region.
- Two-photon calcium imaging measures simultaneously calcium signals evoked by visual stimuli on hundreds of such neurons at different depths (from 130 to 290μ by 20μ steps).

- One finds pinwheels with the same orientation wheel.
- « This demonstrates the columnar structure of the orientation map at a very fine spatial scale ».

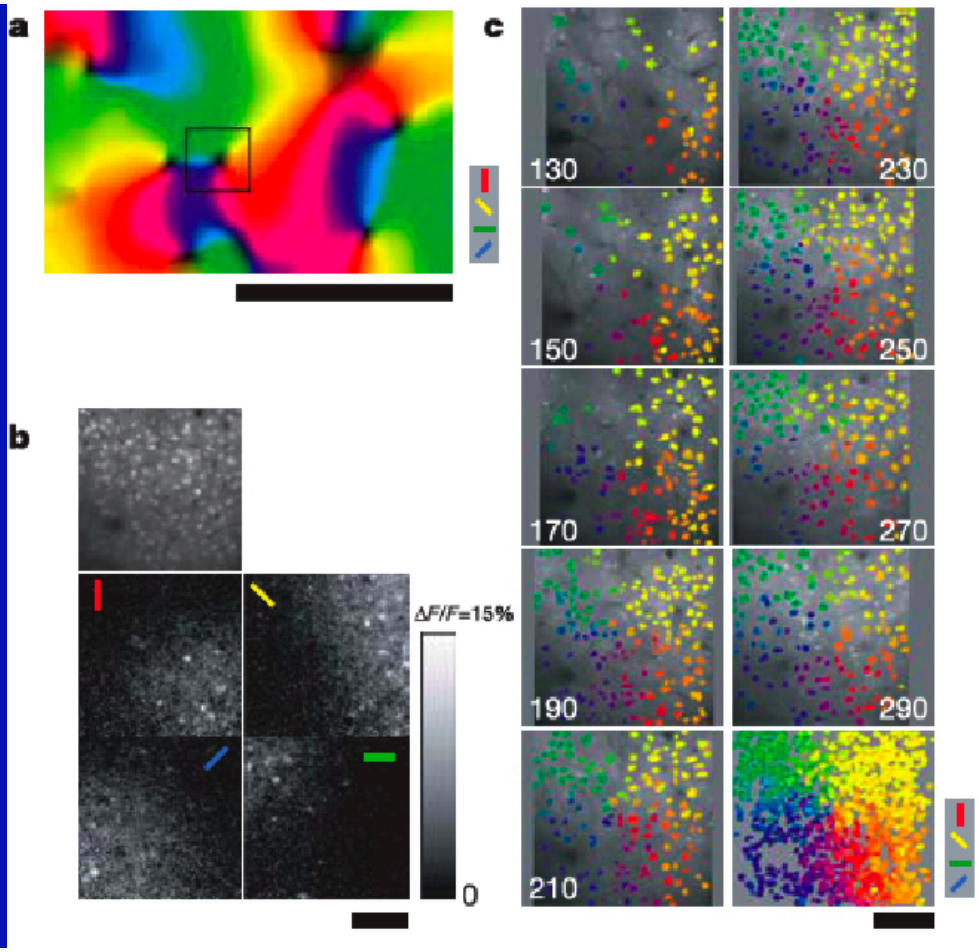

The fibration position / orientation

- Analyzing carefully the pattern of neural activity elicitated by a thin and long line stimulus, William Bosking (*Nature Neuroscience*, 5, 9, 2002) has shown the independance of position and orientation.
- The fibration $\pi : R \times P \to R$ is really implemented.

- The following picture (a) shows the population (stripe) of V1 neurons activated by a line stimulus located at a precise (vertical) position (scale bar = 1mm).
- (b) The stripe is embedded in the population of V1 neurons responding to the same vertical orientation but at different positions.

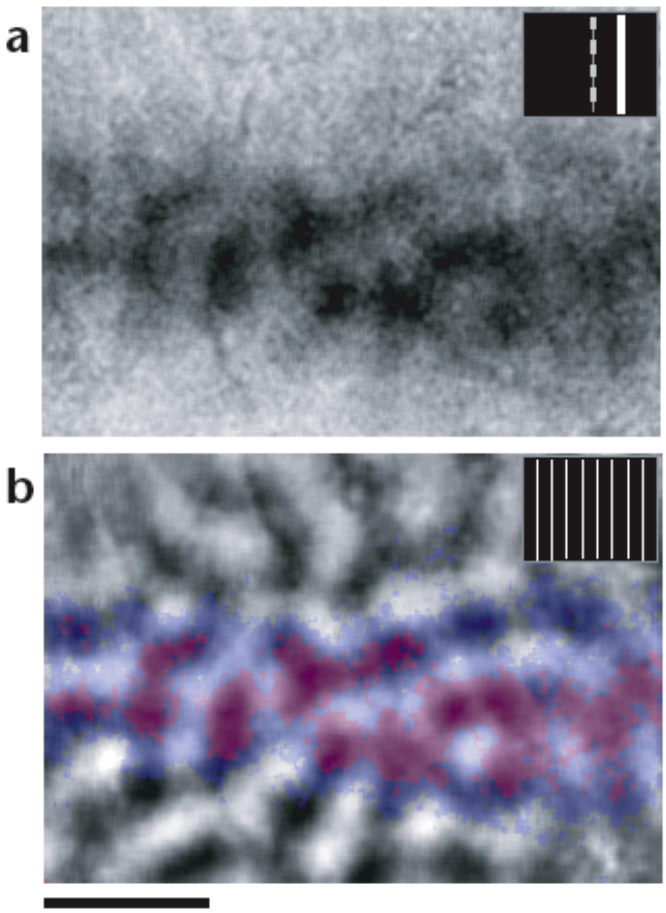

- When the position of the line moves in the visual field, the stripe moves in V1.
- The following picture shows that the position preference map (stripes, 0.5° intervals) and the orientation preference map (pinwheels) are essentially independent.

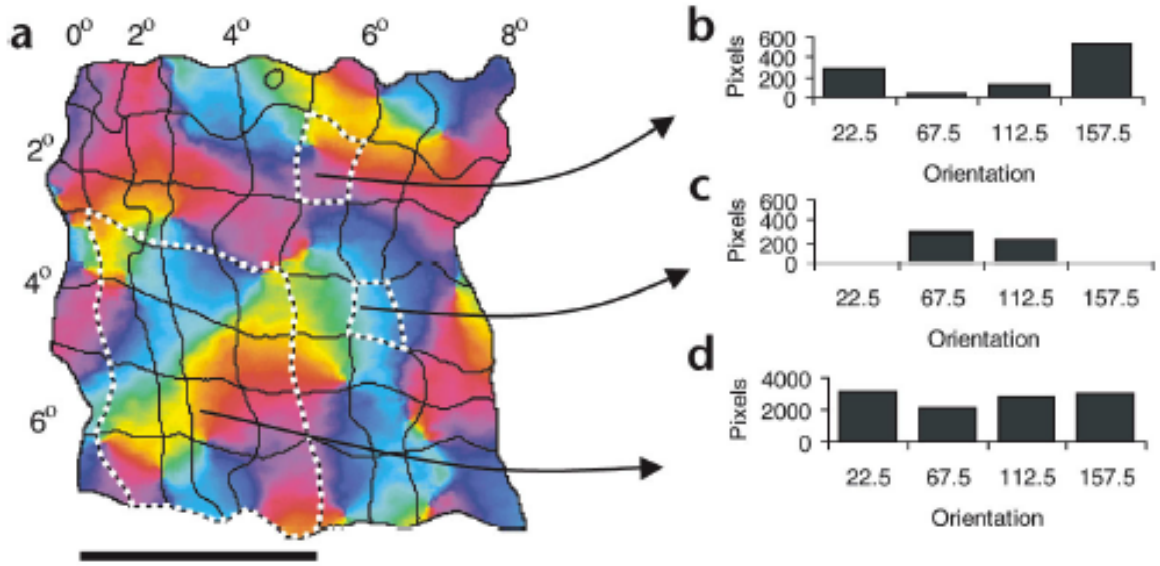

- So, Bosking has shown that

  « the map of visual space in V1 is orderly at a fine scale and has uniform coverage of position and orientation whithout local relationships in the mapping of these features. »

- This means that the local triviality of the fibration $\pi : R \times P \rightarrow R$ is neurally implemented.

Gluing processes

- A good example of neural implementation of a gluing process is given by the callosal connexions between the two hemispheric parts of V1.
- The region near the visual midline (VM) is mapped on the two parts of V1 near the boundary V1 / V2.

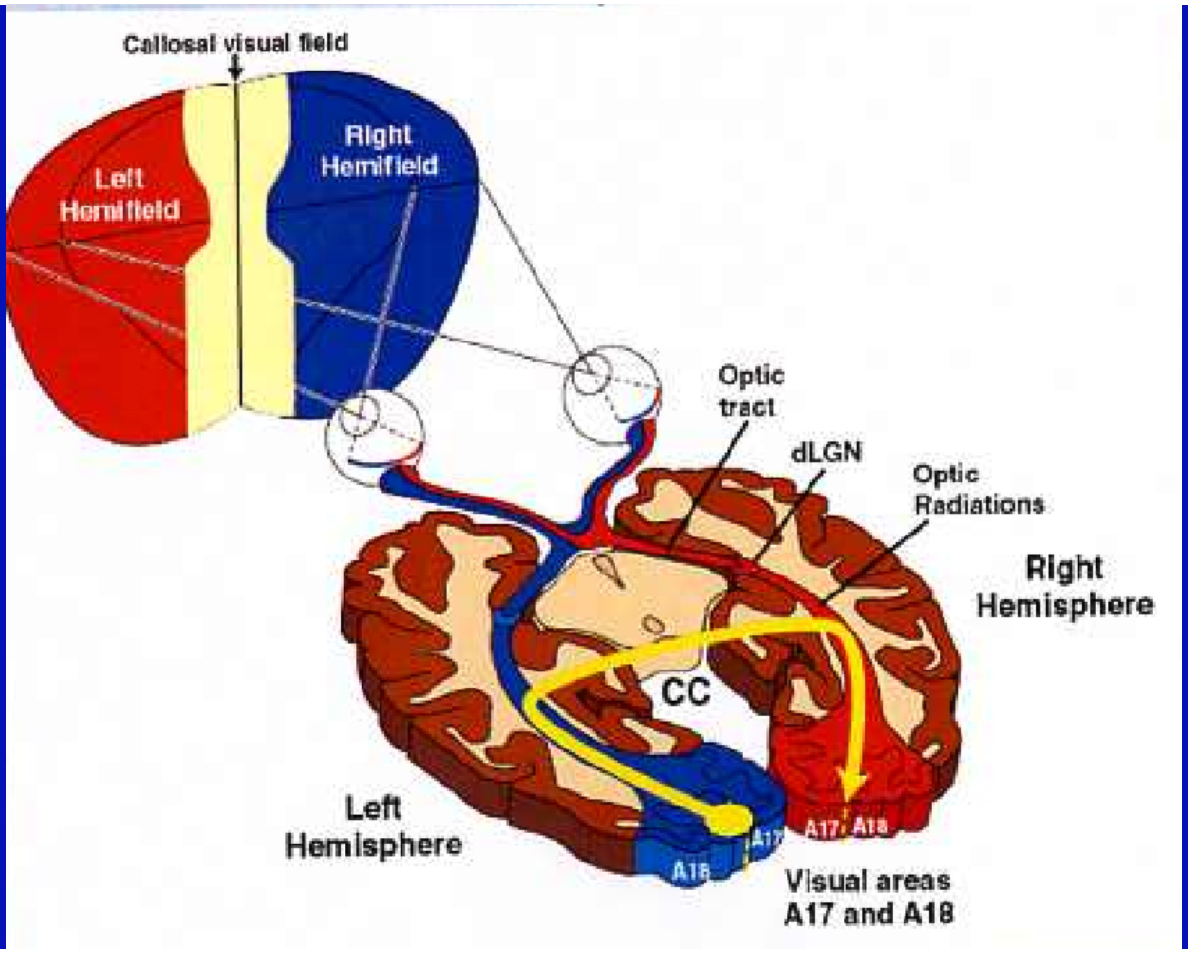

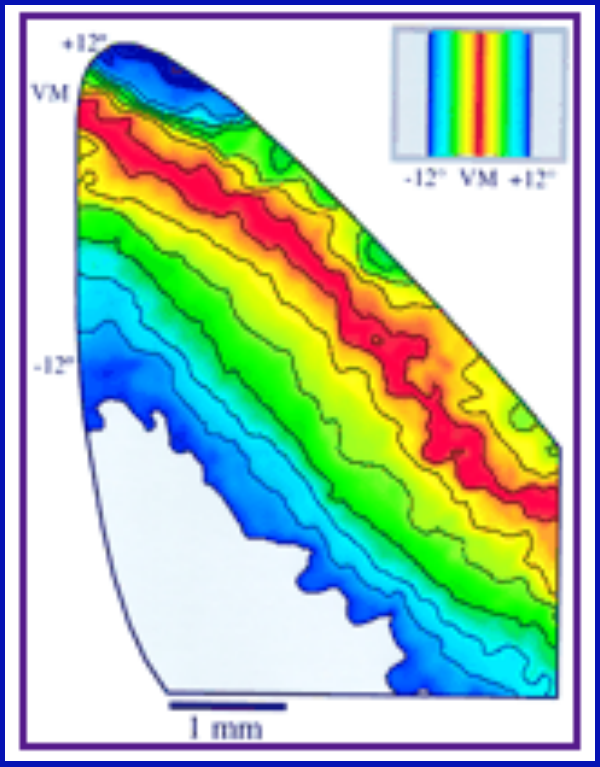

- For the tree shrew, if one injects rhodamine in a small region of $V1_L$ with vertical preference (red circle in a black region) and fluorescein in another small region with horizontal preference (green circle in a nearby white region), the callosal projections on $V1_R$ show no orientation specificity.

W. Bosking et al., *The Journal of Neuroscience*, 2000, 20(6), 2346-2359

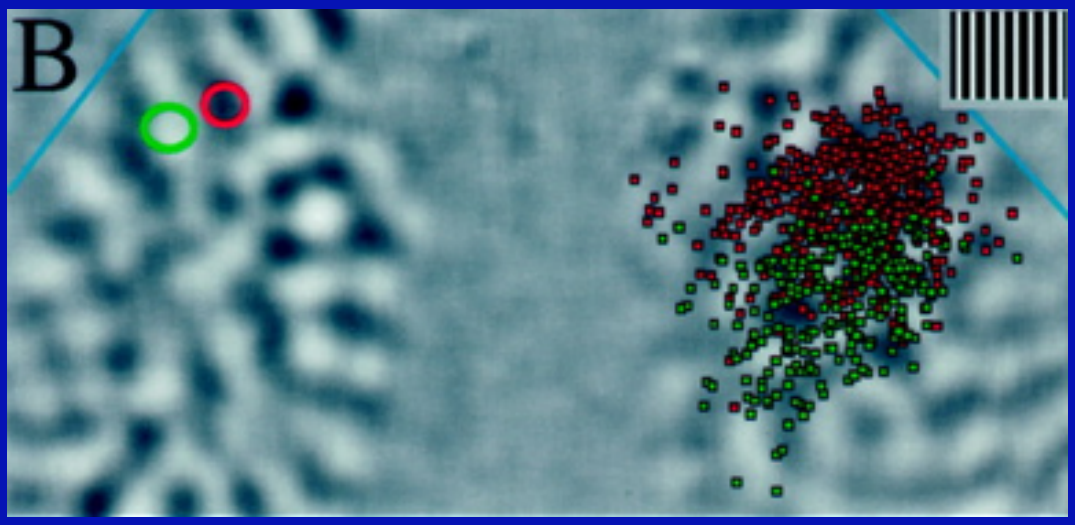

- Chantal Milleret and Nathalie Rochefort (Collège de France, Paris) have shown that it is completely different for the cat : callosal connections preserve orientation selectivity.
- If one cuts the chiasma, the right visual hemifield projects onto the left V1 via the the left eye and the activity of the right V1 is entirely due to the callosal connections.

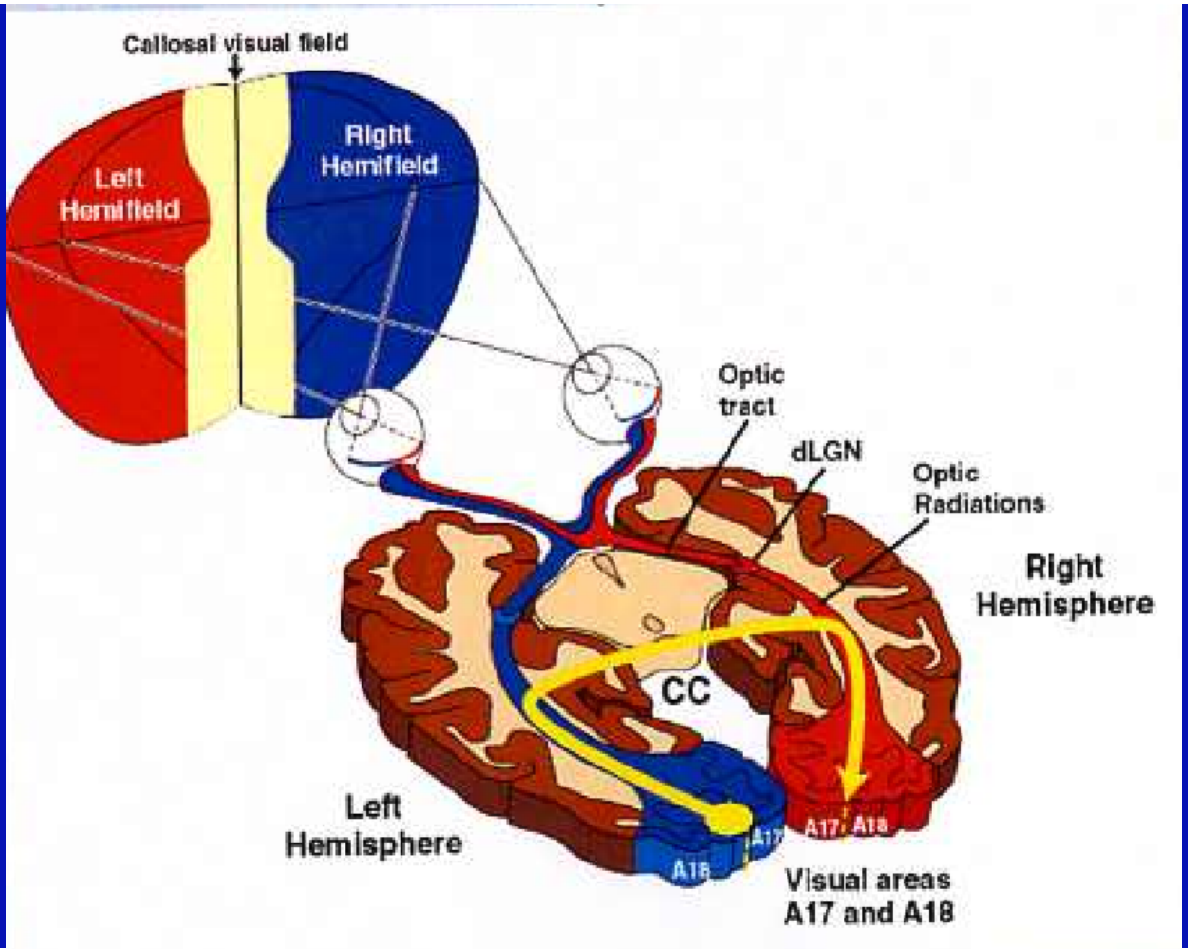

- The principal result is that, for each orientation, the domains activated by the callosal connections are the same as those activated by the retino-geniculo-cortical pathway.

Other “engrafted” variables

- Other variables are “engrafted” in the pinwheel structure, in particular :
  - The spatial frequency distributed along the rays of the pinwheels. Hübener : boundaries of the low spatial frequencies (gray) domains . Statistically, the pinwheels are centered in the frequency regions and the iso-orientation lines are orthogonal to the boundaries.

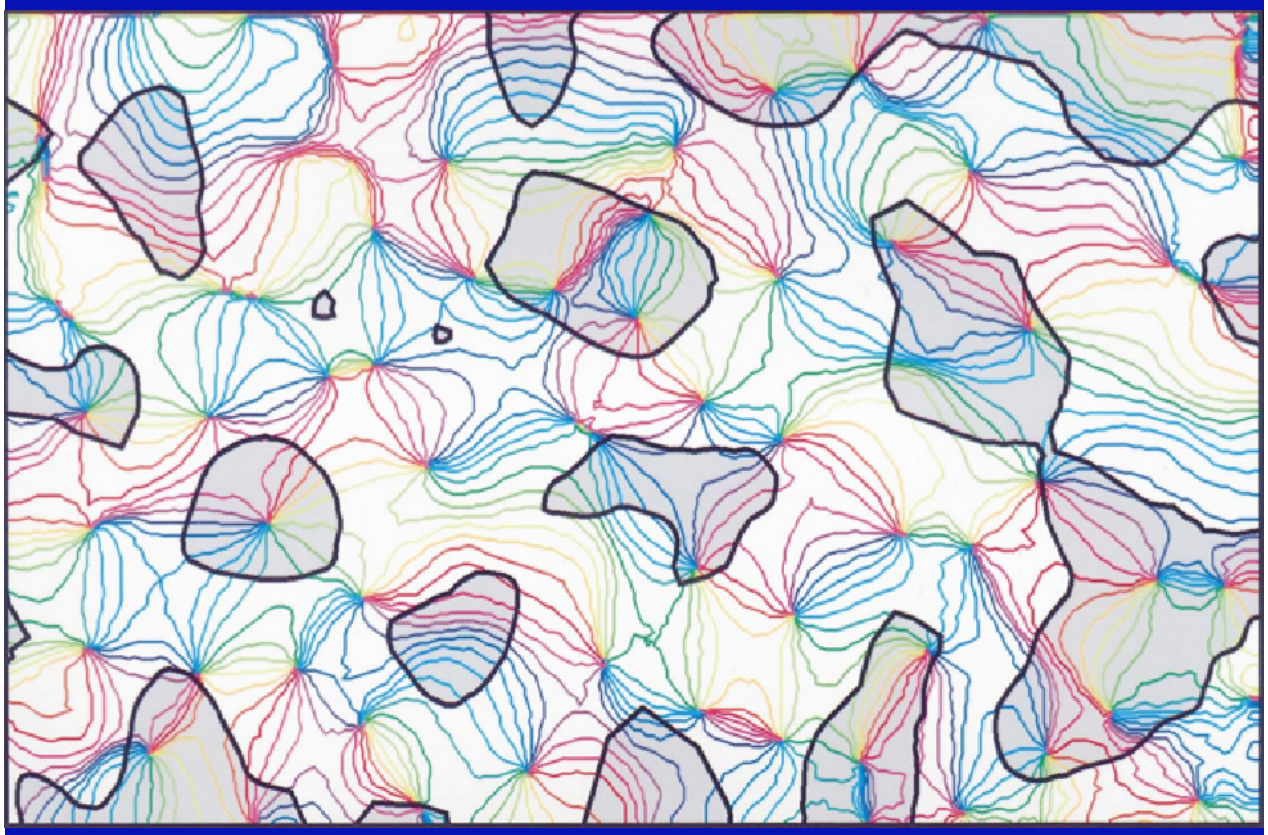

- The variation of phase (De Angelis 1999) : in a single column « spatial phase is the single parameter that accounts for most of the difference between receptive fields of nearby neurons ».
- The figure compares the complete RFs (*X*, *Y* = space and *T* = time = delay correlation) of two nearby cells in a column.
- Stimuli = randomly flashed (40ms) small bars (1.5°) of the prefered orientations of 2 simple neurons in the same column which are simultaneously recorded.

- One measures the cross-correlation between the sequence of stimuli and the response (spike trains) with several correlation delays.
- Visuotopy, orientations, spatial frequencies are essentially the same, but not the spatial phases.

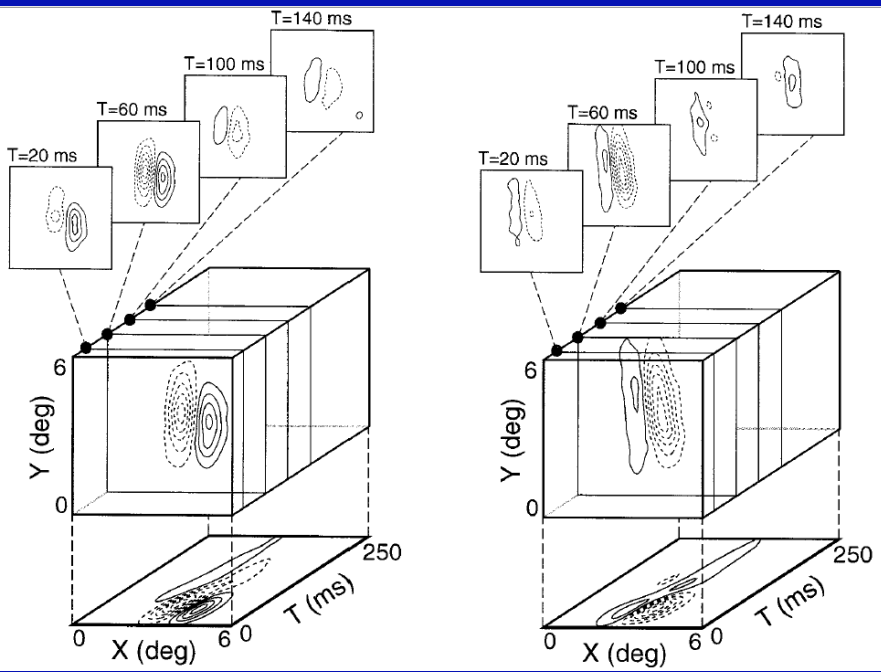

- The relation between the pinwheels and the domains of ocular dominance is also very interesting : their boundaries are essentially orthogonal to the iso-orientation lines.

- Hübener (Hübener, Shoham, Grinvald, Bonhöffer, “Spatial relationships among three columnar systems in cat area 17”, *J. of Neurosc.*, 17 (1997) 9270-84) :
  - Many iso-orientation lines cross the borders between ocular dominance domains close to right angles, and the pinwheel centers are preferentially located in the middle of these OD domains.

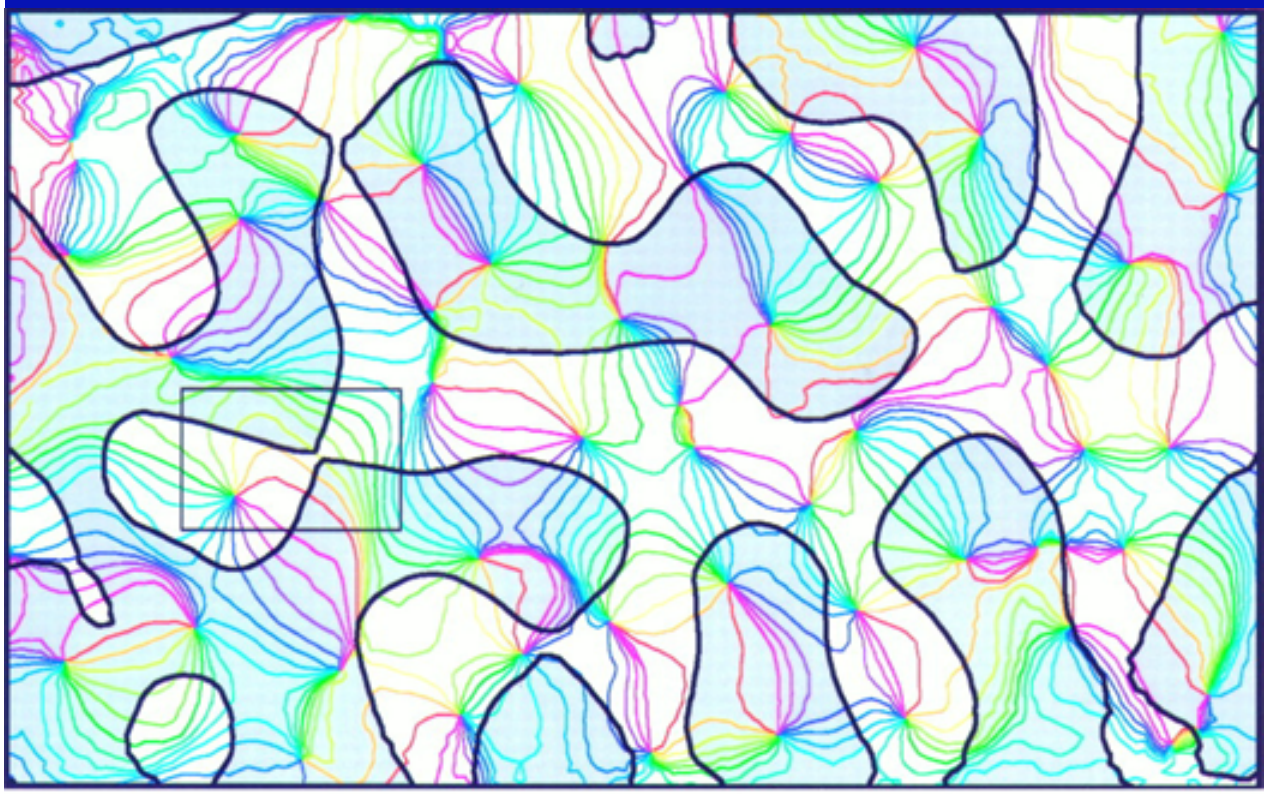

- Michael Crair has shown that the peaks of ocular dominance are localized near the centers of the pinwheels.
  - M. Crair et al., “Ocular Dominance Peaks at Pinwheels Center Singularities of the Orientation Map in Cat Visual Cortex”, *J. of Neurophysiology*, 77 : 3381-3385, 1997.

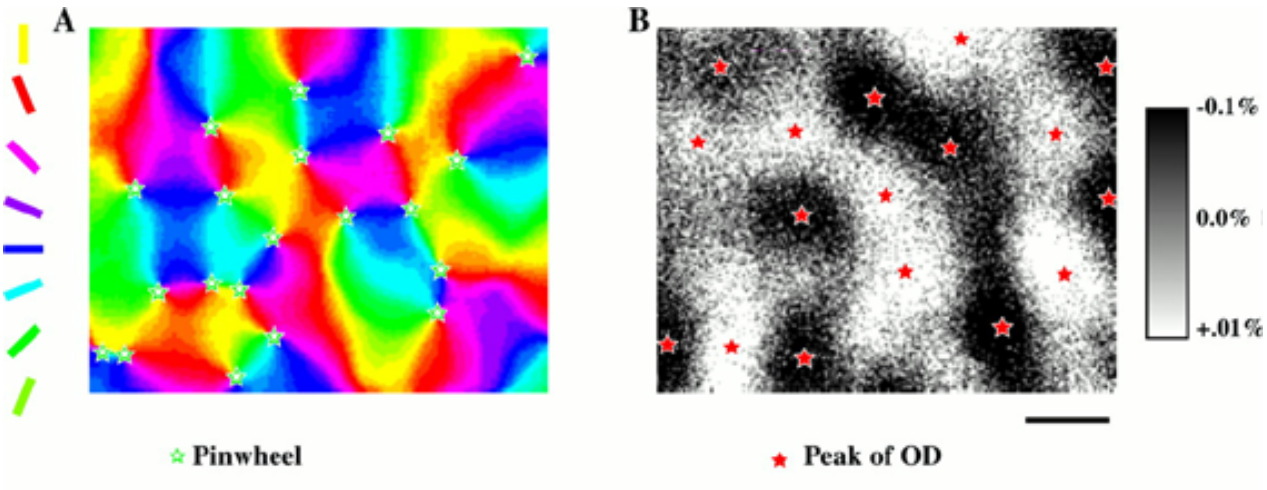

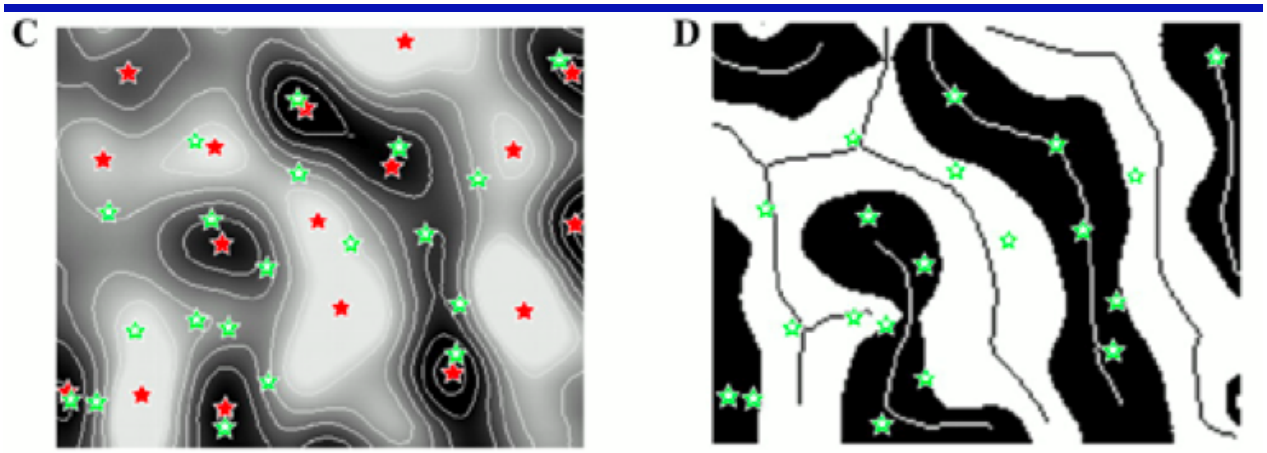

The horizontal structure

- The “vertical” retinotopic structure and the trivial locality are not sufficient.
- To achieve global coherence, the visual system must be able to compare two fibers P_a et P_b over two neighboring points *a* and *b*.
- This is a problem of parallel transport. At the neural level it is implemented in the horizontal cortico-cortical connections.

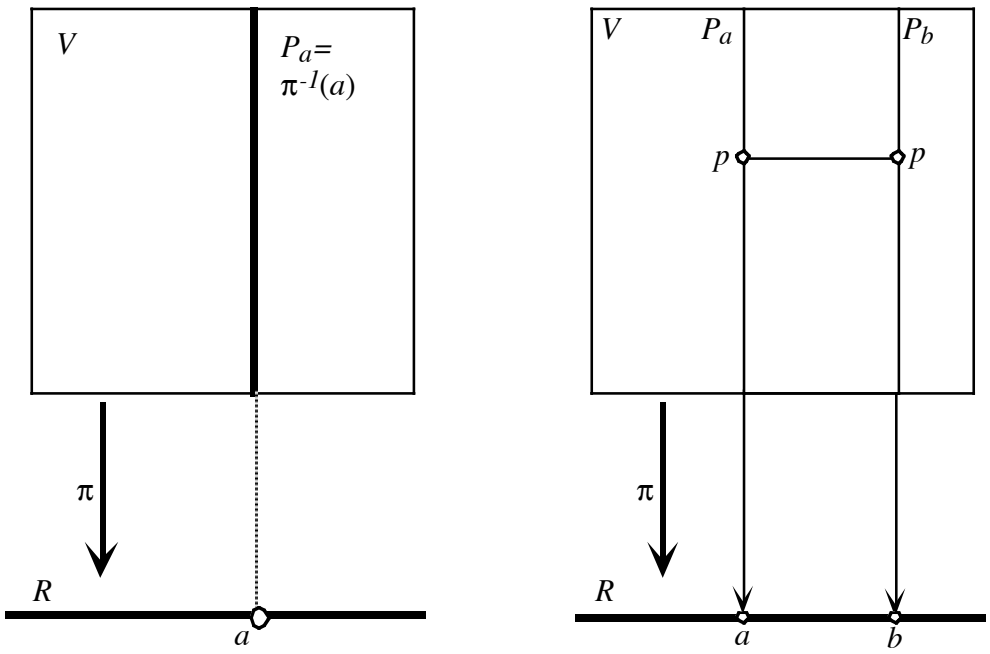

- Cortico-cortical connections are slow (≈ 0.2m/s) and weak. They essentially connect neurons of the same orientation in neighboring hypercolumns.
- This means that the system is able to know, for *b* near *a*, if the orientation *q* at *b* is the same as the orientation *p* at *a* (local parallelism).

- The retino-geniculo-cortical "vertical" connections give an *internal* meaning for the relations between (*a*, *p*) and (*a*, *q*) (*different* orientations *p* and *q* at the *same* point *a*) .
- While the "horizontal" cortico-cortical connections give an *internal* meaning for the relations between (*a*, *p*) and (*b*, *p*) (*same* orientation *p* at *different* points *a* and *b*).

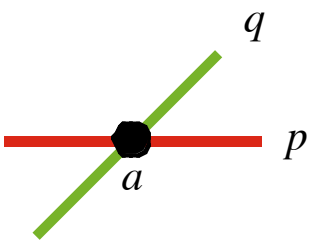

Vertical connections :
$a=b$
$p \neq q$

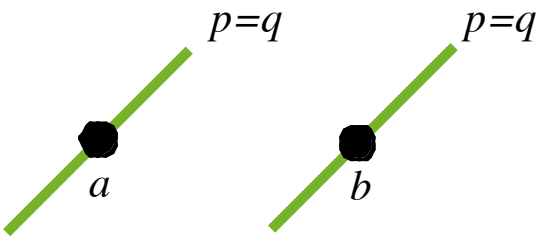

Horizontal connections :
$a \neq b$
$p=q$

- The next slide (William Bosking) shows how biocytin injected locally in a zone of specific orientation (green-blue) diffuses via horizontal cortico-cortical connections. The key fact is that :
  - short range (inside a single hypercolumn) diffusion is isotropic, but
  - long range diffusion (between different hypercolumns) is on the contrary highly anisotropic and restricted to zones of the same orientation (the same color) as the initial one.

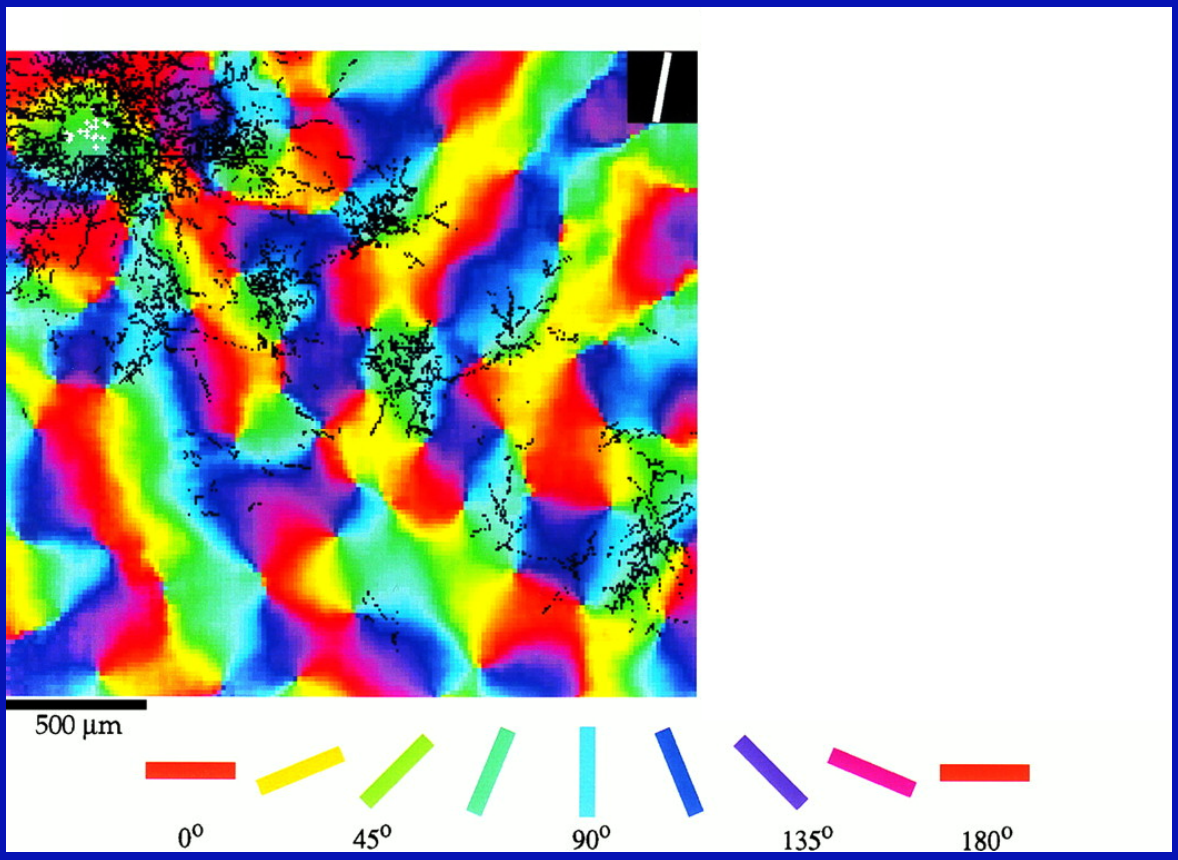

- Moreover, cortico-cortical connections connect neurons coding pairs (*a*, *p*) and (*b*, *p*) *such that p is the orientation of the axis ab* (William Bosking).
- « The system of long-range horizontal connections can be summarized as preferentially linking neurons with co-oriented, co-axially aligned receptive fields ».

Alignement :
$a \neq b$
$p = q = ab$

- These results mean essentially that the contact structure of the fibration $\pi : R \times P \rightarrow R$ is neurally implemented.

The contact structure of V1

- First model.
- We work in the fibration $\pi : V = R \times P \to R$ with base space R and fiber P = set of orientations p.
- A local coordinate system for V is given by triples (x, y, p).

- Let C be a smooth curve in the base space R. We have seen that it can be lifted to a curve Γ in V : its 1-jet or Legendrian lift.
- If $y = y(x)$ is a local equation of C, the equation of Γ is

$$(x, y, p) = (x, y, y').$$

- The contact elements are connected by horizontal connections.

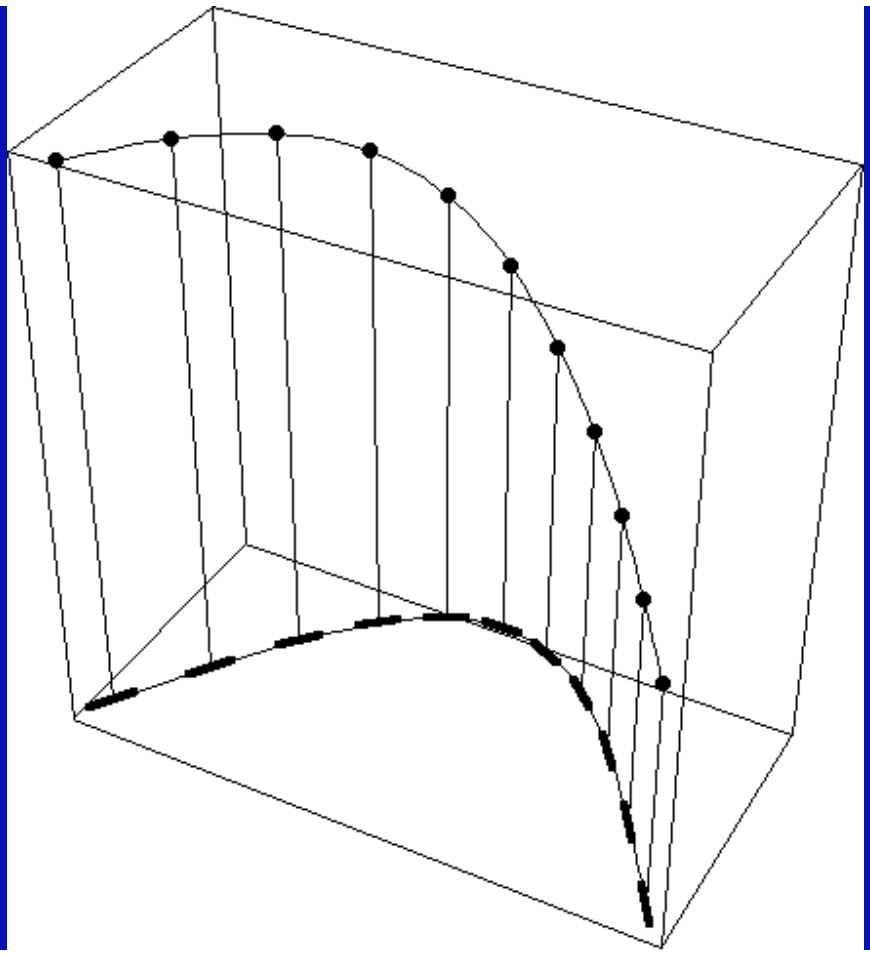

- Conversely, let $\Gamma = (x(s), y(s), p(s))$ be a curve in V with projection C in R.
- Γ is the lifting of C *iff*

$$p(s) = y'(s) / x'(s).$$

- Frobenius integrability condition .
- In the following slide we show curves in V which don't satisfy the integrability condition. The contact elements are not connected by horizontal connections.

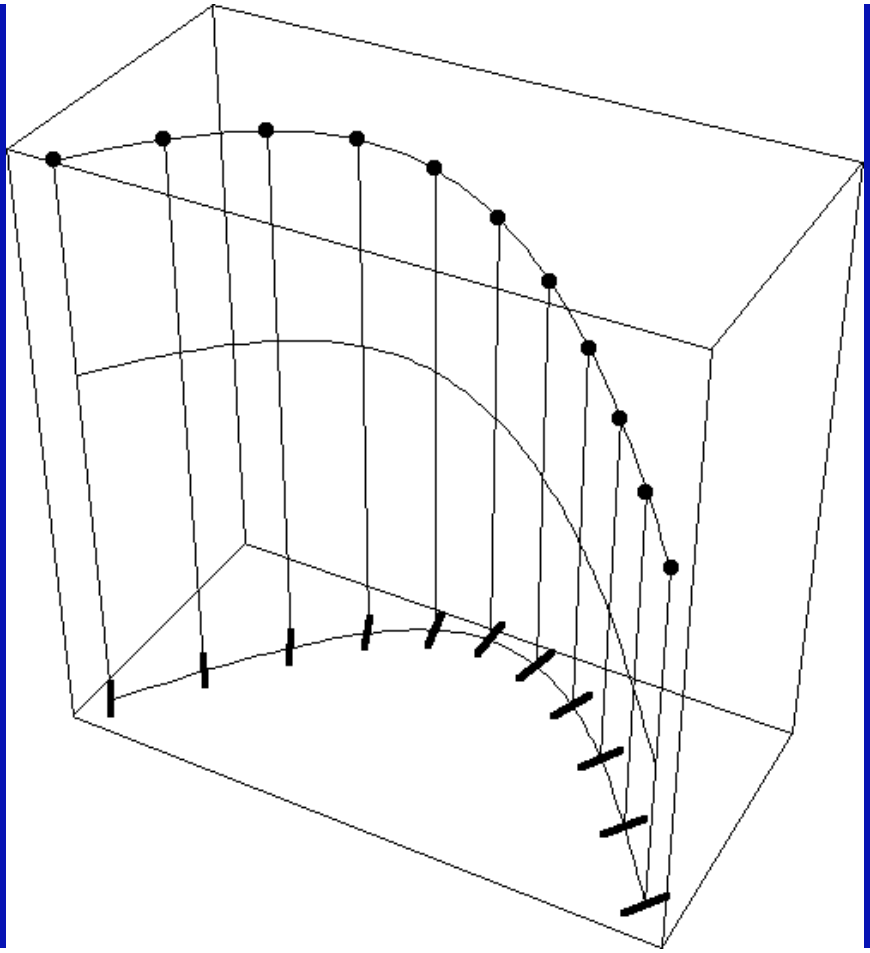

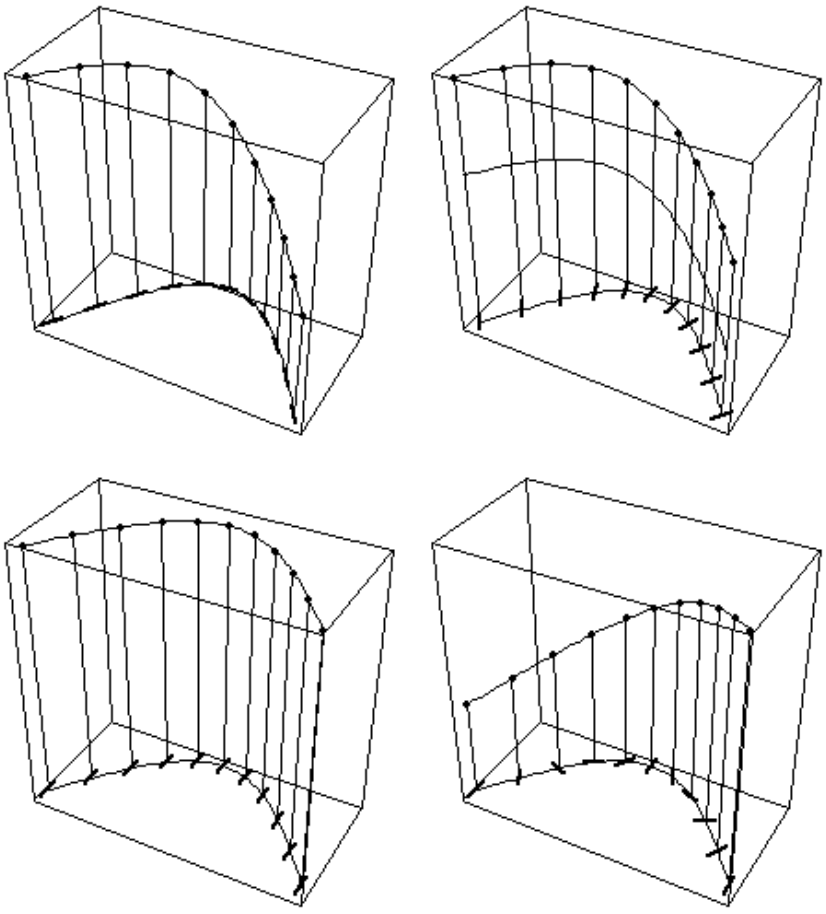

- Geometrically, the integrability condition means the following. We suppose x is the basic variable. Let

$$t = (x, y, p; 1, y', p')$$

be a *tangent vector* to V at the point

$$(a, p) = (x, y, p).$$

If $y' = p$ we have

$$t = (x, y, p; 1, p, p').$$

- This is equivalent to the fact that t is in the kernel of the 1-form

$$\omega = dy - pdx$$

$\omega = 0$ means simply $p = dy / dx$.

- But this kernel is in fact a plane called the contact plane of V at (a, p).

- The curves in V of the form j^1C are therefore the integral curves the field of planes $\mathcal{K}: v \to K_v$.
- This non integrable field is the contact structure of V, and ω is its contact form.
- If we add scale, we get the symplectification of the contact structure.

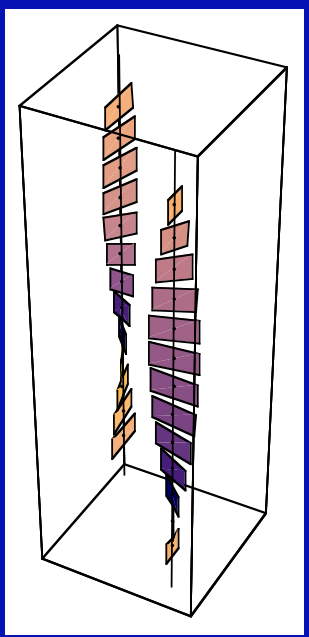

Application to the association field

- The Frobenius integrability condition is a geometrical formulation of the Gestalt law of “good continuation” (J-M. Morel, Y. Frégnac, S. Mallat) .
- Its empirical counterpart has been studied psychophysically by David Field, Anthony Hayes and Robert Hess and explained via the concept of association field.

- Let (a_i, p_i) be a set of segments embedded in a background of distractors. They generate a perceptively salient curve (pop-out) iff the p_i are tangent to « the » curve C interpolating between the a_i.
- Experiments show that some curvature is admissible. This means that the contact plane is implemented (the curvature of C is the vertical component of the lifting).
- But there is a limit to curvature. It has to be added to the model.

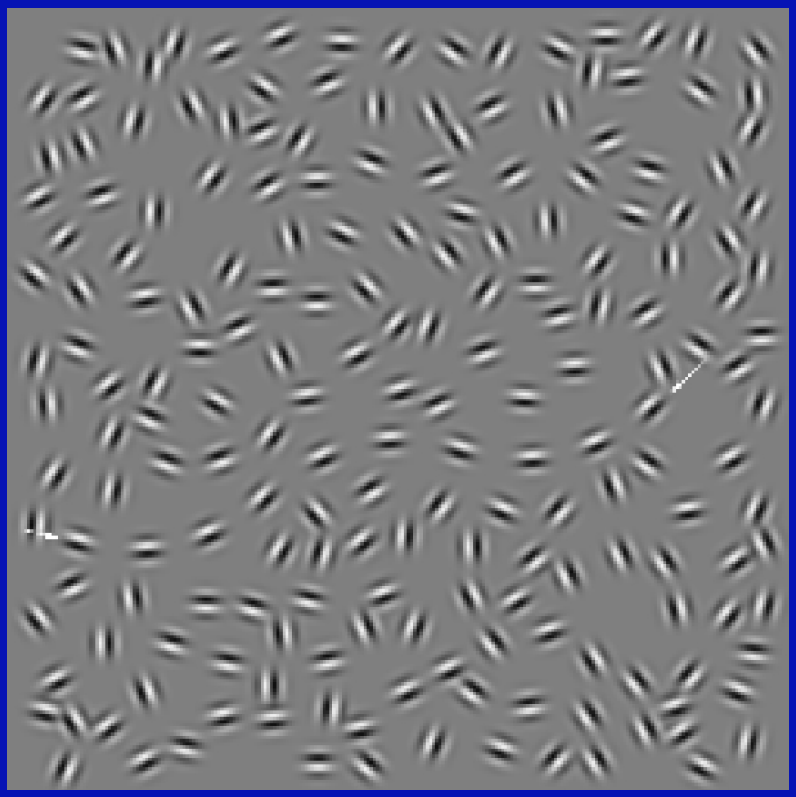

- « Elements are associated according to joint constraints of position and orientation. »
- « The orientation of the elements is locked to the orientation of the path; a smooth curve passing through the long axis can be drawn between any two successive elements. »

- This is a psychophysical formulation of the integrability condition.

- The pop-out of the global curve generated by the (a_i, p_i) is a typical translocal phenomenon resulting from a binding induced by the horizontal connections.
- Binding is a wave of activation along horizontal connections which synchronizes the cells (Singer, Gray, König).

- Second model. It is more natural to work with angles in the fibration $\pi : V = R \times P \to R$ with $P = \mathbf{S}^1$ and with the contact form

$$\omega = -\sin(\theta)dx + \cos(\theta)dy$$

- The contact planes are spanned by

$$X_1 = \cos(\theta)\,\partial_x + \sin(\theta)\,\partial_y$$

$$X_2 = \partial_\theta$$

with Lie bracket

$$[X_1, X_2] = \sin(\theta)\,\partial_x - \cos(\theta)\,\partial_y = -X_3$$

- *V* becomes a Lie group isomorphic to the Euclidean group *E*(2) which is the semi-direct product

$$E(2) = SO(2) \ltimes \mathbb{R}^2$$

$$\begin{pmatrix} x_1 \\ y_1 \\ \theta_1 \end{pmatrix} \cdot \begin{pmatrix} x_2 \\ y_2 \\ \theta_2 \end{pmatrix} = \begin{pmatrix} x_1 + x_2\cos(\theta_1) - y_2\sin(\theta_1) \\ y_1 + x_2\sin(\theta_1) + y_2\cos(\theta_1) \\ \theta_1 + \theta_2 \end{pmatrix}$$

- Inverse

$$(-x\cos(\theta) - y\sin(\theta), x\sin(\theta) - y\cos(\theta), -\theta)$$

- Left invariance

$$\{\partial_x, \partial_y, \partial_\theta\}_0$$

translates into

$$\{\cos(\theta)\,\partial_x + \sin(\theta)\,\partial_y = X_1, -\sin(\theta)\,\partial_x + \cos(\theta)\,\partial_y = X_3, \partial_\theta = X_2\}_q$$

- And

$$\omega_0 = dy$$

translates into the contact form ω.

Contact structure and Heisenberg group

- The group structure on V of the first model is isomorphic to the Heisenberg group :

$$(x, y, p).(x', y', p') = (x + x', y + y' + px', p + p')$$

- If $t = (\xi, \eta, \pi)$ are the tangent vectors of T_0V, the Lie algebra of V has the Lie bracket

$$[t, t'] = [(\xi, \eta, \pi), (\xi', \eta', \pi')] = (0, \xi'\pi - \xi\pi', 0)$$

- It is generated by

$$\left\{ t_1 = \frac{\partial}{\partial x} + p\frac{\partial}{\partial y} = (1, p, 0), t_2 = \frac{\partial}{\partial p} = (0, 0, 1) \right\}$$

(spanning the contact plane)

- We have

$$[t_1, t_2] = t_3 = -\frac{\partial}{\partial y} = (0, -1, 0)$$

(the other brackets = 0).

- This Lie algebra can be represented by nilpotent matrices $m(\xi, \eta, \pi)$

$$\begin{pmatrix} 0 & \pi & \eta \\ 0 & 0 & \xi \\ 0 & 0 & 0 \end{pmatrix}$$

and the elements (x, y, p) of the group V by matrices $M(x, y, p) = I + m(x, y, p)$

$$\begin{pmatrix} 1 & p & y \\ 0 & 1 & x \\ 0 & 0 & 1 \end{pmatrix}$$

- But we can also exponentiate and represent the elements (x, y, p) of the group V by matrices

$$\exp(m(\xi, \eta, \pi)) =$$

$$I + m(x, y, p) + 1/2\ m(0, px, 0) =$$

$$M(x, p, y+1/2px)$$

- The group law on V becomes

$$(x, y, p).(x', y', p') =$$

$$(x + x', y + y' + 1/2(px' - xp'), p + p')$$

- This is the Heisenberg group.
- The center Z of the two groups is the y axis.
- So harmonic analysis on V is strongly related to that on the Heisenberg group, which is very well known in quantum mechanics.
- We can therefore transfer many results (Gerald Folland : *Harmonic Analysis in Phase Space*, Vladimir Kisil, etc.).

- In particular, the Stone – Von Neumann theorem implies that every irreducible unitary representation in an Hilbert space which is not trivial on the center Z is equivalent to a Schrödinger representation :

$$\rho_h(x,y,p)f(t) = e^{2i\pi hy}e^{2i\pi(hpD+xT)}f(t)$$

with $f(t) \in L^2(\mathbf{R})$, $D = \partial/\partial t$ and $T =$ multiplication by t (h is the Planck constant).

Coherent states and harmonic analysis on Lie groups

- The natural context of signal analysis in natural vision is therefore that of coherent states. We have
  - An Hilbert space $\mathcal{H} = L^2(\mathbb{R}^2)$
  - A (locally compact) Lie group *G* acting on $\mathcal{H}$ via an irreducible unitary representation π.
  - A well localized « mother » wavelet $\varphi_0 \in \mathcal{H}$

- Coherent state = *G*-orbit $\{\varphi_g\}_{g \in G}$ of φ_0
- Harmonic analysis of a signal *f* :

$$f(x) = \int_G T_f(g)\, \varphi_g(x)\, d\mu(g)$$

with

$$T_f(g) = \langle f, \varphi_g \rangle \in L^2(G)$$

- The Gabor transform corresponds to the analysis

$$G_f(a,\omega) = \int_{\mathbb{R}} f(x) e^{-i\omega(x-a)} g(x-a)^* \, dx \in L^2(\mathbb{R}^2)$$

with the synthesis

$$f(x) = \frac{1}{2\pi \|g\|^2} \int_{\mathbb{R}} G_f(a,\omega) \, e^{i\omega(x-a)} g(x-a) \, da d\omega.$$

- The coherent states are

$$g_{a,\omega}(x) = e^{i\omega(x-a)} g(x-a)$$

- For classical wavelets, the coherent states are

$$\varphi_{a,s}(x) = \frac{1}{\sqrt{s}} \varphi\left(\frac{x-a}{s}\right)$$

and must satisfy the admissibility condition

$$c_\varphi = \int_R |\widehat{\varphi}(\xi)|^2 \frac{d\xi}{\xi} < \infty$$

- The synthesis is given by Calderon identity with

$$T_f(a,s) = \langle f, \varphi_{a,s} \rangle$$

$$f(x) = \frac{1}{c_\varphi} \int_{\mathbb{R}_+^* \times \mathbb{R}} T_f(a,s) \, \varphi_{a,s}(x) \frac{ds}{s} \frac{da}{s}$$

- Coherent states enable to represent a signal $f \in \mathcal{H}$ by its transform

$$T_f(g) = \langle f, \varphi_g \rangle \in L^2(G)$$

- It is what is done by V1, the $\langle f, \varphi_g \rangle$ being the measure of f by the receptive profiles φ_g.

An application : Kanizsa illusory contours

- A typical example of the problems of neurogeometry is given by well known Gestalt phenomena such as Kanizsa illusory contours.
- The visual system (V1 with probably some feedback from V2) constructs very long range sharp virtual contours.

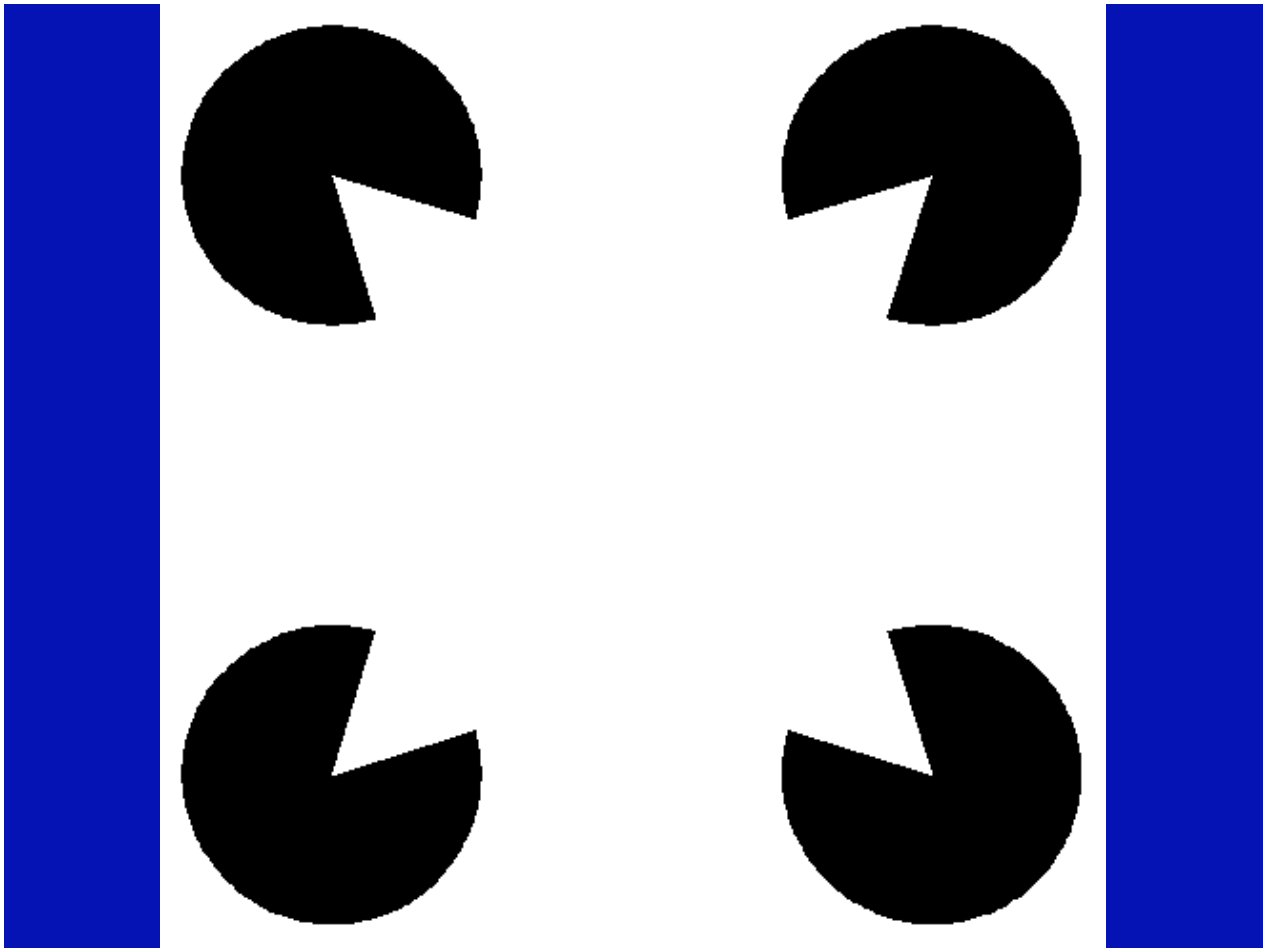

- In the neon effect, virtual boundaries are boundaries for the diffusion of color.

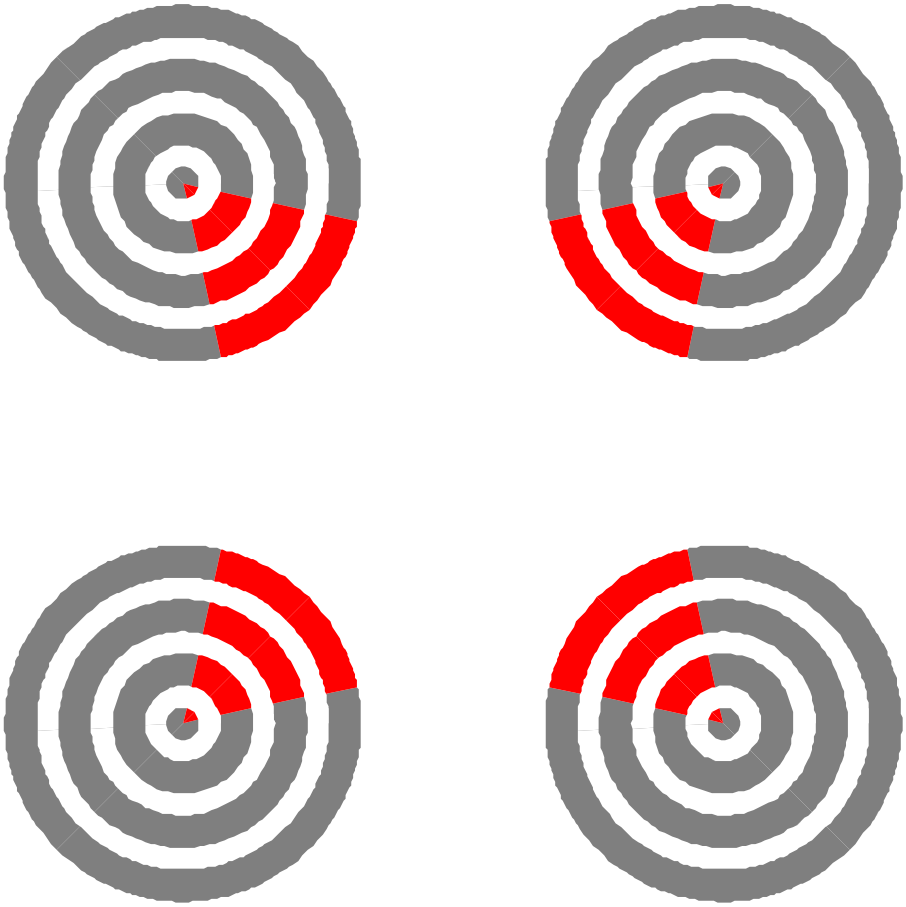

- Kanizsa subjective modal contours manifest a deep neurophysiological phenomenon.
- Here is a result of Catherine Tallon-Baudry in « Oscillatory gamma activity in humans and its role in object representation » (*Trends in Cognitive Science*, 3, 4, 1999).
- Subjects are presented with coherent stimuli (illusory and real triangles) « leading to a coherent percept through a bottom-up feature binding process ».

- « Time–frequency power of the EEG at electrode Cz (overall average of 8 subjects), in response to the illusory triangle (top) and to the no-triangle stimulus (bottom ».
- « Two successive bursts of oscillatory activities were observed.
  - A first burst at about 100 ms and 40 Hz. It showed no difference between stimulus types.
  - A second burst around 280 ms and 30-60 Hz. It is most prominent in response to coherent stimuli. »

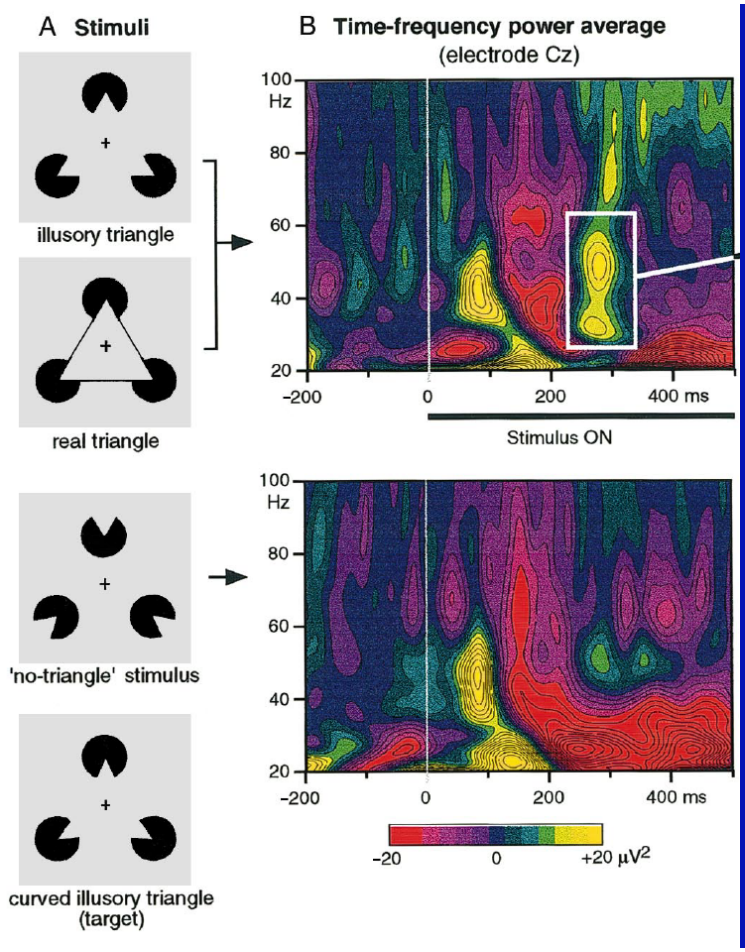

Sub-Riemannian geometry and Kanizsa contours

- The contact structure $\mathcal{K}$ defines sub-Riemannian metrics on V.
- One considers metrics $g_{\mathcal{K}}$ defined only on the planes of $\mathcal{K}$ and only curves Γ in V which are integral curves of $\mathcal{K}$.
- We apply sub-Riemannian geometry to the analysis of curved Kanizsa illusory contours (the sides of the internal angles of the pacmen are not aligned).

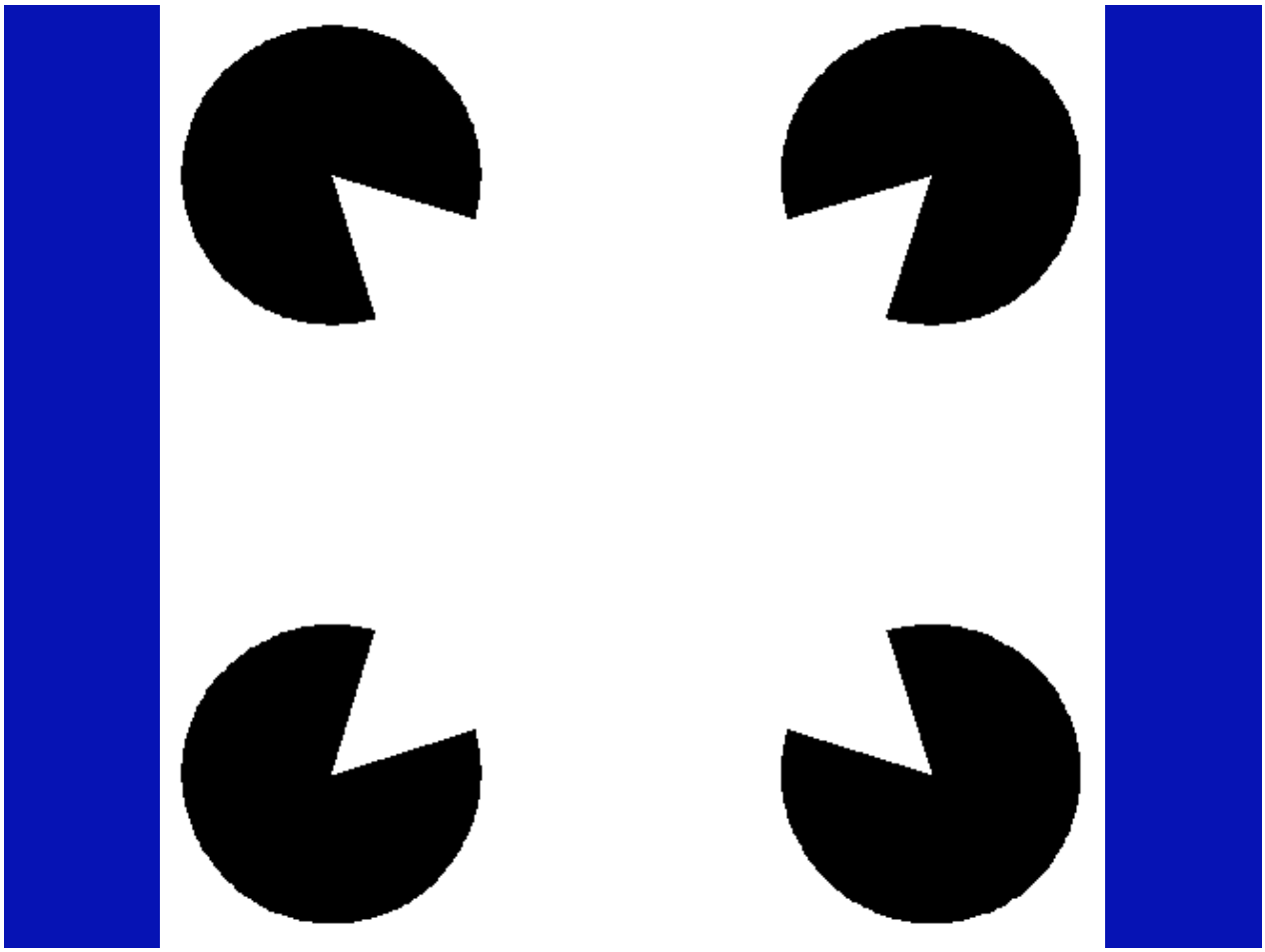

- Shimon Ullman (1976) introduced the idea of *variational models*.

  « A network with the local property of trying to keep the contours “ as straight as possible ” can produce curves possessing the global property of minimizing total curvature. »

- Horn (1983) introduced the curves of least energy.
- David Mumford (1992) used elastica: « Elastica and Computer Vision », *Algebraic Geometry and Applications*, Springer.

  Elastica are curves minimizing the integral of the square of the curvature κ, i.e. the energy

$$E = \int (\alpha\kappa+\beta)^2 ds$$

- For natural vision, we have developped a slightly different variational model using the sub-Riemannian geometry associated to the contact structure.

- Two pacmen of respective centers *a* and *b* with a specific aperture angle define two contact elements (*a*, *p*) and (*b*, *q*) of *V*.
- A *K*-contour interpolating between (*a, p*) and (*b, q*) is
  - 1. a curve *C* from *a* to *b* in *R* with tangent *p* at *a* and tangent *q* at *b*;
  - 2. a curve minimizing an "energy" (variational problem).

- We lift the problem in V. We must find in V a curve Γ interpolating between (a, p) and (b, q) in V, wich is at the same time:
  - 1. "as straight as possible", that is "geodesic" ;
  - 2. an integral curve of the contact structure.
- In general Γ will not be a straight line because it will have to satisfy the Frobenius integrability condition.
- It is "geodesic" only in the class of integral curves of the contact structure.

- We have to solve constrained Euler-Lagrange equations for satisfying the condition of minimal length.
- This is a typical problem of sub-Riemannian geometry.

- Let v and v' be 2 points of V. We define their distance $d_{\mathcal{K}}(v,v')$ as the inf of the $g_{\mathcal{K}}$-length of the integral curves joining v to v'.
- It can be shown – Chow theorem – that such curves always exist due to the fact that the Lie brackets of $\mathcal{K}$ generate the whole tangent bundle TV.

$$d_{\mathcal{K}}(v,v') = \inf_{\substack{\Gamma \text{ integral curve of } \mathcal{K}, \\ \Gamma(0)=v, \Gamma(1)=v'}} \int_I \|\Gamma'(s)\|\, ds$$

- A geodesic between v and v' for the sub-Riemannian metric is then an integral curve of $\mathcal{K}$ which realizes everywhere locally the distance $d_{\mathcal{K}}$.

SR geometry and contact structures

- One of the specificity of sub-Riemannian geometry is that there can be many geodesics (even an infinity) sharing the same initial conditions.
- There exists a quite good theory for sub-Riemannian geometry of contact manifold, especially in dimension 3.

- In particular, for the 1-form

$$\omega = -\sin(\theta)dx + \cos(\theta)dy$$

and the metric making $\{X_1, X_2, X_3\}$

$$X_1 = \cos(\theta)\,\partial_x + \sin(\theta)\,\partial_y$$
$$X_2 = \partial_\theta$$
$$[X_1, X_2] = \sin(\theta)\,\partial_x - \cos(\theta)\,\partial_y = -X_3$$

an orthonormal basis, the problem has been recently solved by Andrei Agrachev and Igor Moiseev (SISSA, Trieste).

- They work in the fibration $V = R \times \mathbf{S}^1$ where the Legendrian lifts are solutions of the control system :

$$\begin{cases} \dot{x} = u_1 \cos(\theta) \\ \dot{y} = u_1 \sin(\theta) \\ \dot{\theta} = u_2 \end{cases}$$

- Sub-Riemannian geodesics are the projections on R of the integral curves of an Hamiltonian system on V.

$$H(p,q) = \frac{1}{2}\left(u_1^2 + u_2^2\right) = \frac{1}{2}\left(\left(p_x \cos(\theta) + p_y \sin(\theta)\right)^2 + p_\theta^2\right)$$

- Hamilton equations in the cotangent bundle *T*V* are :

$$\begin{cases} \dot{x} = \frac{\partial H}{\partial p_x} = p_x \cos^2(\theta) + p_y \cos(\theta) \sin(\theta) \\ \dot{y} = \frac{\partial H}{\partial p_y} = p_y \sin^2(\theta) + p_x \cos(\theta) \sin(\theta) \\ \dot{\theta} = \frac{\partial H}{\partial p_\theta} = p_\theta \end{cases}$$

$$\begin{cases} \dot{p}_x = -\frac{\partial H}{\partial x} = 0 \\ \dot{p}_y = -\frac{\partial H}{\partial y} = 0 \\ \dot{p}_\theta = -\frac{\partial H}{\partial \theta} = (p_x \cos(\theta) + p_y \sin(\theta))(-p_x \sin(\theta) + p_y \cos(\theta)) \end{cases}$$

- p_x and p_y are constant. Write

  $(p_x, p_y) = \rho \exp(i\beta)$. Then

$$\dot{p}_\theta = \frac{1}{2}\rho^2 \sin(2(\theta - \beta))$$

  and *H* yields the first integral :

$$\rho^2 \cos^2(\theta - \beta) + p_\theta^2 = c$$

  and the ODE for θ (c , ρ and β are cst.) :

$$\dot{\theta}^2 = p_\theta^2 = c - \rho^2 \cos^2(\theta - \beta)$$

- For $\beta = 0$ (rotation invariance), the equations become :

$$\begin{cases} \dot{x} = \rho \cos^2(\theta) \\ \dot{y} = \rho \cos(\theta) \sin(\theta) = \frac{1}{2}\rho \sin(2\theta) \\ \dot{\theta} = p_\theta \\ \dot{p}_\theta = \frac{1}{2}\rho^2 \sin(2\theta) \end{cases}$$

- For $\rho = 1$, $\varphi = \pi/2 - \theta$, and $\mu = 2\varphi = \pi - 2\theta$, we get a pendulum equation

$$\ddot{\mu} = -\sin(\mu)$$

with first integral

$$\dot{\varphi}^2 + \sin^2(\varphi) = c$$

- We show the trajectories in the $(\varphi, \dot{\varphi})$ plane :

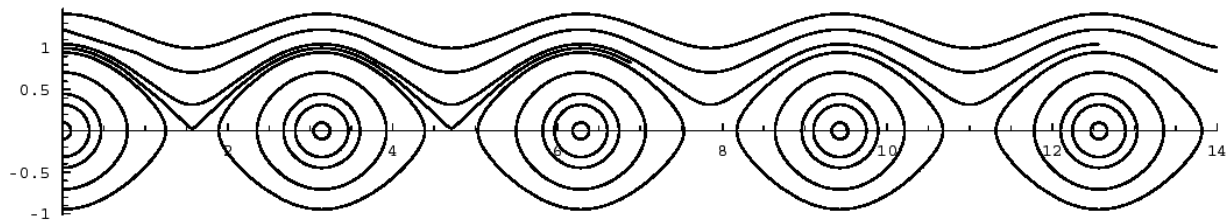

- As

$$dt = \pm \frac{1}{\sqrt{c}} \frac{d\varphi}{\sqrt{1 - \frac{1}{c}\sin^2(\varphi)}}$$

the system can be integrated via elliptic functions.

- For the modulus $1/c < 1$:

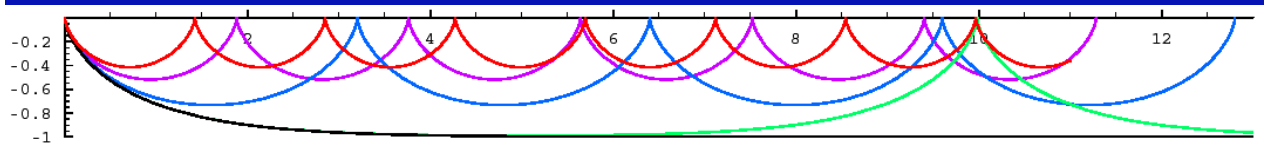

FIGURE 30. Différentes géodésiques sous-riemanniennes pour c décroissant de 2 à 1 : $c = 2$ (rouge), $c = 1.5$ (violet), $c = 1.1$ (bleu), $c = 1.001$ (vert), $c = 1$ (noir). (D'après les calculs d'A. Agrachev).

- For the modulus $1/c > 1$:

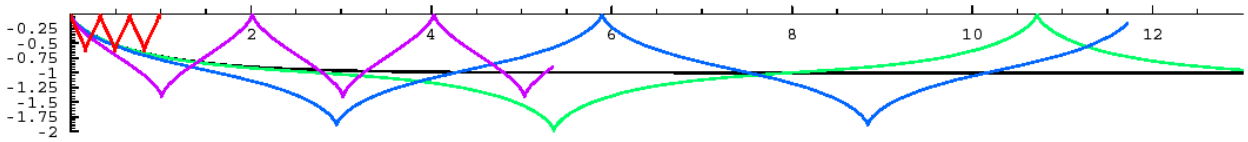

FIGURE 31. Différentes géodésiques sous-riemanniennes pour c croissant de 0.1 à 1 : $c = 0.1$ (rouge), $c = 0.5$ (violet), $c = 0.9$ (bleu), $c = 0.99$ (vert), $c = 1$ (noir). (D'après les calculs d'A. Agrachev).

The sub-Riemannian sphere of the Heisenberg group

- The sub-Riemannian sphere and the wave front are more complex than those of the Heisenberg group.
- For the Heisenberg group, the formulas for geodesics are much simpler (R. Beals, B. Gaveau, P. Greiner, A.M. Vershik, V.Y. Gershkovich) and the wave front can be explicitely computed.

- Let $v = (x_1, x_2, t)$ coordinates for H. The group law is:

$$(x_1, x_2, t)\cdot(x_1', x_2', t') = (x_1 + x_1', x_2 + x_2', t + t' + 2\left(x_2 x_1' - x_1 x_2'\right))$$

- It is isomorphic to the jet space (x, y, p) through the change of variables :

$$x = x_1,\ y = t + 2x_1x_2,\ p = 4x_2.$$

- The tangent vectors X_1 and X_2 generating the contact planes K_v are :

$$X_1 = (1, 0, 2x_2),\ X_2 = (0, 1, -2x_1).$$

- If $T = (0,0,1)$, $[X_1, X_2] = -4T$, $[X_1, T] = 0$, $[X_2, T] = 0$.

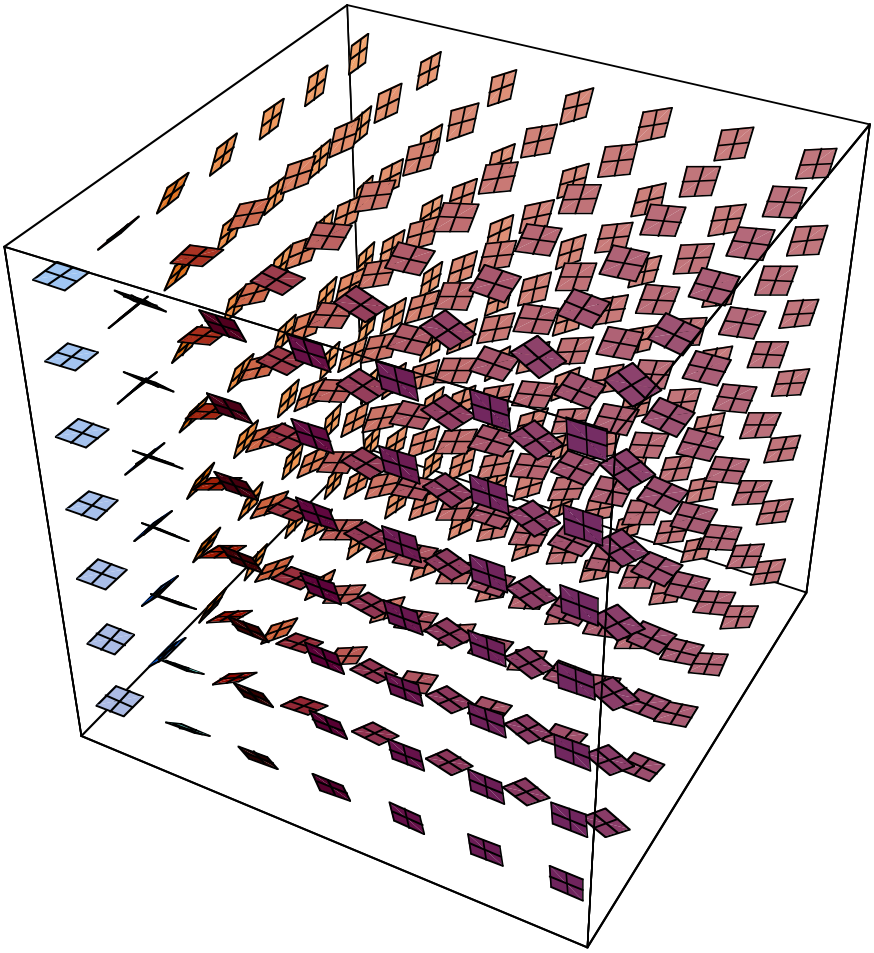

- Many geodesics can have the same initial conditions

$$v(0) = (x_1(0), x_2(0), t(0))$$

$$\dot{v}(0) = (\dot{x}_1(0), \dot{x}_2(0), \dot{t}(0)) .$$

- In the Hamiltonian formalism, initial conditions are no longer defined by tangent vectors but by cotangent vectors

$$\varpi(0) = (\xi_1(0), \xi_2(0), \theta(0))$$

- Geodesics are projections on $\mathbf{R}^3$ of Hamiltonian trajectories of an Hamiltonian H defined on the cotangent bundle $T^*\mathbf{R}^3$.
- They define an exponential map which can be expressed in the following way. Let $v \in \mathbf{R}^3$ and $\mathcal{C}_v$ the submanifold of $T_v{}^*\mathbf{R}^3$ of energy $H = 1/2$.

- $T_v{}^*\mathbf{R}^3$ is isomorphic to $\mathbf{R} \times \mathcal{C}_v$ and the exponential is the map $\mathcal{E}_v : \mathbf{R} \times \mathcal{C}_v \to \mathbf{R}^3$ which associates to (s, ϖ) the projection of the end at time = 1 of the H-trajectory starting at (s, ϖ) .

- The problem is that $\mathscr{E}_v$ has singularities.
- Sphere $S(v, r) = \{ w : d(v, w) = r \}$.
- Wave front $W(v, r) = \{ w : \exists$ a geodesic $\gamma : v \to w$ of length $r \}$.
- Cut locus of $v = \{ w : w$ end point of a geodesic $\gamma : v \to w$ which is no longer globally minimizing $\}$.
- Conjugate locus of v = caustic = Σ_v = { singular locus of $\mathscr{E}_v$ }.

- The geodesics are the projections of the trajectories associated to the Hamiltonian

$$H(x_1, x_2, t, \xi_1, \xi_2, \theta) = \frac{1}{2}\left[(\xi_1 + 2x_2\theta)^2 + (\xi_2 - 2x_1\theta)^2\right]$$

(as H is independent of t, θ is constant) and their equations from (0, 0, 0) to $(x_1 = x_1(\tau), x_2 = x_2(\tau), t = t(\tau))$ are

$$\begin{cases} x_1(s) = \frac{\sin[2s\theta]}{\sin[2\tau\theta]}\left(\cos[2(s-\tau)\theta]\ x_1 + \sin[2(s-\tau)\theta]\ x_2\right) \\ x_2(s) = \frac{\sin[2s\theta]}{\sin[2\tau\theta]}\left(\cos[2(s-\tau)\theta]\ x_2 - \sin[2(s-\tau)\theta]\ x_1\right) \\ t(s) = \frac{4s\theta - \sin[4s\theta]}{2(\sin[2\tau\theta])^2}\left((x_1)^2 + (x_2)^2\right) \end{cases}$$

- We have with $t = \mu(2\tau\theta)\,\|\mathbf{x}\|^2$

$$\mu(\varphi) = \frac{\varphi}{\sin^2(\varphi)} - \frac{1}{2}\frac{\sin(2\varphi)}{\sin^2(\varphi)} = \frac{\varphi}{\sin^2(\varphi)} - \cot(\varphi)$$

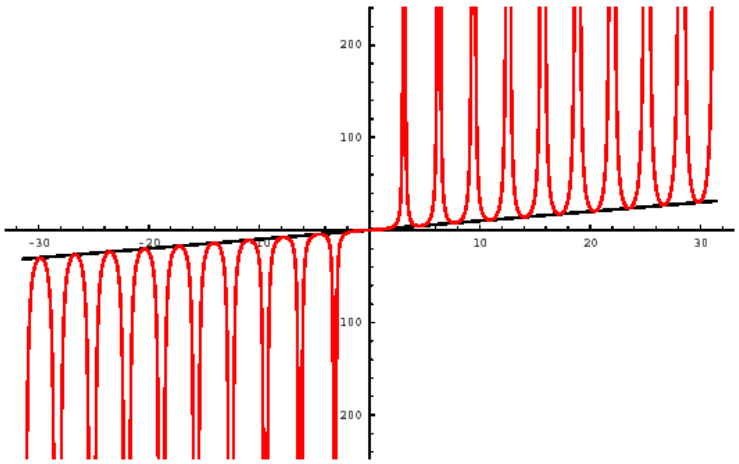

FIGURE 32. La fonction $\mu(\varphi)$ intervenant dans la construction des géodésiques sous-riemanniennes du groupe de Heisenberg.

To get geodesics with the same end point
$(x_1 = x_1(\tau), x_2 = x_2(\tau), t = t(\tau))$
we have to solve $t = \mu(2\tau\theta) \|\mathbf{x}\|^2$ in $\tau\theta$.

For instance for $\mu(\varphi) = 20$ (and $\theta = 1$) we get 11 solutions: $\tau_1 = 1.36$, $\tau_2 = 1.77$, $\tau_3 = 2.84$, $\tau_4 = 3.44$, $\tau_5 = 4.34$, $\tau_6 = 5.09$, $\tau_7 = 5.83$, $\tau_8 = 6.75$, $\tau_9 = 7.32$, $\tau_{10} = 8.42$, $\tau_{11} = 8.80$. If we take for instance $x_1 = x_1(\tau) = 2$ and $x_2 = x_2(\tau) = 1$, we get $t = 100$ and 11 geodesics joining $(0, 0, 0)$ to $(2, 1, 100)$. In the following figure we show the two cases τ_1 and τ_{10}.

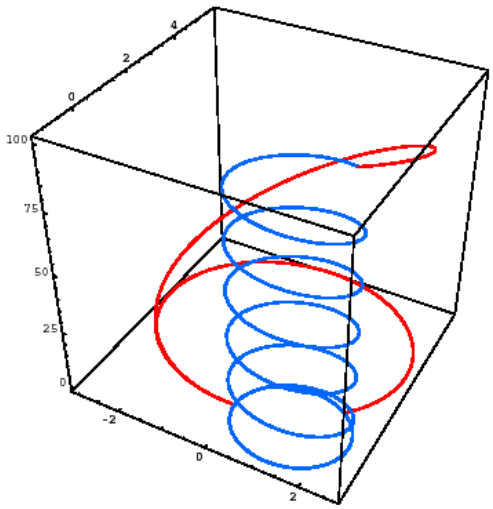

FIGURE 33. Deux géodésiques sous-riemanniennes du groupe de Heisenberg joignant $(0, 0, 0)$ à $(2, 1, 100)$. On représente les géodésiques dans V et leur projection sur le plan z.

- This structure of geodesics implies that the sub-Riemannian sphere *S* and the wave front *W* are rather strange.
- We show first their section in one quadrant, then their entire structure.

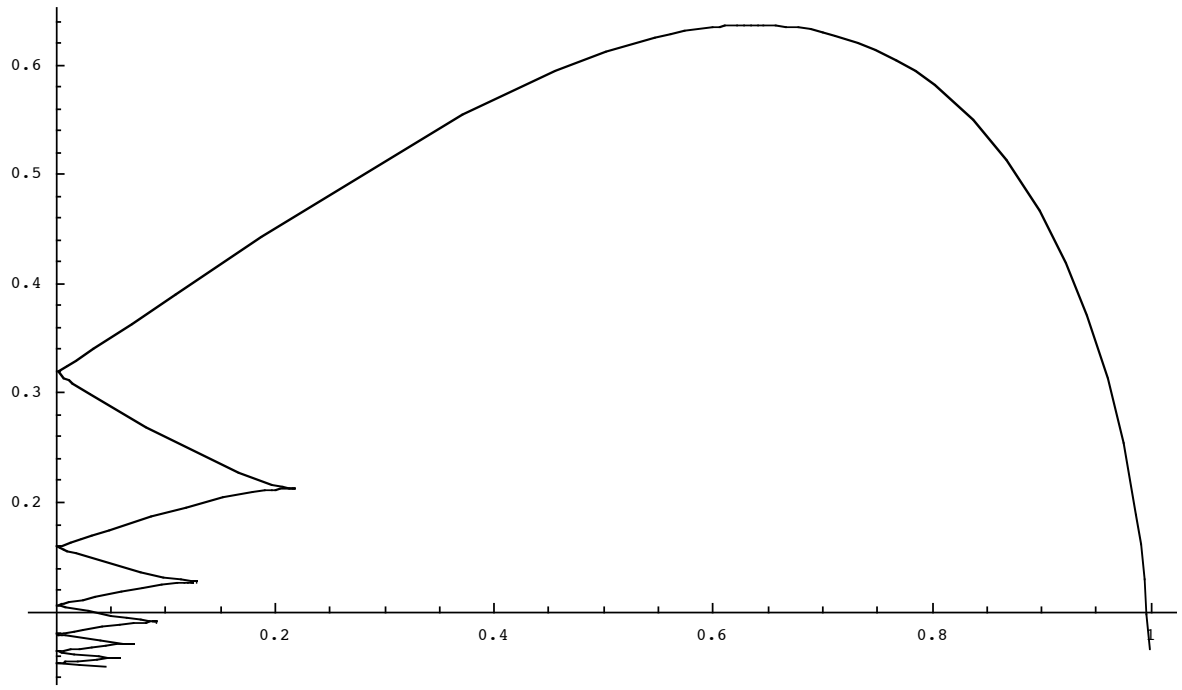

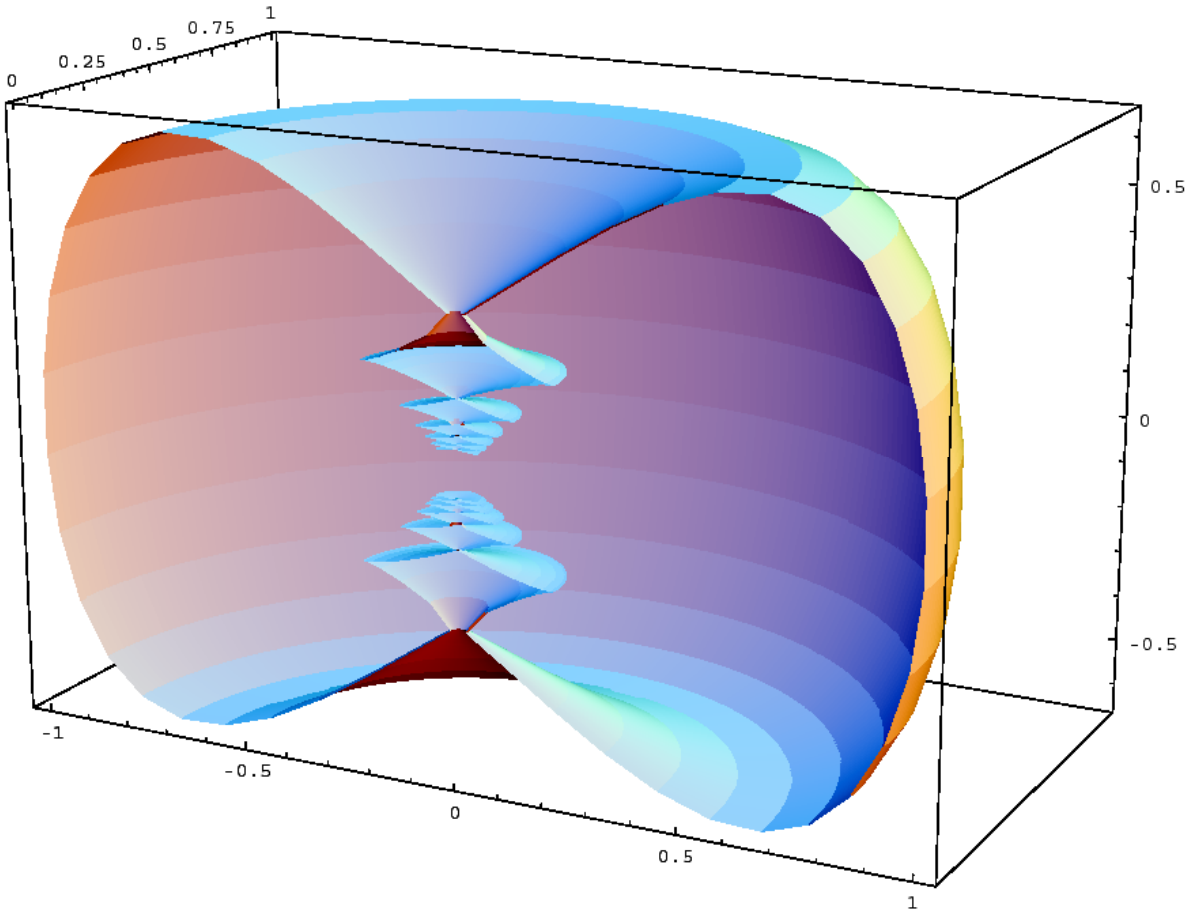
0
0.25
0.5
0.75
1
0.5
0
-0.5
-1
-0.5
0
0.5
1

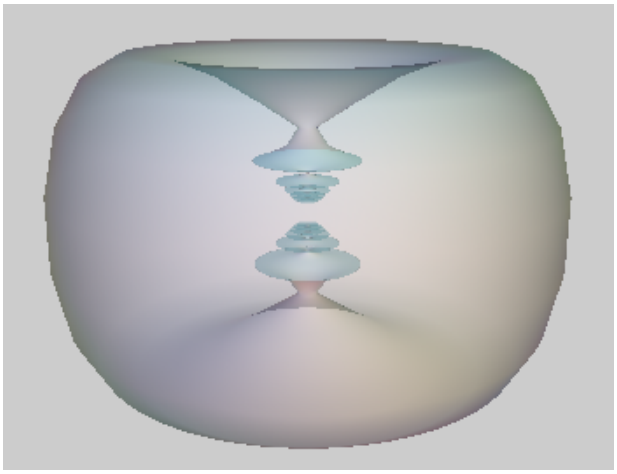

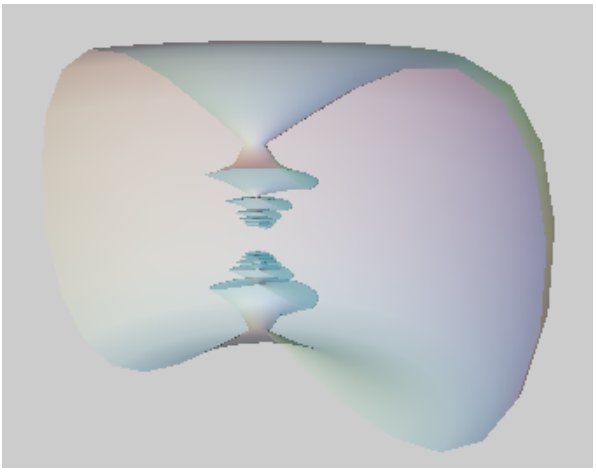

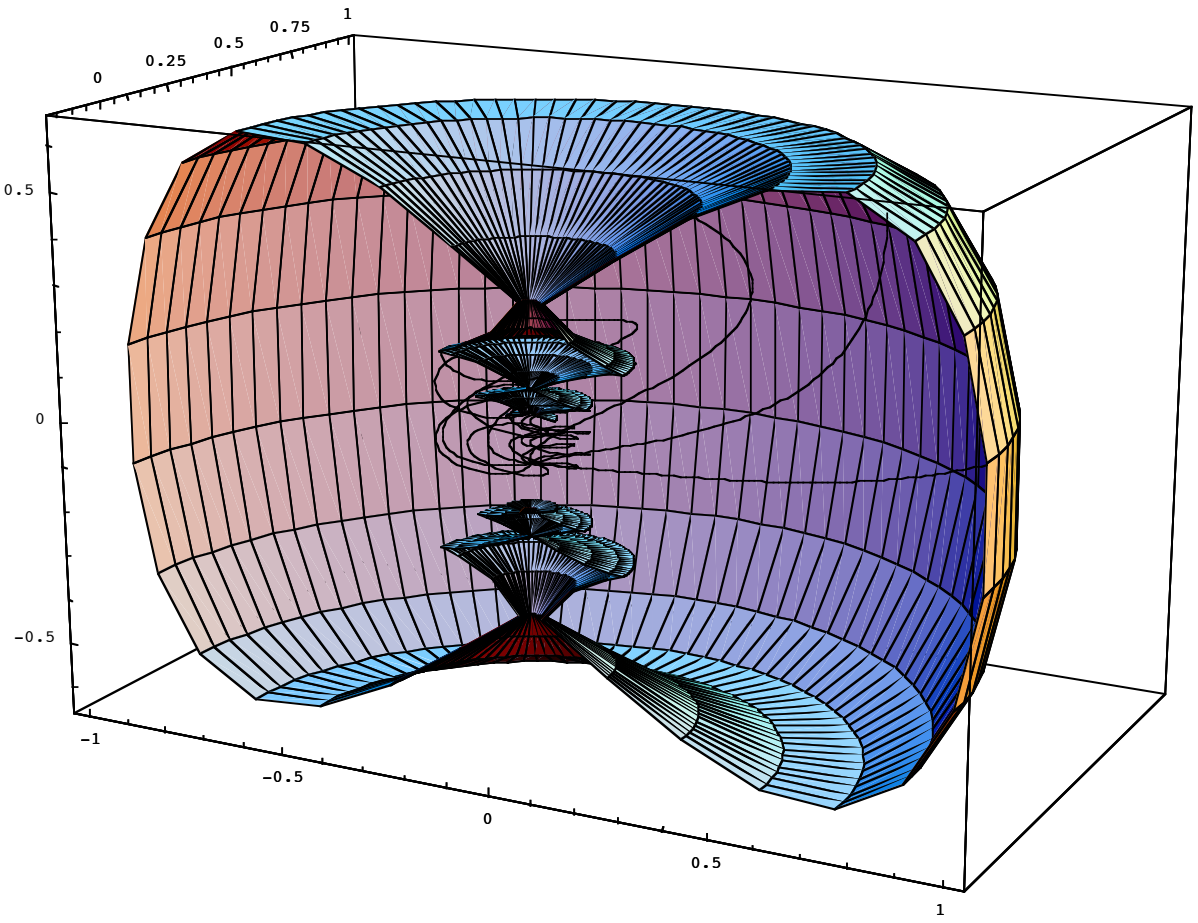

Sub-Riemannian caustics of contact structures

- A. Agrachev, Gauthier and Zakalyukin gave the normal forms of generic caustics of sub-Riemannian metric on contact structures in $\mathbf{R}^3$.

- There exists normal coordinates w.r.t. which the Hamiltonian H writes as a deformation of the Heisenberg case

$$H\left(x_1, x_2, t, \xi_1, \xi_2, \theta\right) = \frac{1}{2}\left[\left(\xi_1 + 2x_2\theta\right)^2 + \left(\xi_2 - 2x_1\theta\right)^2\right]$$

$$\begin{aligned} & H(x_1, x_2, t, \xi_1, \xi_2, \theta) \\ = \; & \frac{1}{2}\left[\left(\xi_1 + \beta\left(\xi_1 x_2 - \xi_2 x_1\right) + 2\gamma x_2\theta\right)^2 + \left(\xi_2 - \beta\left(\xi_1 x_2 - \xi_2 x_1\right) - 2\gamma x_1\theta\right)^2\right] \end{aligned}$$

where $\beta(x_1, x_2, t)$ and $\gamma(x_1, x_2, t)$ satisfy the boundary conditions $\beta(0, 0, t) = 0$, $\gamma(0, 0, t) = 1$, $\nabla_{x,y}\gamma(0, 0, t) = 0$.

- At 0, $\beta = \gamma = x_1 = x_2 = 0$ and $\gamma = 1$ and

$$H = \frac{1}{2}\left[\xi_1^2 + \xi_2^2\right]$$

so, $H = 1/2$ implies

$$\xi_1^2 + \xi_2^2 = 1, \xi_1 = \cos\left(\varphi\right), \xi_2 = \sin\left(\varphi\right)$$

- For Heisenberg, the caustic Σ is the t-axis.

- For the generic case it is, in the new variables $z = x_1 + i\,x_2$, $t = h^2$ and φ, at 4th order in h

$$\begin{cases} z(h,\varphi) = h^3\,(3e^{-i\varphi} + e^{3i\varphi}) + ih^4\left(2e^{-i(2\varphi+\varphi_0)} + e^{i(4\varphi+\varphi_0)}\right) \\ t(h) = h^2 \end{cases}$$

- φ_0 is a module for the diffeo-equivalence.
- In the following figure we see the 4th order approximation :

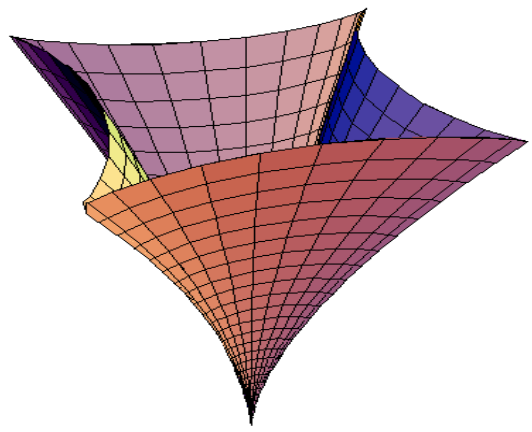

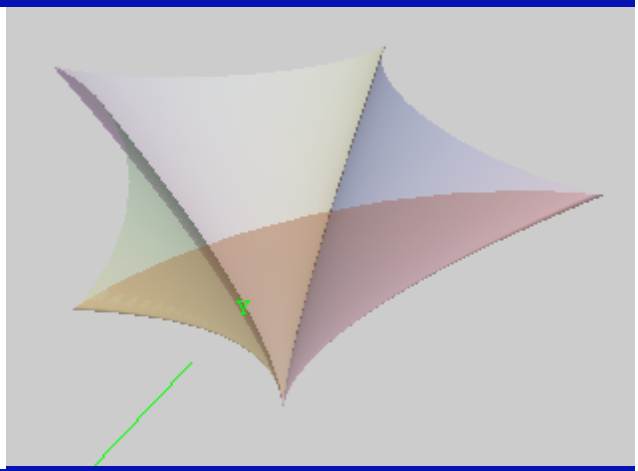

- The intersection of the cuspidal edges with the plane $t = h^2$ is given by $dz / d\varphi = 0$, i.e.

$$3ih^3\left(e^{3i\varphi} - e^{-i\varphi}\right) + 4h^4\left(e^{i(4\varphi+\varphi_0)} + e^{-i(2\varphi+\varphi_0)}\right) = 0$$

Harmonic analysis and SR geometry

- To understand correctly V1, we would have to correlate harmonic analysis and sub-Riemannian geometry, and in particular investigate the sub-elliptic Laplacian and the heat kernel.
- For the Heisenberg group, there are works of R. Beals, B. Gaveau, P. Greiner, D-Ch Chang.

- The problem is rather difficult since there are cut points in every neighborhood of each point and the classical analysis of heat equation fails at these singular points (B. Gaveau, IHP, 26-10-2005).

Scale-space and symplectic structures

- The contact structure of V is defined as the kernel field of the 1-form ω .
- But this field is only defined up to a scale factor $s = e^{\sigma}$, $\omega$and $s\omega$ having the same kernels.
- It is therefore natural to enlarge the 3 dimensional contact space $V = R^2 \times S^1$ to the 4 dimensional space $G = R^2 \times S^1 \times R$ with coordinates (x, y, θ, σ).

- G is the affine group of the plane and its invariant basis is now

$$\begin{cases} X_1 = e^{\sigma}\left(\cos(\theta)\partial_x + \sin(\theta)\partial_y\right) \\ X_2 = \partial_\theta \\ X_3 = e^{\sigma}\left(-\sin(\theta)\partial_x + \cos(\theta)\partial_y\right) \\ X_4 = \partial_\sigma \end{cases}$$

the invariant 1-form being now

$$\omega = e^{-\sigma}\left(-\sin(\theta)dx + \cos(\theta)dy\right)$$

- $d\omega$ is the symplectic 2-form on G

$$\begin{aligned} d\omega &= \left(e^{-\sigma}\cos(\theta)dx + e^{-\sigma}\sin(\theta)dy\right) \wedge d\theta + \\ &\quad \left(-e^{-\sigma}\sin(\theta)dx + e^{-\sigma}\cos(\theta)dy\right) \wedge d\sigma. \end{aligned}$$

deduced via left translations from the canonical symplectic 2-form at 0

$$dx \wedge d\theta + dy \wedge d\sigma$$

- Indeed, the translated of dx and dy are

$$\begin{cases} \upsilon = e^{-\sigma}\left(\cos(\theta)dx + \sin(\theta)dy\right) \\ \omega = e^{-\sigma}\left(-\sin(\theta)dx + \cos(\theta)dy\right) \end{cases}$$

and $d\omega = \upsilon \wedge d\theta + \omega \wedge d\sigma$

- $d\omega$ can be writen using an antisymmetric matrix B

$$d\omega(X, X') = \langle BX, X' \rangle$$

$$B = e^{-\sigma}\begin{pmatrix} 0 & 0 & -\cos(\theta) & \sin(\theta) \\ 0 & 0 & -\sin(\theta) & -\cos(\theta) \\ \cos(\theta) & \sin(\theta) & 0 & 0 \\ -\sin(\theta) & \cos(\theta) & 0 & 0 \end{pmatrix}$$

- $-B^2 = BB^*$ is positive definite $-B^2 = e^{-2\sigma}I$ and we can therefore consider

$$P = \sqrt{-B^2} = e^{-\sigma} I$$

- Then, $J = BP^{-1} = e^{\sigma} B$ satisfies $J^2 = -I$ and defines a complex structure

$$J = \begin{pmatrix} 0 & 0 & -\cos(\theta) & \sin(\theta) \\ 0 & 0 & -\sin(\theta) & -\cos(\theta) \\ \cos(\theta) & \sin(\theta) & 0 & 0 \\ -\sin(\theta) & \cos(\theta) & 0 & 0 \end{pmatrix}$$

- If we define a new scalar product by

$$(X|Y) = e^{-\sigma} \langle X|Y \rangle$$

then $d\omega(X,Y) = (JX|Y)$

- The planes $\{ X_1, X_2 \}$ and $\{ X_3, X_4 \}$ are complex planes, on which J acts as multiplication by i.

Harmonic analysis and symmetry axis

- We can apply this to the mother wavelet

$$\varphi_{(0,\sigma)}(x,y) = \frac{1}{e^{2\sigma}} e^{\frac{-(x^2+y^2)}{e^{2\sigma}}} e^{\frac{2iy}{e^{\sigma}}}$$

  and look at the associatated coherent state.

- Let *C* be a closed boundary in *R* and *a* = (*x*, *y*) a point inside *C*.

- Citti-Sarti : If we look at the maximal responses of the receptive profiles centered at *a*, and if *c* is the nearest point of *C* relative to *a*, then

$$d\left((x,y),c\right) = \frac{1}{\sqrt{2}} e^{\bar{\sigma}}$$

  and $\bar{\theta}$ is the direction of *C* at *c*.

- We can therefore lift *R* to a surface Σ in *G*

$$\Sigma = \left\{(x, y, \bar{\theta}(x,y), \bar{\sigma}(x,y))\right\}$$

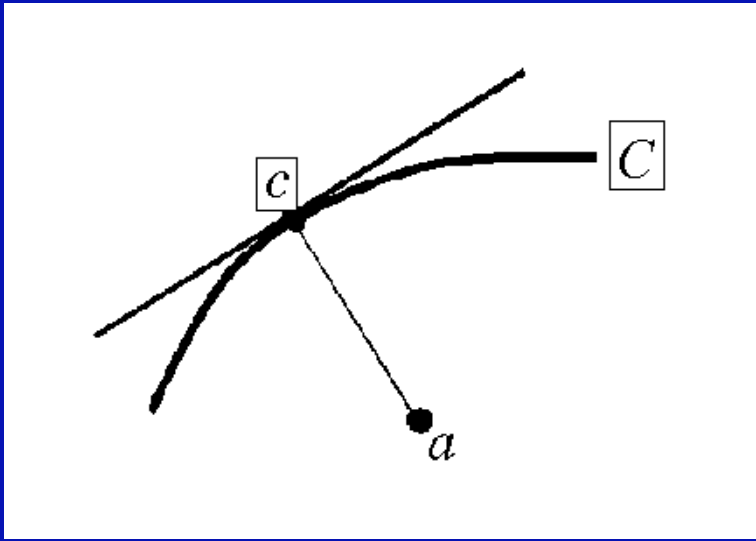

- The tangent vecteur over *a* = (*x*, *y*)

$$X_1 = e^{\bar{\sigma}} \left(\cos(\bar{\theta}) \partial_x + \sin(\bar{\theta}) \partial_y \right)$$

is parallel to *C* at *c* which is at minimal distance and therefore, as a derivative, satisfies

$$X_1 \left(\bar{\sigma} \right) = 0$$

- The tangent vector over $a = (x, y)$

$$X_3 = e^{\bar{\sigma}} \left(-\sin(\bar{\theta})\partial_x + \cos(\bar{\theta})\partial_y \right)$$

is orthogonal to C at c and $\bar{\theta}$ is constant along this direction. Therefore

$$X_3 \left(\bar{\theta} \right) = 0$$

- Now, the tangent plane to Σ: $T_{x,y,\bar{\theta},\bar{\sigma}} \Sigma$ is generated by the 2 vectors

$$\begin{cases} X_1 + X_1 \left(\bar{\theta} \right) X_2 + X_1 \left(\bar{\sigma} \right) X_4 \\ X_3 + X_3 \left(\bar{\theta} \right) X_2 + X_3 \left(\bar{\sigma} \right) X_4 \end{cases}$$

- But, since

$$X_1 \left(\bar{\sigma} \right) = X_3 \left(\bar{\theta} \right) = 0$$

it is in fact generated by

$$\begin{cases} X_1 + X_1 \left(\bar{\theta} \right) X_2 \\ X_3 + X_3 \left(\bar{\sigma} \right) X_4 \end{cases}$$

- As $d\omega = \upsilon \wedge d\theta + \omega \wedge d\sigma = \omega_1 \wedge \omega_2 + \omega_3 \wedge \omega_4$

we see that $d\omega$ vanishes on $T\Sigma$: Σ is a *Lagrangian* submanifold of G.

- The transform of a closed contour *C* by this coherent state realizes the propagation of *C* via the eikonal equation of geometrical optics (Huyghens or « grassfire » model).
- The singular locus of this propagation is like the « symmetry axis » or « medial axis » whose role in vision has been strongly emphasized by many authors after Harry Blum : René Thom, David Marr, David Mumford, Steve Zucker, James Damon, Benjamin Kimia, etc.

- MA of a rectangle

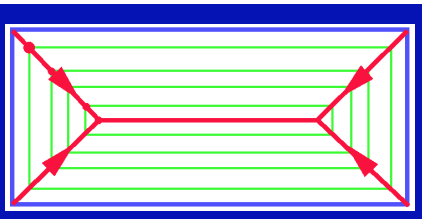

- MA of an ellipse computed by A. Sarti using the coherent state

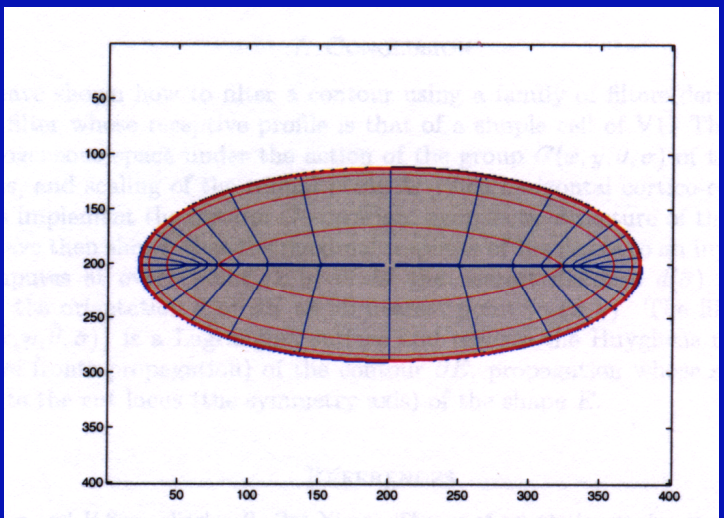

FIGURE 11. Level curves of $\bar{\theta}(x, y)$ (blue) and $\bar{\sigma}(x, y)$ (red).

Minimal surfaces in V1

- It seems that illusory contours are in fact boundaries of illusory minimal surfaces in V1.
- The theory of surfaces *S* in a contact manifold endowed with a sub-Riemannian geometry is rather difficult.
- There are in general “characteristic” points where S is tangent to the contact plane and where the normal vector relative to $\mathcal{K}$ is not defined.
- See Scott Pauls : « Minimal surfaces in the Heisenberg group ».

Application to spontaneous geometric visual patterns

- The geometry of the functional architecture of V1 is a rich underlying structure for the physics of neural activity and the dynamics of propagating waves.
- A beautiful application of this concerns entoptic vision (Tyler 1978).
- It can be summarized by the following comparison :

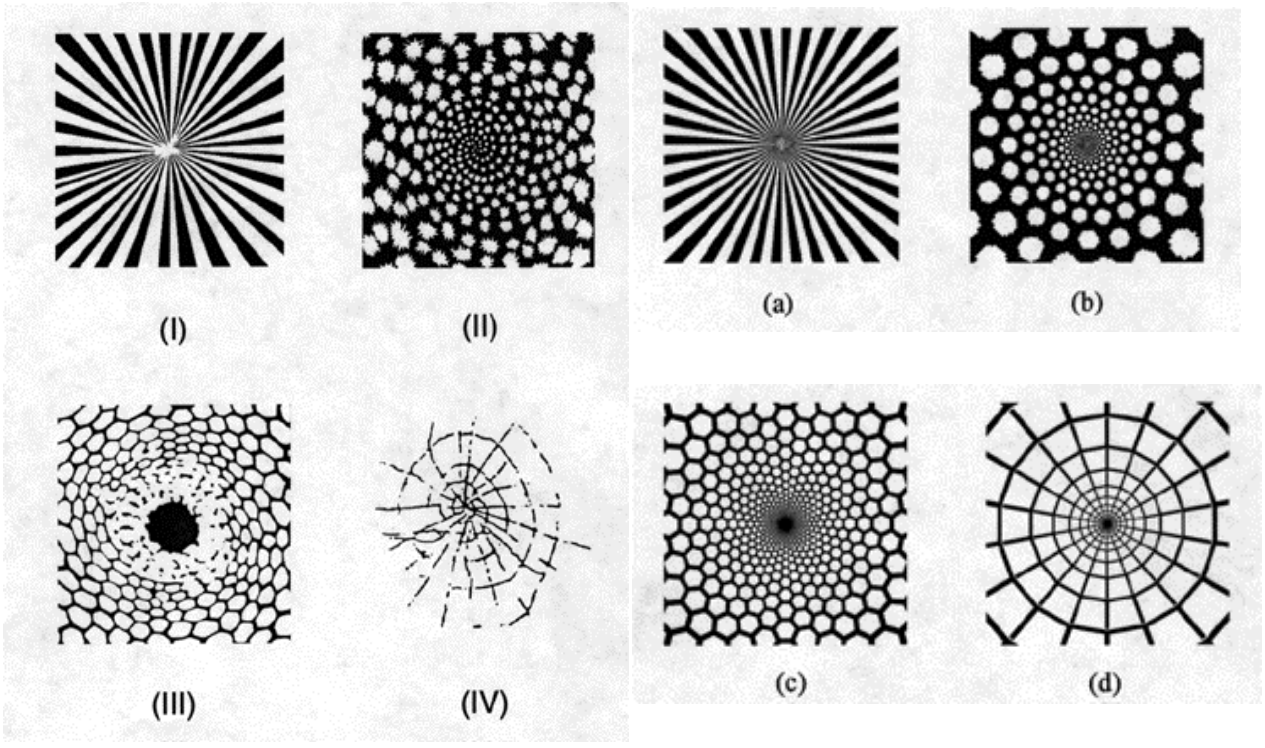

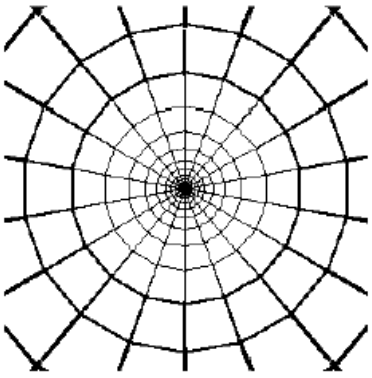

1. Even squares.

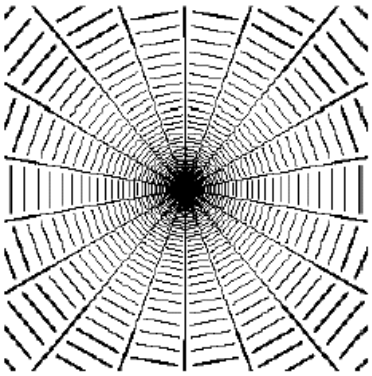

2. Even rolls.

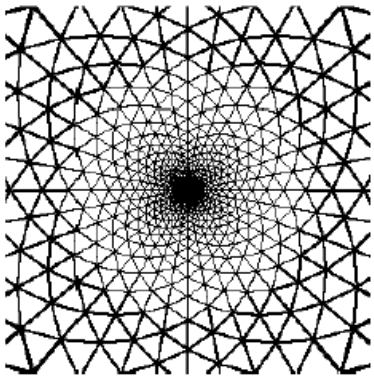

3. Even hexagons I.

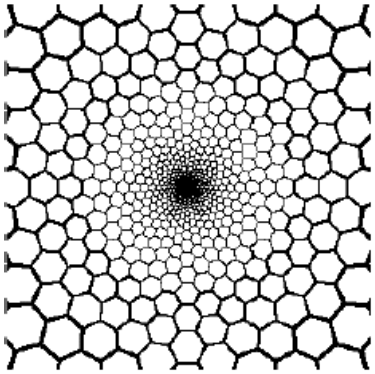

4. Even hexagons II.

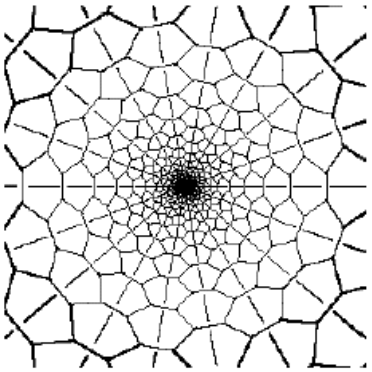

5. Even rhombs.

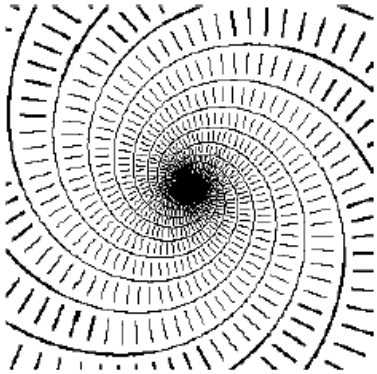

6. Even rhombic rolls.

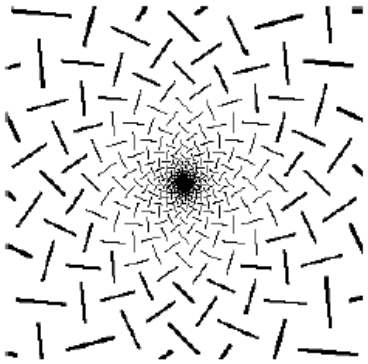

1. Odd squares.

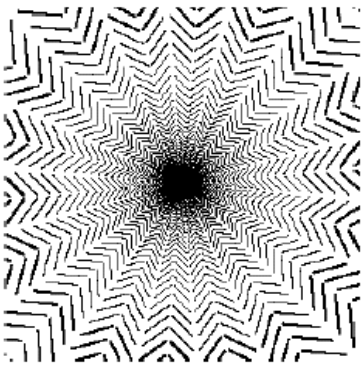

2. Odd rolls.

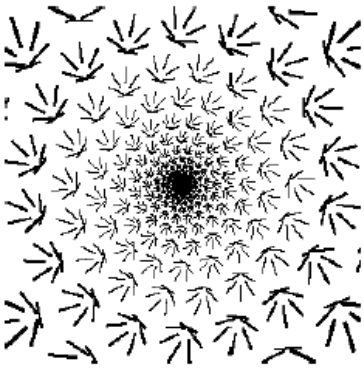

3. Odd hexagons I (triangle

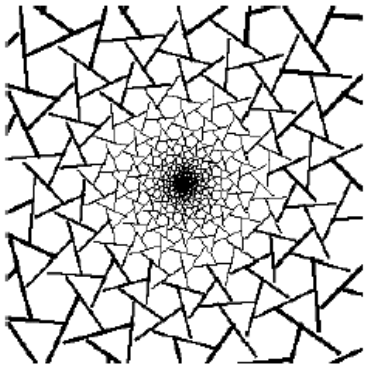

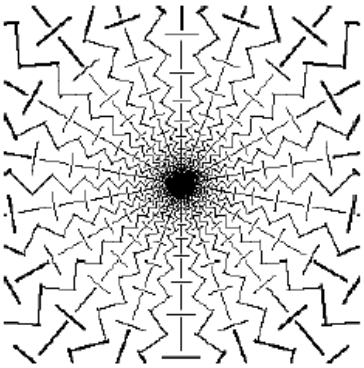

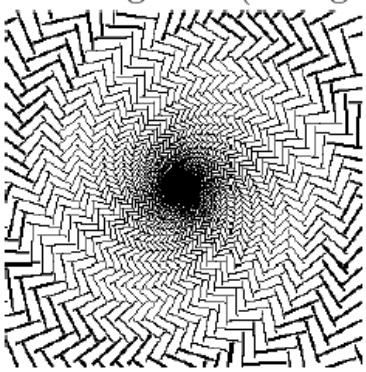

- The key result is that these morphological structures can be deduced from the encoding of the functional architecture of V1 into the Hopfield equations of a neural net.

- Entoptic vision concerns some geometrical patterns of phosphenes which are perceived after strong pressions on the eyeballs (mechanichal stimulation), electro-magnetic stimulations (transcranial magnetic stim., electrical stim. via implanted micro-electrodes), exposures to a violent flickering light, headaches, absorptions of substances such as mescaline, LSD, psilocybin, ketamin, some alkaloids (peyote) (neuropharmaco stim.), or near death experiences.

- They are related with an increased abnormal excitability of the photorecptors and of V1.
- They are in competition with the activity coming from visual inputs (Rauschecker, 2004).

- Subjects see spontaneously vividely typical forms : tunnels and funnels, spirals, lattices (honeycombs, triangles), cobwebs.
- These typical forms can operate on the drawings of any type of objects as in the paintings from Indian Mexican tribes.
- The Huichol are an indigenous ethnic group of Western Central Mexico that live in the Sierra Madre Occidental.

- « Such visual imagery is dynamic and the illusory contours usually explode from the center of gaze to the periphery, appearing initially in black and white before bright colors take over, and eventually pulsate and rotate in time as the experience progresses » (Yves Frégnac, *J. of Physio-Paris*, 97, 2-3).

- These illusory forms were already classified a long time ago (1928) by the great neurophysiologist Heinrich Klüver (1897-1979) who provided many clinical reports on them.
- Klüver was a student of Max Wertheimer and introduced the Gestalt psychology in the United States.
- He called the most typical forms planforms.

The NIMH program

- Programs at the National Institute of Mental Health aiming at probing the neuroreceptors with varied substances.
- In the receptor space each substance shifts the balance of activity of the brain away from the origin, by a vector representing the profile of binding affinities at different receptors.

  - « In a brain-centered reference frame, the origin is based on absolute levels of activity at each receptor population. The state of the brain is constantly on the move. We can think of it as a complex dynamical system, in which the trajectory follows high-dimensional orbits, and switches among many "attractors". »
  - « In this dynamic reference frame, drugs will create a perturbation along the binding vector, thereby pushing the system into a new attractor. » (Thomas Ray, Univ. of Oklahoma)

Spontaneous emergence of geometric visual patterns

Reference papers

- The first paper on the subject was that of Ermentrout and Cowan (1979):

  « A mathematical theory of visual hallucinations », *Biol. Cybernetics*, 34, 137-150.

- Recently, the subject was completely revisited by Paul Bressloff, Jack Cowan, Martin Golubitsky, Peter Thomas, and Matthew Wiener:

  « Geometric visual hallucinations, Euclidean symmetry and the functional architecture of striate cortex », *Phil. Trans. R. Soc. Lond. B* (2001) 356, 299-330.

- See also the very recent Bressloff's Cowan's paper:

  « The functional geometry of local and horizontal connections in a model of V1 », *Neurogeometry and Visual Perception* (J. Petitot, J. Lorenceau, eds.), *J. Physiology (Paris)*, 97, 2-3, 221-236.

Neural nets and Hopfield equations

- The authors work in the fibration

$$\pi : V = R \times \mathbf{S}^1 \rightarrow R$$

  with local coordinates (**x**, θ) (θ = the angle of the orientation p).

- Let $a(\mathbf{x}, \theta, t)$ be the activity of V1. We look for the PDE (partial differential equation) governing the evolution of a.

- Standard Hopfield equations.

- Let u_i , i = 1, …, N be formal neurons with activity $a_i(t)$.
- If time and space are discrete, standard Hopfield equations are (local rules of interaction):

$$a_i(t+1) = \sum_{j=1}^{j=N} w_{ij}\sigma\left(a_j(t)\right) + h_i(t)$$

where σ is a non linear gain function (with σ(0) = 0), h an external input and w_{ij} the weight of the connection between u_i and u_j.

- If time is continuous and space discrete, we get a system of N ordinary differential equations :

$$\frac{da_i}{dt}(t) = -a_i(t) + \sum_{j=1}^{j=N} w_{ij}\sigma\left(a_j(t)\right) + h_i(t)$$

- If time and space are continuous, we get a partial differential equation :

$$\frac{\partial a(q,t)}{\partial t} = -a(q,t) + \int_V w\left\langle q|q'\right\rangle \sigma\left(a(q',t)\right) dq' + h(q,t)$$

- The authors use the following Hopfield equation :

$$\frac{\partial a(\mathbf{x},\theta,t)}{\partial t} = -\alpha a(\mathbf{x},\theta,t) + \frac{\mu}{\pi}\int_0^{\pi}\int_{\mathbb{R}} w\left\langle \mathbf{x},\theta|\mathbf{x}',\theta'\right\rangle \sigma\left(a(\mathbf{x}',\theta',t)\right) d\mathbf{x}' d\theta' + h(\mathbf{x},\theta,t)$$

where $w\left\langle \mathbf{x},\theta|\mathbf{x}',\theta'\right\rangle$ is the weight of the connection between the neuron $v = (\mathbf{x}, \theta)$ and the neuron $v' = (\mathbf{x}', \theta')$, α a parameter of decay and μ a parameter of excitability of V1.

- The increasing of μ models an increasing of the excitability of V1 due to the action of the substances on the nuclei (locus coerulus, raphé) which produce neurotransmitters such as serotonin or noradrenalin.

Encoding the functional architecture in the synaptic weights

- The local vertical connections inside a single hypercolumn yield a term:

$$w\left\langle \mathbf{x},\theta|\mathbf{x}',\theta'\right\rangle = w_{\mathrm{loc}}\left(\theta-\theta'\right)\delta\left(\mathbf{x}-\mathbf{x}'\right)$$

where δ is a Dirac function imposing

x = x´

- The lateral horizontal connections between different hypercolumns yield a term:

$$w\left\langle \mathbf{x},\theta|\mathbf{x}',\theta'\right\rangle = w_{\mathrm{lat}}\left(\mathbf{x}-\mathbf{x}',\theta\right)\delta\left(\theta-\theta'\right)$$

where the factor

$$\delta\left(\theta-\theta'\right)$$

imposes $\theta = \theta'$ and expresses the fact that the horizontal cortico-cortical connections connect coaxial pairs.

- Moreover, the coaxiality $\theta = \theta' = \mathbf{x}\mathbf{x}'$ is expressed by the fact that

$$w_{\mathrm{lat}}\left(\mathbf{x}-\mathbf{x}',\theta\right) = w_{\mathrm{lat}}\left(s\right)\delta\left(\mathbf{x}-\mathbf{x}'-se_{\theta}\right) = \widehat{w}\left(r_{-\theta}\left(\mathbf{x}-\mathbf{x}'\right)\right)$$

where e_θ is the unit vector in the direction θ.

- As the weights *w* are *E*(2)-invariant under the roto-translation group of motions of the plane *E*(2), the PDE is itself *E*(2)-equivariant if $h = 0$.
- The *E*(2) action is given by

$$\begin{cases} \mathbf{y}(\mathbf{x},\theta) = (\mathbf{x}+\mathbf{y},\theta) \\ \varphi(\mathbf{x},\theta) = (r_\varphi \mathbf{x}, \theta+\varphi) \\ \kappa(\mathbf{x},\theta) = (\kappa\mathbf{x}, -\theta) \end{cases}$$

- The action on the activity function *a* is :

$$\gamma a(\mathbf{x},\theta) \;=\; a\left(\gamma^{-1}(\mathbf{x},\theta)\right)$$

and on the synaptic weights is :

$$\gamma w\left\langle \mathbf{x},\theta|\mathbf{x}',\theta'\right\rangle \;=\; w\left\langle \gamma^{-1}(\mathbf{x},\theta)|\gamma^{-1}(\mathbf{x}',\theta')\right\rangle$$

The $E(2)$-invariances imply that the PDE

$$\frac{\partial a(\mathbf{x},\theta,t)}{\partial t} = F\left(a(\mathbf{x},\theta,t)\right)$$

(we suppose the input $h = 0$) is $E(2)$-*equivariant*: $\gamma F(a) = F(\gamma a)$.
Martin Golubitsky,

> " The equivariance of the operator F with respect to the action of $E(2)$ has major implications for the nature of solutions bifurcating from the homogeneous resting state. "

Dynamically emerging morphologies and bifurcations

- We suppose that there exist no external input, that is $h = 0$. For $\mu = 0$, the state $a \equiv 0$ is trivially the state of the network and it is stable (you see nothing in a black room).
- $a \equiv 0$ is the ground state.

- Now, the analysis of the PDE shows that, as the parameter μ increases, this initial activation state $a \equiv 0$ can become unstable and bifurcate for critical values μ_c of μ.

- The new stable activation states present spatial patterns generated by an **E**(2) symmetry breaking.
- The bifurcations can be analyzed using classical methods:
  - Linearization of the PDE near the solution $a \equiv 0$ and the critical value μ_c.
  - Spectral analysis of the linearized equation.
  - Computation of its eigenvectors (eigenmodes).
- Here are some examples of eigenmodes.

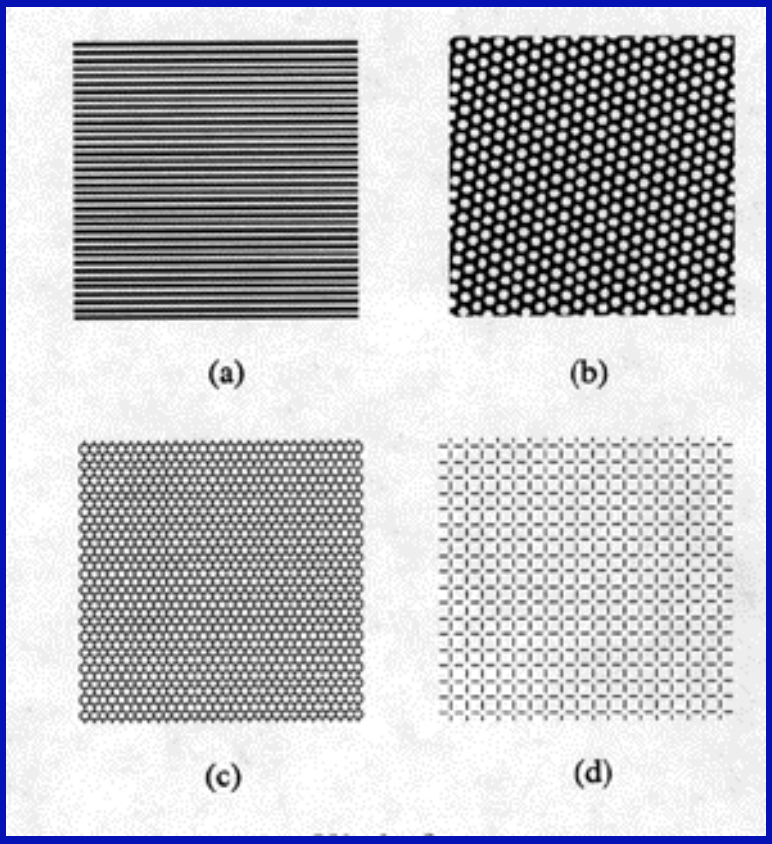

- Spectral analysis of the PDE.

– After having linearized the PDE around the trivial solution $a \equiv 0$ we look at solutions of the form :

$$a(\mathbf{x}, \theta, t) = e^{\lambda t}\, a(\mathbf{x}, \theta)$$

When $\mu = 0$, $\lambda = -\alpha$ and the solution is $a(\mathbf{x}, \theta, t) = e^{-\alpha t}\, a(\mathbf{x}, \theta)$.

– The solutions are stationary only if $\lambda = 0$. Otherwise they decay ($\lambda < 0$) or diverge ($\lambda > 0$) exponentially. In that case saturation imposed by the non linear gain function stabilizes them.

- We get an equation for the eigenvalues λ of the form :

$$\lambda a(\mathbf{x},\theta) = -\alpha a(\mathbf{x},\theta) + \sigma'(0)\mu\left(\int_0^{\pi} w_{\mathrm{loc}}(\theta-\theta')a(\mathbf{x},\theta')\frac{d\theta'}{\pi} + \beta\int_R w_{\mathrm{lat}}(\mathbf{x}-\mathbf{x}',\theta)a(\mathbf{x}',\theta)d\mathbf{x}'\right)$$

where β is a constant measuring the relative strength of the vertical and horizontal connections.

- Using Fourier series of a, w_{loc} and w_{lat} for the periodic variable θ and Fourier transforms for the spatial variable **x**, and identifying the coefficients of the terms of the two sides of the equation we get dispersion relations of the form

$$\lambda = -\alpha + \mu F(\ )$$

where F is a function of the Fourier coefficients.

- $\lambda = 0$ yields equations for critical μ.

- For $\mu = 0$, $\lambda = -\alpha$. When μ increases, λ will vanish for a certain $F(W_{loc,n}, W_{lat}(q))$ (where $W_{loc,n}$ and $W_{lat}(q)$ are Fourier coefficients) and a certain critical value μ_c.
- The bifurcation activates the corresponding terms in the Fourier series and transforms. Hence the eigenmodes.
- Symmetries imply very strong constraints.

- Solutions of the form : plane wave of wave vector $\mathbf{k} = (\rho\cos\psi, \rho\sin\psi)$

  modulated by a phase function

  $$a(\mathbf{x}, \theta) = u(\theta - \psi)e^{i\mathbf{k}.\mathbf{x}} + c.c.$$

  Let $u(\theta) = \sum_{n\in\mathbb{Z}} U_n e^{2in\theta}$

  $$w_{\mathrm{loc}}(\theta) = \sum_{n\in\mathbb{Z}} W_{\mathrm{loc},n} e^{2in\theta}$$

  be the Fourier series of u and w_{loc}

- Symmetries imply u even and $U_{-n} = U_n$ or u odd and $U_{-n} = U_n$
- Dispersion relations :

$$\left(\frac{\lambda+\alpha}{\sigma'(0)\mu} - W_{\mathrm{loc},m}\right) U_m = \beta \sum_{n\in\mathbb{Z}} \widehat{W}_{\mathrm{lat},m-n}(\rho) U_n$$

$$\widehat{W}_{\mathrm{lat},n}(\rho) = \int_0^{\pi} e^{-2in\theta} \left(\int_R w_{\mathrm{lat}}(\mathbf{x},0) e^{-i\mathbf{k}.r_\theta(\mathbf{x})} d\mathbf{x} \right) \frac{d\theta}{\pi}$$

- They imply typical forms for u (see text).

- When μ crosses the critical μ_c, some eigenmodes are activated and we get solutions like :

$$a(\mathbf{x},\theta) = \sum_{j=1}^{j=N} c_j u(\theta - \psi_j) e^{i\ \mathbf{k}_j.\mathbf{x}} + c.c.$$

- Problem : infinite degree of degeneracy . The dispersion relations depend only on ρ. All the wave vectors k sharing the same critical module ρ_c become unstable together.
- Main hypothesis.

The authors suppose that the solutions are *spatially doubly periodic* relative to a lattice $\mathcal{L}$ of R.

The solutions restricted by this double periodicity constraint are called *planforms*. They are well known and

> " There is a common approach to all lattice bifurcation problems " (Bressloff *et al.*)

The authors work in three lattices of the plane R: $\mathcal{L} = \{2\pi m_1 \mathbf{l}_1 + 2\pi m_2 \mathbf{l}_2\}$ $(m_1, m_2 \in \mathbb{Z})$ and their dual lattices $\mathcal{L}^*$ generated by the wave vectors $\mathbf{k}_1, \mathbf{k}_2$ such that $\mathbf{l}_i.\mathbf{k}_j = \delta_{ij}$.

If $\mathbf{k} \in \mathcal{L}^*$, the plane wave $e^{i\mathbf{k}.\mathbf{x}}$ is $\mathcal{L}$-periodic.

	$\mathbf{l}_1$	$\mathbf{l}_2$	$\mathbf{k}_1$	$\mathbf{k}_2$
Square	$(1, 0)$	$(0, 1)$	$(1, 0)$	$(0, 1)$
Hexagonal	$\left(1, \frac{1}{\sqrt{3}}\right)$	$\left(0, \frac{2}{\sqrt{3}}\right)$	$(1, 0)$	$\frac{1}{2}\left(-1, \sqrt{3}\right)$
Rhombic	$(1, -\cot\eta)$	$(0, \frac{1}{\sin\eta}$	$(1, 0)$	$(\cos\eta, \sin\eta)$

where, in the rhombic case, $\eta \neq 0, \frac{\pi}{3}, \frac{\pi}{2}$.

The main advantage to restrict to a lattice $\mathcal{L}$ is that the *non compact* Euclidean group $E(2)$ is reduced to the *compact* symmetry group

$$\Gamma_{\mathcal{L}} = H_{\mathcal{L}} \dot{+} T^2$$

where:

1. $H_{\mathcal{L}}$ is the *holohedry group* of $\mathcal{L}$ = the subgroup of rotations and reflexions of $O(2)$ preserving $\mathcal{L}$,
2. T^2 is the 2-*torus* $\mathbb{R}^2/\mathcal{L}$.

- This hypothesis is absolutely not evident (Bennequin) as lines in V1 do not correspond to lines in the visual field (see below).

$$\begin{cases} \mathcal{L} \text{ carré} & c_1 u(\theta) e^{i\mathbf{k}_1.\mathbf{x}} + c_2 u\left(\theta - \frac{\pi}{2}\right) e^{i\mathbf{k}_2.\mathbf{x}} + c.c. \\ \mathcal{L} \text{ hexagonal} & \begin{array}{l} c_1 u(\theta) e^{i\mathbf{k}_1.\mathbf{x}} + c_2 u\left(\theta - \frac{2\pi}{3}\right) e^{i\mathbf{k}_2.\mathbf{x}} + c_3 u\left(\theta + \frac{4\pi}{3}\right) e^{i\mathbf{k}_3.\mathbf{x}} + c.c. \\ \text{avec } \mathbf{k}_3 = -(\mathbf{k}_1 + \mathbf{k}_2) \end{array} \\ \mathcal{L} \text{ rhombique} & c_1 u(\theta) e^{i\mathbf{k}_1.\mathbf{x}} + c_2 u(\theta - \eta) e^{i\mathbf{k}_2.\mathbf{x}} + c.c. \end{cases}$$

Action of the translations T^2. Let $2\pi\tau = (2\pi\tau_1 \mathbf{l}_1 + 2\pi\tau_2 \mathbf{l}_2) \in T^2$ $(\tau_1, \tau_2 \in [0, 1[\,)$. We note it $\tau = [\tau_1, \tau_2]$. It acts as $\tau\left(u(\varphi)e^{i\mathbf{k}.\mathbf{x}}\right) = u(\varphi)e^{i\mathbf{k}.(\mathbf{x}-2\pi\tau)} = e^{-2i\pi\mathbf{k}.\tau} u(\varphi) e^{i\mathbf{k}.\mathbf{x}}$ and therefore

$$\begin{cases} \mathcal{L} \text{ square} & [\tau_1, \tau_2]\,(c_1, c_2) = (e^{-2i\pi\tau_1} c_1, e^{-2i\pi\tau_2} c_2) \\ \mathcal{L} \text{ hexagonal} & [\tau_1, \tau_2]\,(c_1, c_2, c_3) = \left(e^{-2i\pi\tau_1} c_1, e^{-2i\pi\tau_2} c_2, e^{2i\pi(\tau_1+\tau_2)} c_3\right) \\ \mathcal{L} \text{ rhombic} & [\tau_1, \tau_2]\,(c_1, c_2) = (e^{-2i\pi\tau_1} c_1, e^{-2i\pi\tau_2} c_2)\,. \end{cases}$$

- Solutions

$$\begin{cases} \mathcal{L} \text{ carré} & c_1 u(\theta) e^{i\mathbf{k}_1.\mathbf{x}} + c_2 u\left(\theta - \frac{\pi}{2}\right) e^{i\mathbf{k}_2.\mathbf{x}} + c.c. \\ \mathcal{L} \text{ hexagonal} & \begin{array}{l} c_1 u(\theta) e^{i\mathbf{k}_1.\mathbf{x}} + c_2 u\left(\theta - \frac{2\pi}{3}\right) e^{i\mathbf{k}_2.\mathbf{x}} + c_3 u\left(\theta + \frac{4\pi}{3}\right) e^{i\mathbf{k}_3.\mathbf{x}} + c.c. \\ \text{avec } \mathbf{k}_3 = -(\mathbf{k}_1 + \mathbf{k}_2) \end{array} \\ \mathcal{L} \text{ rhombique} & c_1 u(\theta) e^{i\mathbf{k}_1.\mathbf{x}} + c_2 u(\theta - \eta) e^{i\mathbf{k}_2.\mathbf{x}} + c.c. \end{cases}$$

- We can work directly on the coefficients c_i
- Example of the square. ξ is the rotation of $\pi/2$ and κ is the reflection

  $k_1 \rightarrow k_1$, $k_2 \rightarrow -k_2$, $\theta \rightarrow -\theta$.

We know therefore the action of $\Gamma_{\mathcal{L}} = D_4 \dot{+} T^2$ on $\mathcal{K} \simeq \mathbb{C}^2$:

$$
\begin{aligned}
&1\,(c_1, c_2) = (c_1, c_2),\\
&\xi\,(c_1, c_2) = (\overline{c_2}, c_1),\\
&\xi^2\,(c_1, c_2) = (\overline{c_1}, \overline{c_2}),\\
&\xi^3\,(c_1, c_2) = (c_2, \overline{c_1}),\\
&\kappa\,(c_1, c_2) = \pm\,(c_1, \overline{c_2})\ ,\\
&\kappa\xi\,(c_1, c_2) = \pm\,(\overline{c_2}, \overline{c_1}),\\
&\kappa\xi^2\,(c_1, c_2) = \pm\,(\overline{c_1}, c_2),\\
&\kappa\xi^3\,(c_1, c_2) = \pm\,(c_2, c_1),\\
&[\tau_1, \tau_2]\,(c_1, c_2) = (e^{-2i\pi\tau_1} c_1, e^{-2i\pi\tau_2} c_2).
\end{aligned}
$$

Let Γ be a group acting on a $\mathbb{R}$-vector space $\mathcal{K}$ and let Σ be a subgroup of Γ. We note $\mathrm{Fix}\,(\Sigma)$ the subset of $\mathcal{K}$ fixed by Σ (Σ is the *isotropy subgroup* of $\mathrm{Fix}\,(\Sigma)$) and we say that Σ is *axial* if $\mathrm{Fix}\,(\Sigma)$ is of dimension 1.

Equivariant Branching Lemma. Let Γ be a Lie group acting in a way absolutely irreducible on $\mathcal{K}$ (that is the linear maps commuting with the action of Γ are scalar multiples of the identity) and let $F \in \mathcal{E}(\Gamma)$ (where $\mathcal{E}(\Gamma)$ is the space of Γ-equivariant germs at the origin 0 of C^∞ mappings of $\mathcal{K}$ into $\mathcal{K}$) be a bifurcation problem (depending on a bifurcation parameter λ) with symmetry group Γ. Let Σ be an axial isotropy subgroup ($\dim \mathrm{Fix}(\Sigma) = 1$). Then there exists a unique smooth solution branch to $F = 0$ such that the isotropy subgroup of each solution is Σ.

Let $(c_1, c_2) \in \mathcal{K} = \mathbb{C}^2$. Using the T^2 action $[\tau_1, \tau_2]\,(c_1, c_2) = (e^{-2i\pi\tau_1} c_1, e^{-2i\pi\tau_2} c_2)$ we may suppose that $c_1, c_2 \in \mathbb{R}^+$. We look at the isotropy group Σ of (c_1, c_2) and we ask if it is axial.

If $c_1 > 0$, $c_2 > 0$, $[\tau_1, \tau_2]$ must be $[0, 0]$ to fix (c_1, c_2).

The subgroup $\Sigma = \left\{1, \xi^2, \kappa, \kappa\xi^2\right\} = D_2\left(\xi^2, \kappa\right)$ fixes all the (c_1, c_2) real and $\dim \mathrm{Fix}(\Sigma) = 2$. It is not axial.

But if $c_1 = c_2$, the subgroup $\Sigma = D_4(\xi, \kappa)$ fixes the diagonal which is of $\dim \mathrm{Fix}(D_4) = 1$. The subgroup D_4 is therefore *axial* and there will be a bifurcating branch of planforms (eigenfunctions) called *Even Squares*:

$$\begin{aligned} a(\mathbf{x}, \theta) &= u(\theta)\cos(\mathbf{k}_1.\mathbf{x}) + u\left(\theta - \frac{\pi}{2}\right)\cos(\mathbf{k}_2.\mathbf{x}) \\ &= u(\theta)\cos(x) + u\left(\theta - \frac{\pi}{2}\right)\cos(y) \end{aligned}$$

Computation of the case $u(\theta)$ even: $u(\theta) = \cos(2\theta) - 0.5\cos(4\theta)$ which vanishes for $x^\circ = y^\circ = \frac{1}{4}$ ($x = 2\pi x^\circ$, $y = 2\pi y^\circ$).

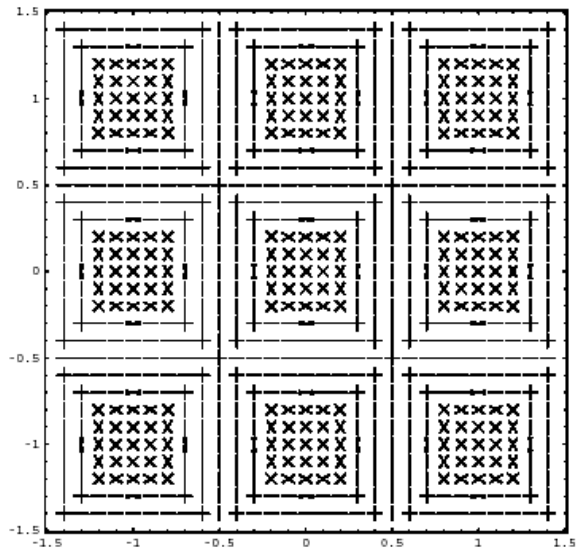

1. Even squares.

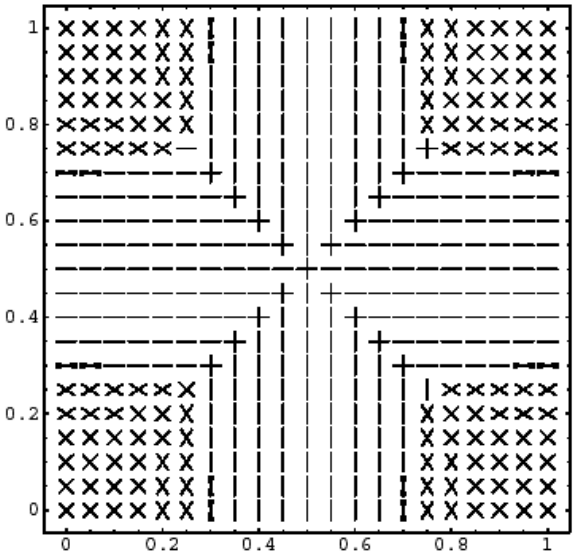

2. Zoom on the even squares.

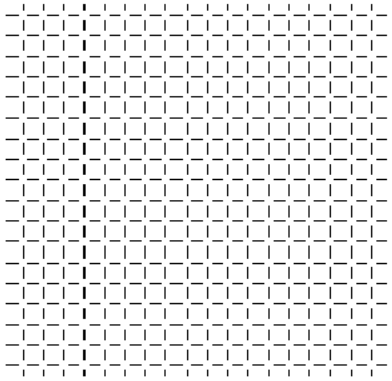

1. Even squares.

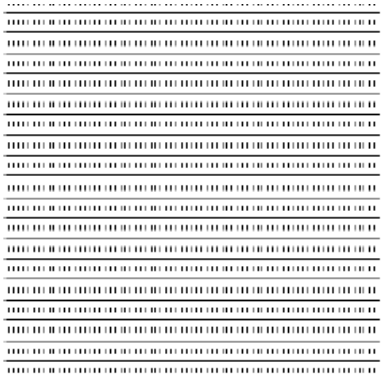

2. Even rolls.

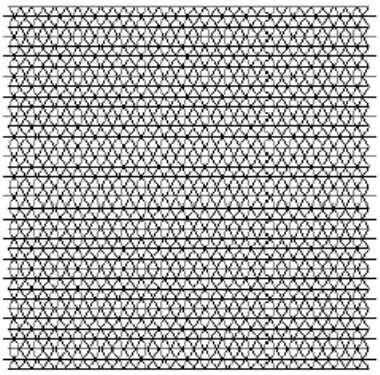

3. Even hexagons I.

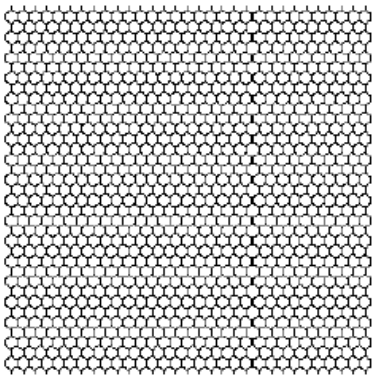

4. Even Hexagons II.

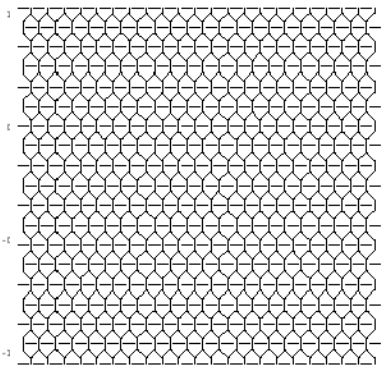

5. Even rhombs.

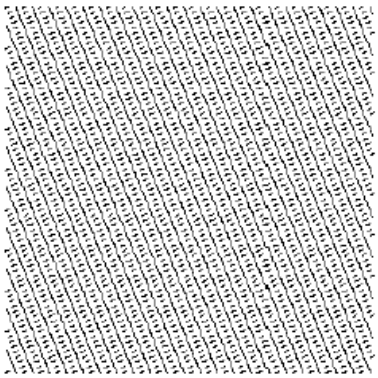

6. Even rhombic rolls.

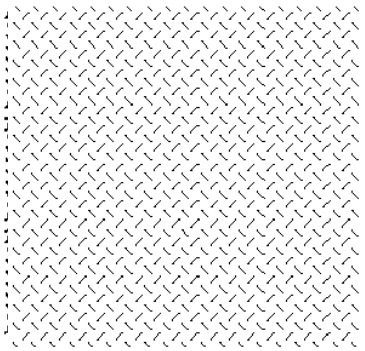

1. Odd squares.

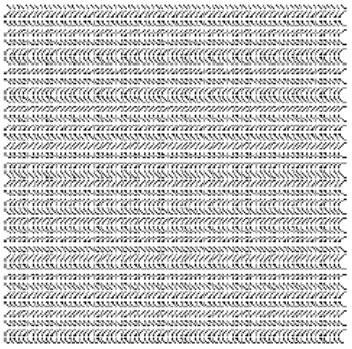

2. Odd rolls.

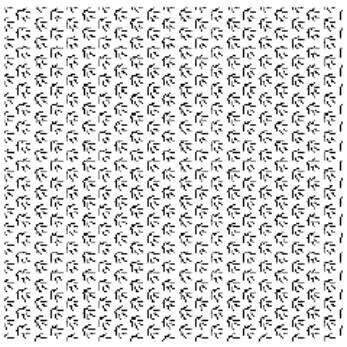

3. Odd hexagons I (triangles).

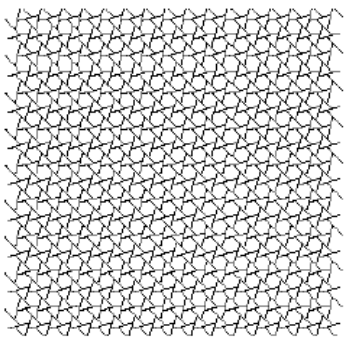

4. Odd hexagons II.

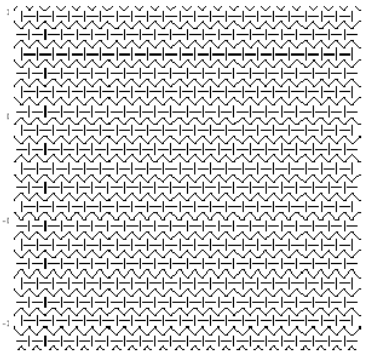

5. Odd rhombs.

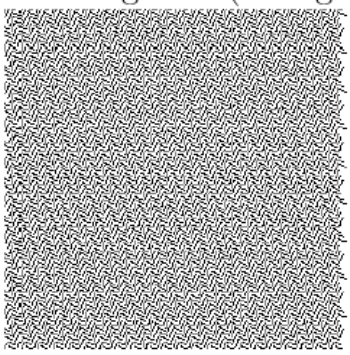

6. Odd rhombic rolls.

Patterns as virtual retinal images

- The last step is to reconstruct from eigenmodes in V1, corresponding virtual retinal images.
- For that, we must take into account the retinotopic conformal map mapping the retina on V1.

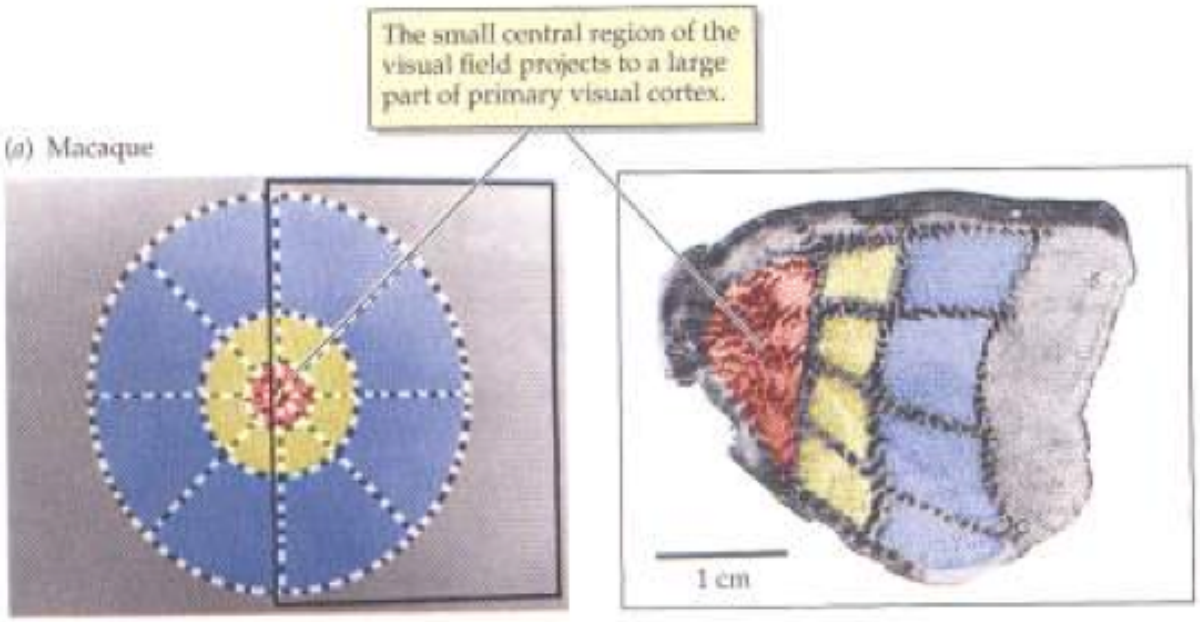

- The first model was a monopole model

$$\text{Log}(z+a)$$

- A better model is a dipole model (Eric Schwartz, 1994), for instance

$$\text{Log}[(z+0.333)/(z+6.66)].$$

- A better model is a wedge-dipole model for V1, V2, and V3

$$\text{Log}[(w(z)+a)/(w(z)+b)]$$

where $w(z)$ wedges the argument.

- Left G : human V1-V2-V3 (Horton & Hoyt 1991).
- Right H : fit with a wedge-dipole model (Schwartz 2002).

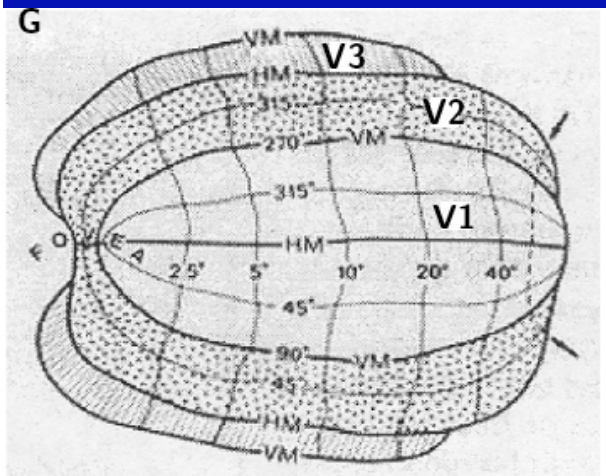

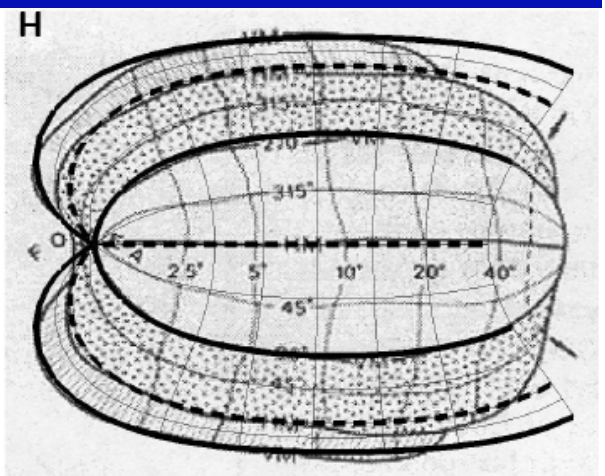

- Lines in V1 correspond to spiral on the retina.

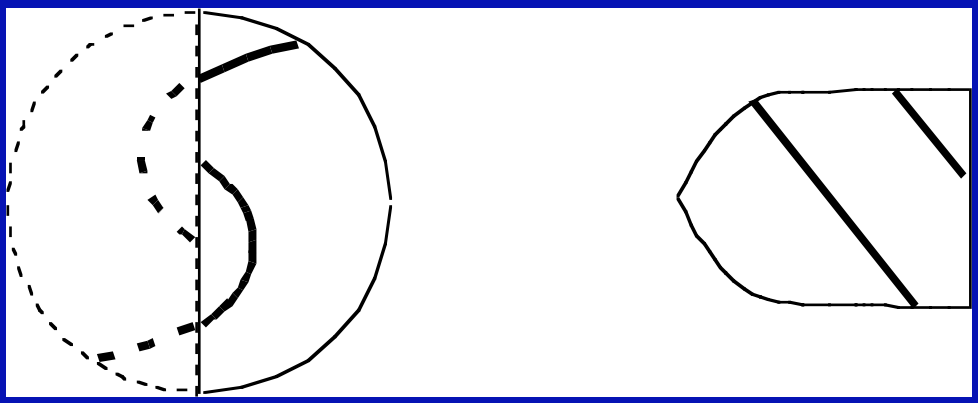

- If we apply the inverse of the conformal map to the eigenstates of the PDE we get quite exact models of Klüver's planforms.
- Klüver's planforms are isomorphic to eigenmodes of the bifurcated solution of the neural network in the synaptic weights of which the functional architecture of V1 is encoded.

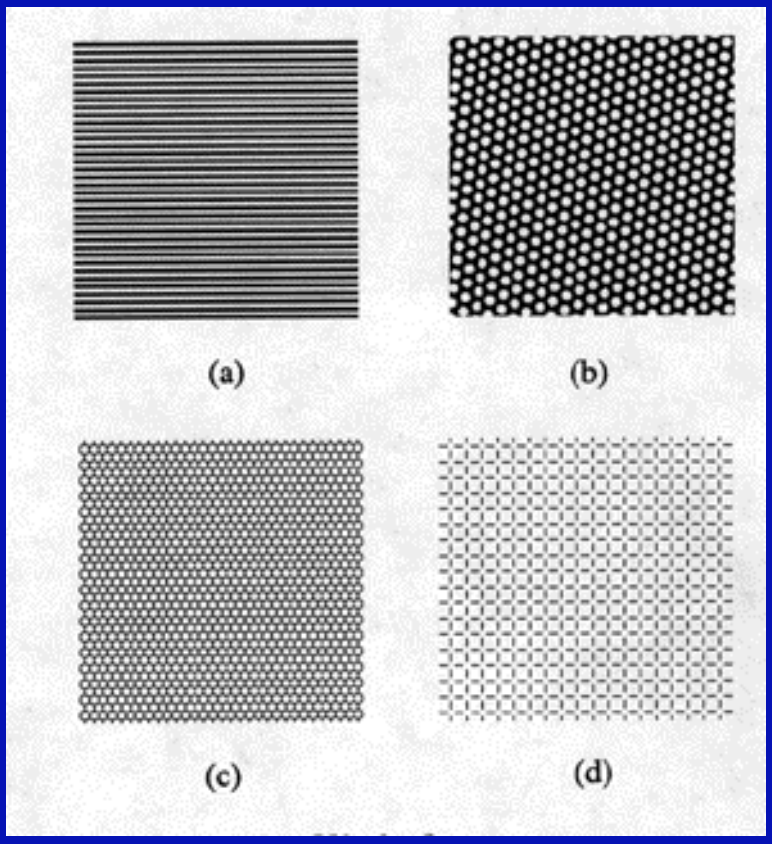
(a)
(b)
(c)
(d)

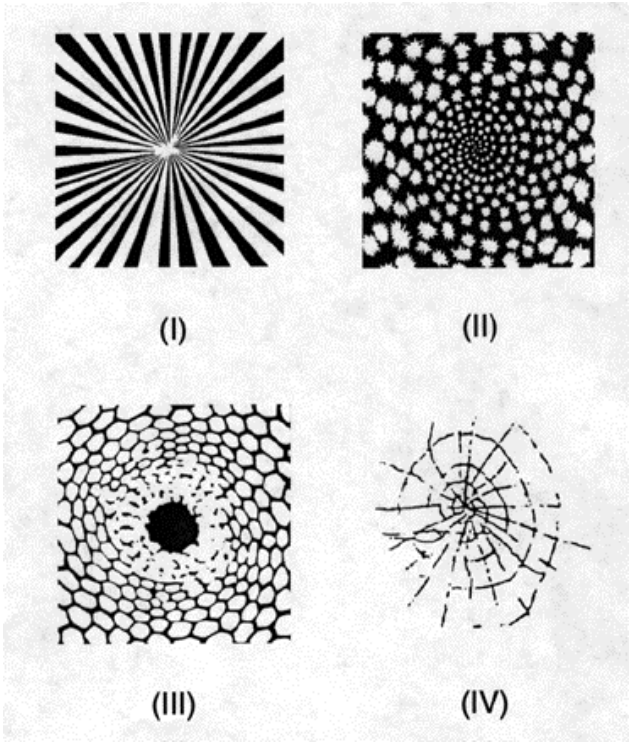
(I)
(II)
(III)
(IV)

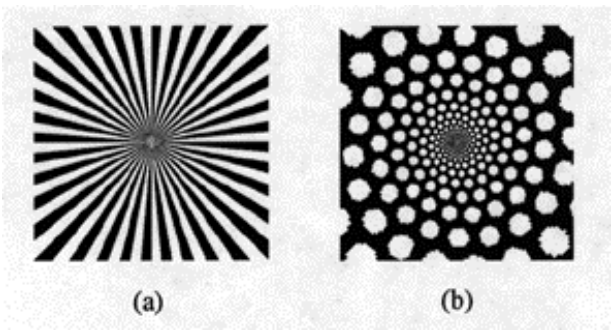
(a)
(b)

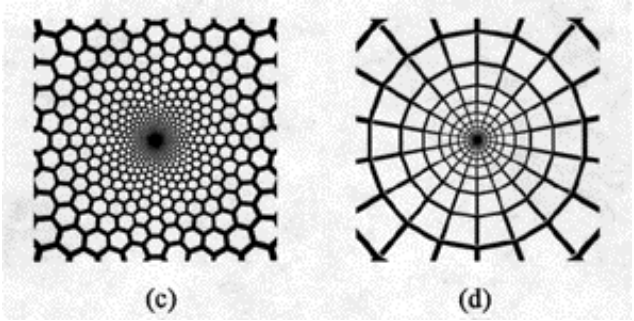
(c)
(d)

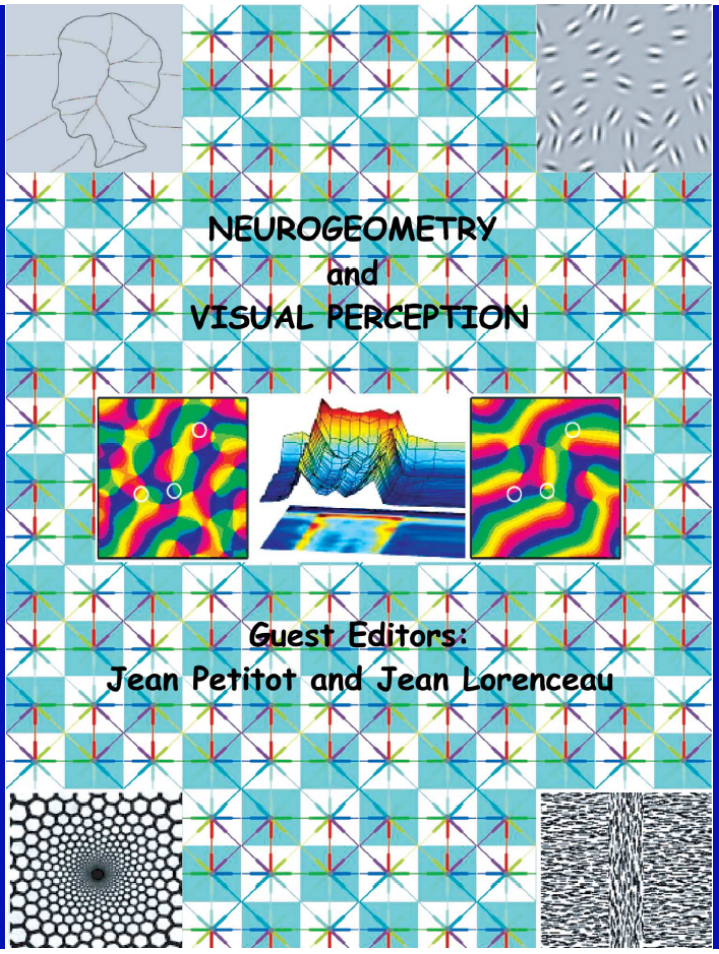
NEUROGEOMETRY
and
VISUAL PERCEPTION
Guest Editors:
Jean Petitot and Jean Lorenceau

E(2) invariance

- The contact structure is invariant under the action of the Euclidean group **E**(2) of rigid motions in the plane :

$$\mathbf{E}(2) = \mathbf{O}(2) \dot{+} \mathbf{R}^2$$

E(2) is the semi-direct product of the orthogonal group **O**(2) and the translation group $\mathbf{R}^2$.

- Let (α, r_φ) an element of **E**(2). (α, r_φ) acts on a point *a* of *R* by

$$(\alpha, r_\varphi)(a) = \alpha + r_\varphi(a)$$

- If (α, r_φ) and (β, r_θ) are 2 elements of E(2), their (non commutative) product is given by the formula:

$$(\beta, r_\theta) \circ (\alpha, r_\varphi) = (\beta + r_\theta(\alpha), r_{\theta+\varphi})$$

- The rotation r_φ acts on the fibration V by

$$r_\varphi(a,\theta) = (r_\varphi(a), \theta+\varphi)$$

- This particular form of action expresses the fact that the alignement of preferential directions is invariant.

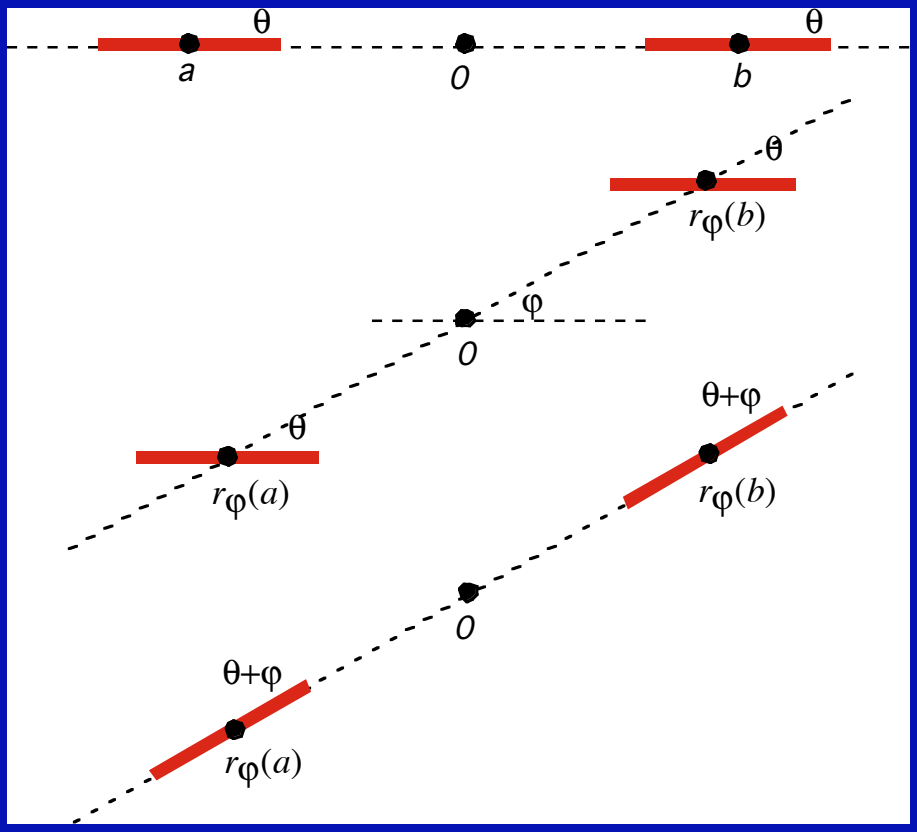

Moving frames

- In fact, the “good” fibration to use would be the principal bundle on the base space *R* associated to the invariance Euclidean group **E**(2). This would lead us to Elie Cartan ’s moving frame method.

- We can think that **E**(2) is neurally implemented if we take into account areas V1 and V2 and the fact that when an element of contour is activated it is also the case for the orthogonal direction.
- The translations of **E**(2) can be kinesthesically interpreted: the motor control of vision allows a change of moving frame (see A. Berthoz).

Contact structure and Lie group structure

- The contact structure of $V = J^1R$ can be recovered as a translation-invariant structure in an appropriate Lie group.
- Indeed, let us define a product in V by the formula:

$$(x, y, p).(x', y', p') = (x+x', y+y'+px', p+p')$$

$(0, 0, 0)$ is the 0 element and
$(-x, -y+px, -p)$ the opposite of (x, y, p).

- The Lie algebra of V is the vector space $\mathfrak{v} = T_0V$ endowed with the Lie bracket

$$[t, t'] = [(\xi, \eta, \pi), (\xi', \eta', \pi')] = (0, \xi'\pi - \xi\pi', 0).$$

Let us consider the *left translation* L_v defined by $L_v(v') = v.v'$. It is a non linear diffeomorphism of V whose tangent application at 0 is the linear map

$$\begin{array}{rccc} T_0L_v: & T_0V & \to & T_vV \\ & t=(\xi,\eta,\pi) & \mapsto & T_0L_v(t)=(\xi,\eta+p\xi,\pi) \end{array}$$

The matrix of T_0L_v is

$$T_0L_v = \begin{pmatrix} 1 & 0 & 0 \\ p & 1 & 0 \\ 0 & 0 & 1 \end{pmatrix} .$$

That shows that the basis $\left\{\frac{\partial}{\partial x}, \frac{\partial}{\partial y}, \frac{\partial}{\partial p}\right\}$ of the tangent bundle $TV = TJ^1R$ associated to the coordinates system $\{x, y, p\}$ is *not* left-invariant. It is the origin of non holonomy. To get a left-invariant basis we must translate the basis $\left\{\frac{\partial}{\partial x}, \frac{\partial}{\partial y}, \frac{\partial}{\partial p}\right\}_0$ at 0 and this yields the basis $\left\{\frac{\partial}{\partial x} + p\frac{\partial}{\partial y}, \frac{\partial}{\partial y}, \frac{\partial}{\partial p}\right\}$ that is $\{t_1, -t_3, t_2\}$.

Let us now consider a vector t of K_0. As $\eta = p\xi$ and $p = 0$, we have $\eta = 0$. Its transform $T_0L_v(t)$ is therefore given by $(\xi, p\xi, \pi)$. As $\eta = p\xi$, $T_0L_v(t)$ is an element of the contact plane K_v and *the contact structure* $\mathcal{K} = \{K_v\}$ *is nothing else than the left invariant field of tangent planes generated by left translating* K_0. Equivalently, we can say that $\mathcal{K}$ is the field of kernels of the 1-form ω which is left invariant. Indeed, at the origin 0, $\omega = dy - pdx$ is simply $\omega_0 = dy$. If we translate ω_0 to the point v we get $\omega_v = T_0L_v^*(\omega_0)$ defined by the formula $\omega_v(t) = \omega_0\left(T_0L_v^{-1}(t)\right)$ for $t = (\xi, \eta, \pi) \in T_vV$.

But

$$T_0L_v^{-1} = \begin{pmatrix} 1 & 0 & 0 \\ -p & 1 & 0 \\ 0 & 0 & 1 \end{pmatrix}$$

and

$$T_0L_v^{-1}(t) = \begin{pmatrix} 1 & 0 & 0 \\ -p & 1 & 0 \\ 0 & 0 & 1 \end{pmatrix} \begin{pmatrix} \xi \\ \eta \\ \pi \end{pmatrix} = \begin{pmatrix} \xi \\ -p\xi + \eta \\ \pi \end{pmatrix}.$$

So

$$\omega_v(t) = dy(\xi, -p\xi+\eta, \pi) = -p\xi+\eta = dy(t)-pdx(t) = \omega(t).$$

Application to the association field

- The Frobenius integrability condition is a geometrical formulation of the Gestalt law of “good continuation” (J-M. Morel, Y. Frégnac, S. Mallat) .
- Its empirical counterpart has been studied psychophysically by David Field, Anthony Hayes and Robert Hess and explained via the concept of association field.

- Let (a_i, p_i) be a set of segments embedded in a background of distractors. The segments generate a perceptively salient curve (pop-out) iff the p_i are tangent to the curve C interpolating between the a_i.

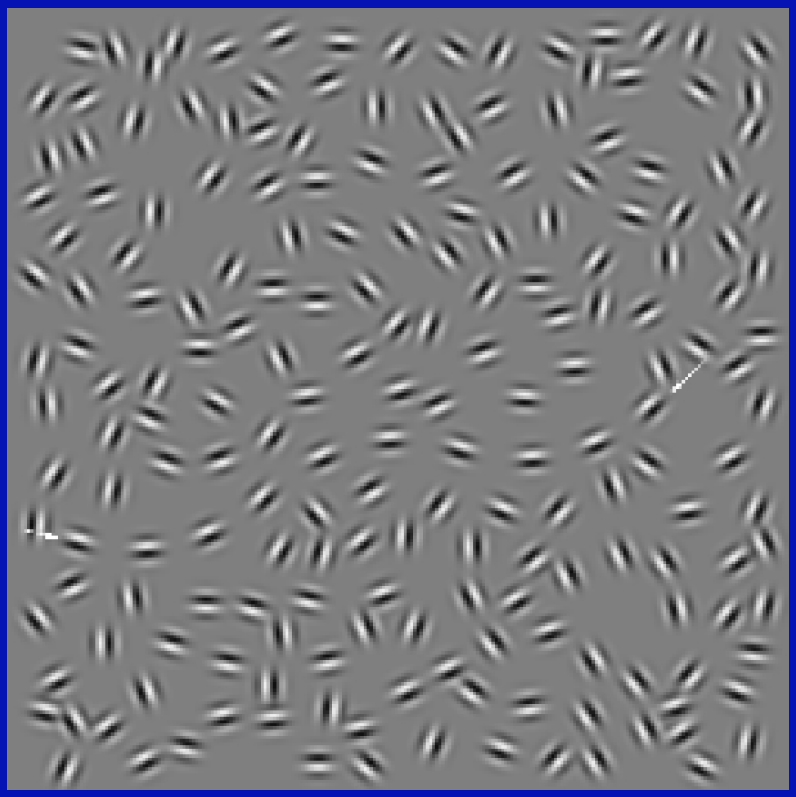

- This is due to the fact that the activation of a simple cell detecting a pair (a, p) preactivates, via the horizontal cortico-cortical connections, cells (b, q) with b roughly aligned with a in the direction p and q close to p. This is exactly a discrete version of the integrability condition.

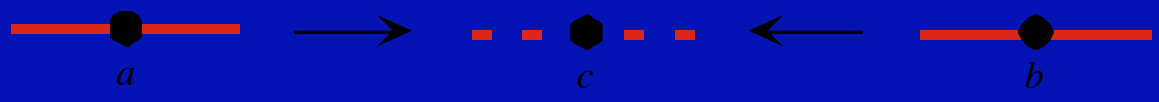

Preactivation of a cell (c,p)

– « Elements are associated according to joint constraints of position and orientation. »

– « The orientation of the elements is locked to the orientation of the path; a smooth curve passing through the long axis can be drawn between any two successive elements. »

- This is a psychophysical formulation of the integrability condition.

- The pop-out of the global curve generated by the (a_i, p_i) is a typical translocal phenomenon resulting from a binding induced by the co-activation.
- Binding is a wave of activation along horizontal connections which synchronizes the cells (Singer, Gray, König).

Scale-space and symplectic structures

- We have seen in the introduction that it is relevant to introduce a scale factor. Its natural interpretation is that the receptive profiles of the visual neurons are of the form DG (with D a differential operator) and a Gaussian G defines a scale.

- When the resolution becomes infinite and G becomes a Dirac distribution it seems that the concept of scale becomes irrelevant. But it is not the case.
- Indeed, the contact structure of $V = J^1R$ is defined as the kernel field $v = (x, y, p) \rightarrow K_v$ of the 1-form $\omega = dy - pdx$.
- But this field is only defined up to a scalar factor, ω and $\sigma\omega$ having the same kernels.

- It is therefore natural to enlarge the 3 dimensional space $V = R^2 \times R$ to the 4 dimensional space $S = R^2 \times R \times R^+$ with coordinates (x, y, p, σ).

Formulae are more symmetrical and simpler if we work with A. Sarti and G. Citti in the fibrations $V = \mathbb{R}^2 \times S^1 \times \mathbb{R}$ and $S = V \times \mathbb{R} = \mathbb{R}^2 \times S^1 \times \mathbb{R}$ with the 1-form

$$\omega = -\sin\theta dx + \cos\theta dy$$

and the scaling e^s.

The contact planes in V are then generated by the orthonormal basis

$$\begin{aligned} X_1 &= \cos\theta\partial_x + \sin\theta\partial_y \\ X_2 &= \partial_\theta \end{aligned}$$

whose Lie bracket is

$$[X_1, X_2] = \sin\theta\partial_x - \cos\theta\partial_y = -X_3$$

which is unitary and orthogonal to the contact plane.

We get

$$\begin{aligned} d\omega &= \cos\theta dx \wedge d\theta + \sin\theta dy \wedge d\theta \\ \omega \wedge d\omega &= -dx \wedge dy \wedge d\theta. \end{aligned}$$

In S we get

$X_1 = e^s(\cos\theta\partial_x + \sin\theta\partial_y)$

$X_2 = \partial_\theta$

$X_3 = e^s(-\sin\theta\partial_x + \cos\theta\partial_y)$

$X_4 = \partial_s$

and we consider the 1-form

$$\alpha = e^{-s}\omega = e^{-s}(-\sin\theta dx + \cos\theta dy)$$

We get the symplectic 2-form

$$\begin{aligned} d\alpha &= -e^{-s}ds \wedge (-\sin\theta dx + \cos\theta dy) \\ &\quad -e^{-s}d\theta \wedge (\cos\theta dx + \sin\theta dy) \end{aligned}$$

If for tangent vectors $\tau = (\xi, \eta, \varphi, \sigma)$ at points (x, y, θ, e^s) we write

$$d\alpha\,(\tau, \tau') = \langle A\tau, \tau' \rangle$$

we get the antisymmetric matrix

$$A = \begin{pmatrix} 0 & 0 & -e^{-s}\cos\theta & e^{-s}\sin\theta \\ 0 & 0 & -e^{-s}\sin\theta & -e^{-s}\cos\theta \\ e^{-s}\cos\theta & e^{-s}\sin\theta & 0 & 0 \\ -e^{-s}\sin\theta & e^{-s}\cos\theta & 0 & 0 \end{pmatrix}$$

We have $A^2 = -e^{-2s}I$, and if $P = \sqrt{-A^2} = e^{-s}I$, the matrix $J = AP^{-1}$ defines a *complex structure* on S satisfying $J^2 = -I$.

$$J = \begin{pmatrix} 0 & 0 & -\cos\theta & \sin\theta \\ 0 & 0 & -\sin\theta & -\cos\theta \\ \cos\theta & \sin\theta & 0 & 0 \\ -\sin\theta & \cos\theta & 0 & 0 \end{pmatrix}$$

J is of course symplectic and we define a new Riemannian structure by

$$\begin{aligned} (\tau|\tau') &= -d\alpha\,(J\tau, \tau') \\ &= \langle P\tau, \tau' \rangle \\ &= e^{-s}\,\langle \tau, \tau' \rangle \end{aligned}$$

It is immediate to verify that $JX_1 = e^s X_2$ and $JX_3 = e^s X_4$. Therefore the planes $\{X_1, X_2\}$ and $\{X_3, X_4\}$ are *complex planes* upon which J acts as the multiplication by i.

All these structures are integrated in an Hermitian product on $\mathbb{R}^4 = \mathbb{C}^2$ defined by

$$\begin{aligned} h(\tau, \tau') &= (\tau|\tau') - id\alpha(\tau, \tau') \\ &= e^{-s}\langle \tau, \tau' \rangle - ie^{-s}\langle J\tau, \tau' \rangle \\ &= e^{-s}\langle (I - iJ)(\tau), \tau' \rangle \end{aligned}$$

In the initial frame, the matrix of h is the Hermitian matrix

$$h = e^{-s} \begin{pmatrix} 1 & 0 & i\cos\theta & -i\sin\theta \\ 0 & 1 & i\sin\theta & i\cos\theta \\ -i\cos\theta & -i\sin\theta & 1 & 0 \\ i\sin\theta & -i\cos\theta & 0 & 1 \end{pmatrix}$$

The sub-Riemannian sphere of the Heisenberg group

- Sub-Riemannian geometry is not intuitive. To illustrate it, we have computed the sub-Riemannian sphere of the Heisenberg group which is isomorphic to the jet space.
- We used explicit formulas for geodesics due to R. Beals, B. Gaveau, P. Greiner, A. Agratchev, A.M. Vershik, V.Y. Gershkovich.

- Let $v = (x_1, x_2, t)$ coordinates for H. The group law is:

$$(x_1, x_2, t)\cdot(x_1', x_2', t') = (x_1 + x_1', x_2 + x_2', t + t' + 2\,(x_2 x_1' - x_1 x_2'))$$

- It is isomorphic to the jet space (x, y, p) through the change of variables :

$$x = x_1,\ y = t + 2x_1x_2,\ p = 4x_2.$$

- The tangent vectors X_1 and X_2 generating the contact planes K_v are :

$$X_1 = (1, 0, 2x_2),\ X_2 = (0, 1, -2x_1).$$

- If $T = (0,0,1)$, $[X_1, X_2] = -4T$, $[X_1, T] = 0$, $[X_2, T] = 0$.

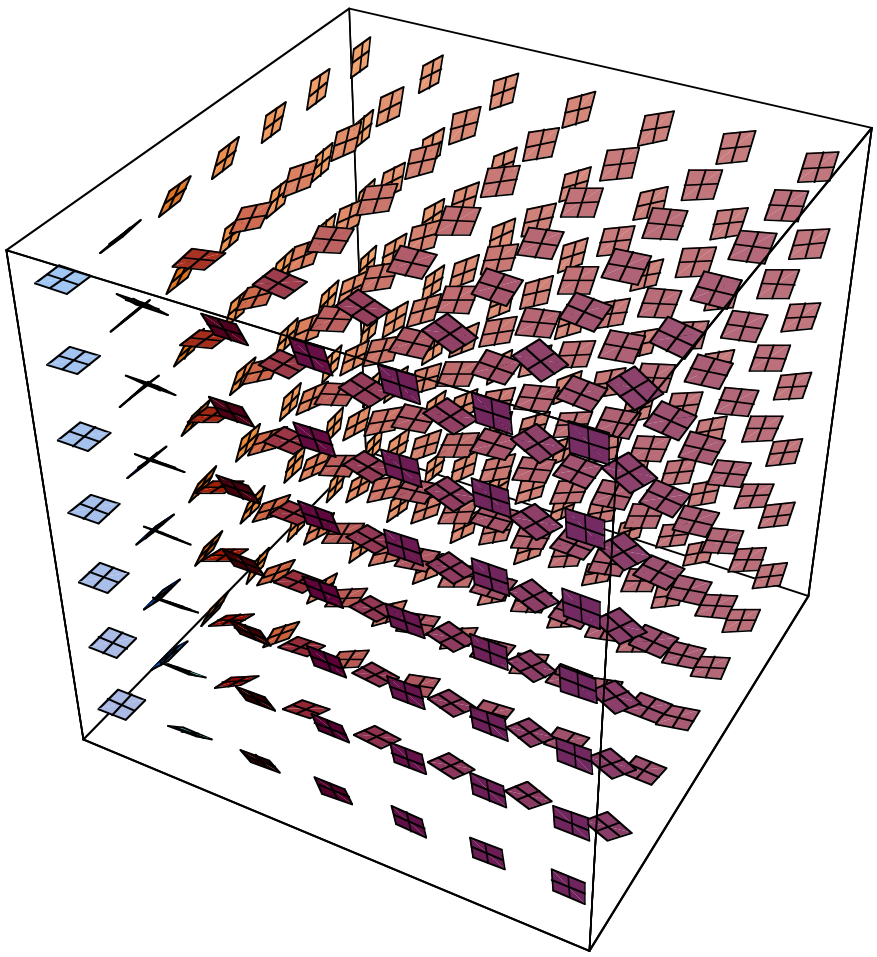

- The Hamiltonian is :

$$H\left(x_1, x_2, t, \xi_1, \xi_2, \theta\right) = \frac{1}{2}\left[\left(\xi_1 + 2x_2\theta\right)^2 + \left(\xi_2 - 2x_1\theta\right)^2\right]$$

and the equations of geodesics from (0, 0, 0) to $(x_1 = x_1(\tau), x_2 = x_2(\tau), t = t(\tau))$

$$\begin{cases} x_1(s) = \frac{\sin[2s\theta]}{\sin[2\tau\theta]}\left(\cos[2(s-\tau)\theta]\ x_1 + \sin[2(s-\tau)\theta]\ x_2\right) \\ x_2(s) = \frac{\sin[2s\theta]}{\sin[2\tau\theta]}\left(\cos[2(s-\tau)\theta]\ x_2 - \sin[2(s-\tau)\theta]\ x_1\right) \\ t(s) = \frac{4s\theta - \sin[4s\theta]}{2(\sin[2\tau\theta])^2}\left(\left(x_1\right)^2 + \left(x_2\right)^2\right) \end{cases}$$

- We have $t = \mu(2\tau\theta)\left\|\mathbf{x}\right\|^2$

with

$$\mu(\varphi) = \frac{\varphi}{\sin^2(\varphi)} - \frac{1}{2}\frac{\sin(2\varphi)}{\sin^2(\varphi)} = \frac{\varphi}{\sin^2(\varphi)} - \cot(\varphi)$$

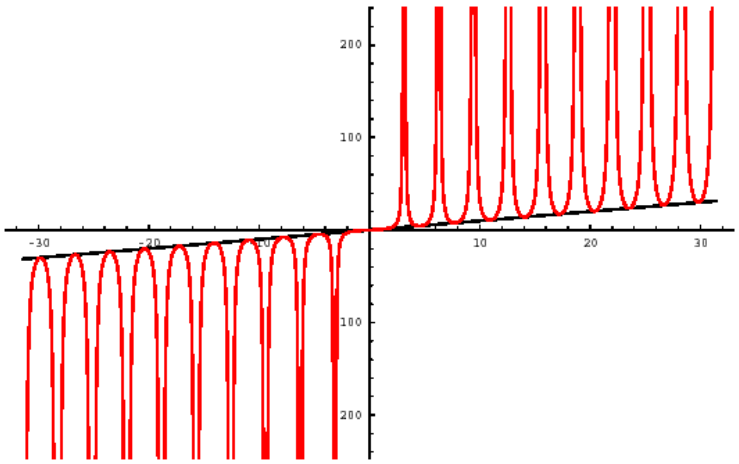

FIGURE 32. La fonction $\mu(\varphi)$ intervenant dans la construction des géodésiques sous-riemanniennes du groupe de Heisenberg.

To get geodesics with the same end point
$(x_1 = x_1(\tau), x_2 = x_2(\tau), t = t(\tau))$
we have to solve $t = \mu(2\tau\theta) \|\mathbf{x}\|^2$ in $\tau\theta$.

For instance for $\mu(\varphi) = 20$ (and $\theta = 1$) we get 11 solutions: $\tau_1 = 1.36$, $\tau_2 = 1.77$, $\tau_3 = 2.84$, $\tau_4 = 3.44$, $\tau_5 = 4.34$, $\tau_6 = 5.09$, $\tau_7 = 5.83$, $\tau_8 = 6.75$, $\tau_9 = 7.32$, $\tau_{10} = 8.42$, $\tau_{11} = 8.80$. If we take for instance $x_1 = x_1(\tau) = 2$ and $x_2 = x_2(\tau) = 1$, we get $t = 100$ and 11 geodesics joining $(0, 0, 0)$ to $(2, 1, 100)$. In the following figure we show the two cases τ_1 and τ_{10}.

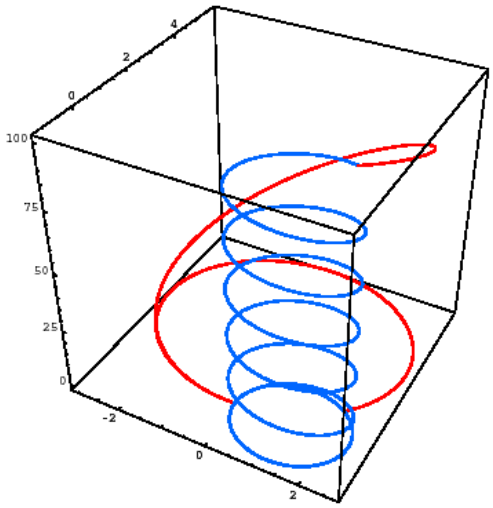

FIGURE 33. Deux géodésiques sous-riemanniennes du groupe de Heisenberg joignant $(0,0,0)$ à $(2,1,100)$. On représente les géodésiques dans V et leur projection sur le plan z.

- This structure of geodesics implies that the sub-Riemannian sphere *S* and the wave front are rather strange.
- We show first their section in one quadrant, then their entire structure.

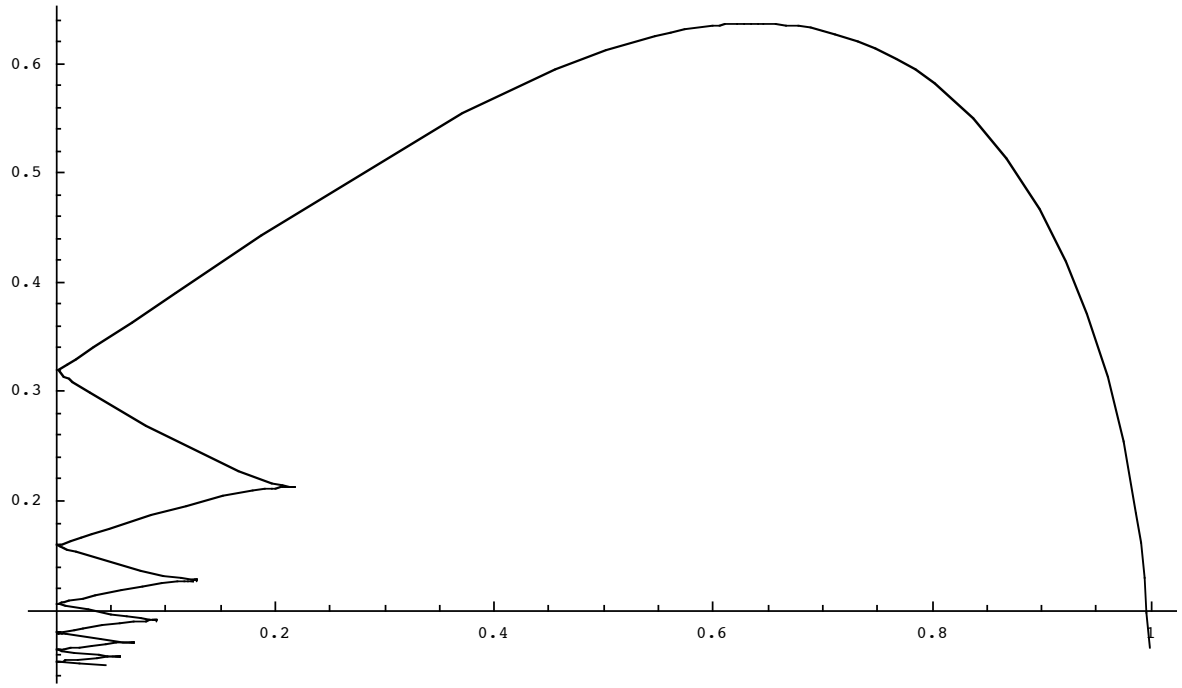
0.6
0.5
0.4
0.3
0.2
0.2
0.4
0.6
0.8
1

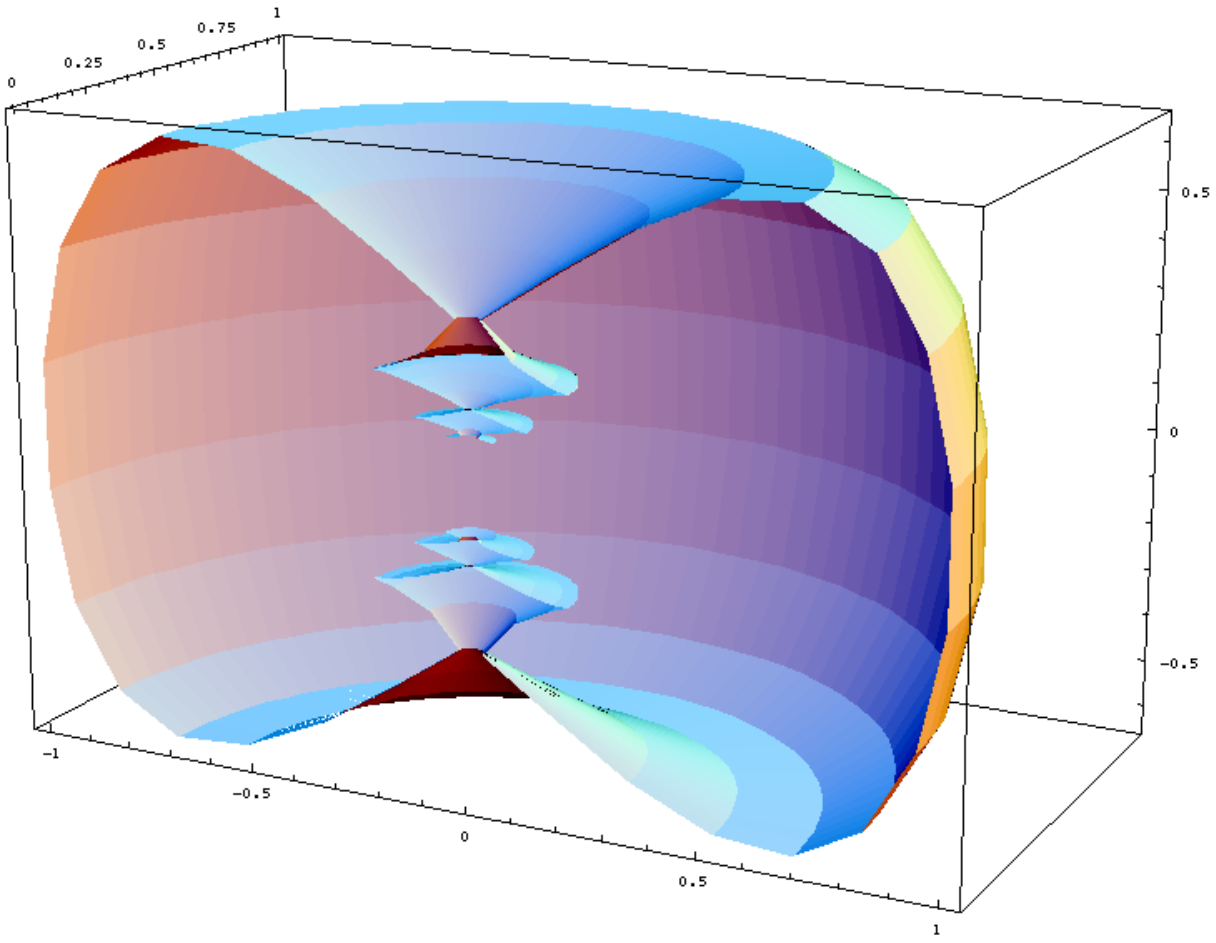
0
0.25
0.5
0.75
1
0.5
0
−0.5
−1
−0.5
0
0.5
1

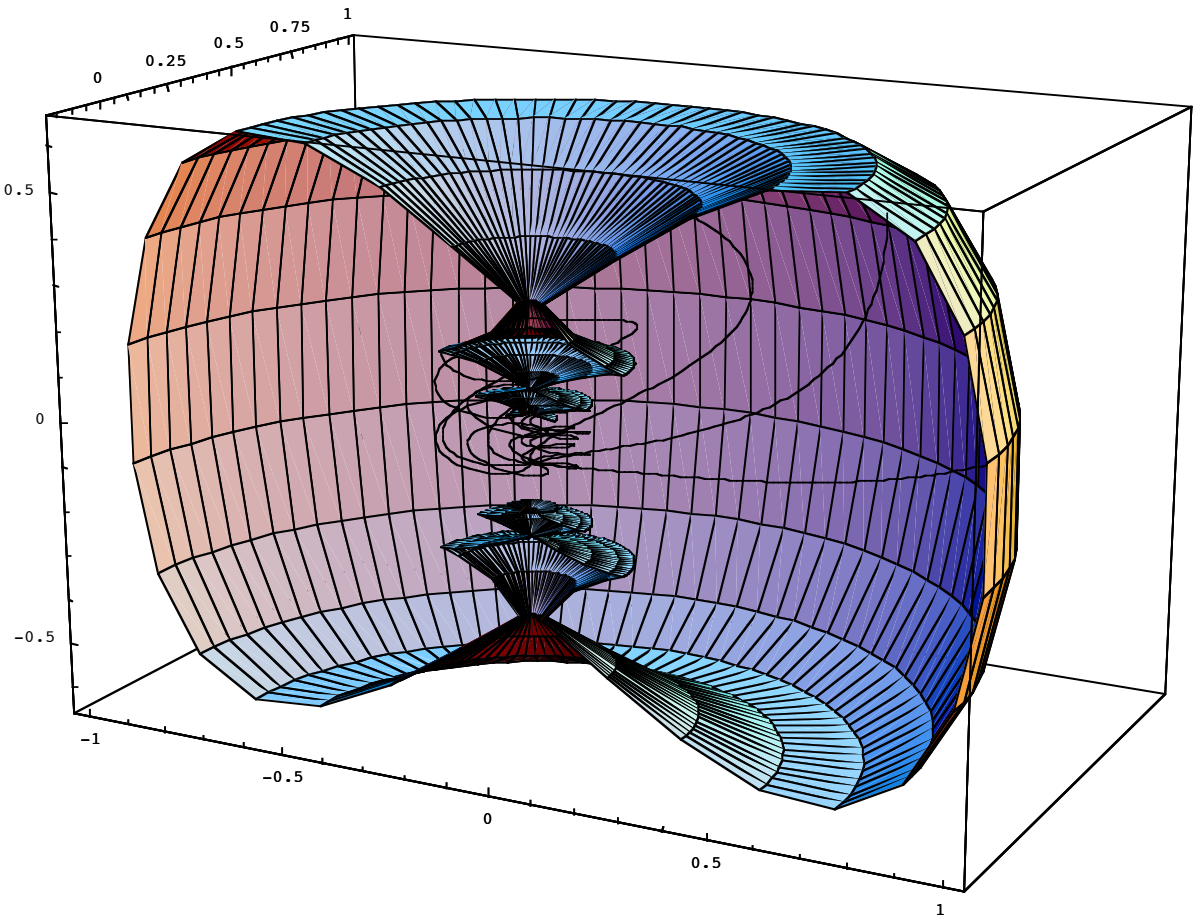

- The dynamics of NA^{+}, K^{+}, Ca^{++}, Cl^{-} ions accross the ionic channels of the membrane defines a rest potential (RP) $V \approx -75$ mV
- The respective equilibrium potential (EP) of ions are :

  $NA^{+} = +62$ mV,

  $K^{+} = -80$ mV,

  $Ca^{++} = +123$ mV,

  $Cl^{-} = -65$ mV.

- A depolarization increases RP. When it crosses the threshold of –45 mV the neuron “fires” and emits a spike (action potential) which propagates along the axon.
- There is a positive feedback of depolarization on the (fast) aperture of NA^+ channels and RP increases catastrophically up to +60 mV (≈ EP of NA^+).
- Afterwards, NA^+ channels are inactivated.

- But this strong depolarization opens the (slow) K^+ channels and the membrane is repolarized and returns to the RP after a period of hyperpolarization (–85 mV ≈ EP of K^+) .
- Equations of Hodgkin & Huxley (1952, Nobel Prize 1963).
- Dynamical analysis by C. Zeeman (1972).

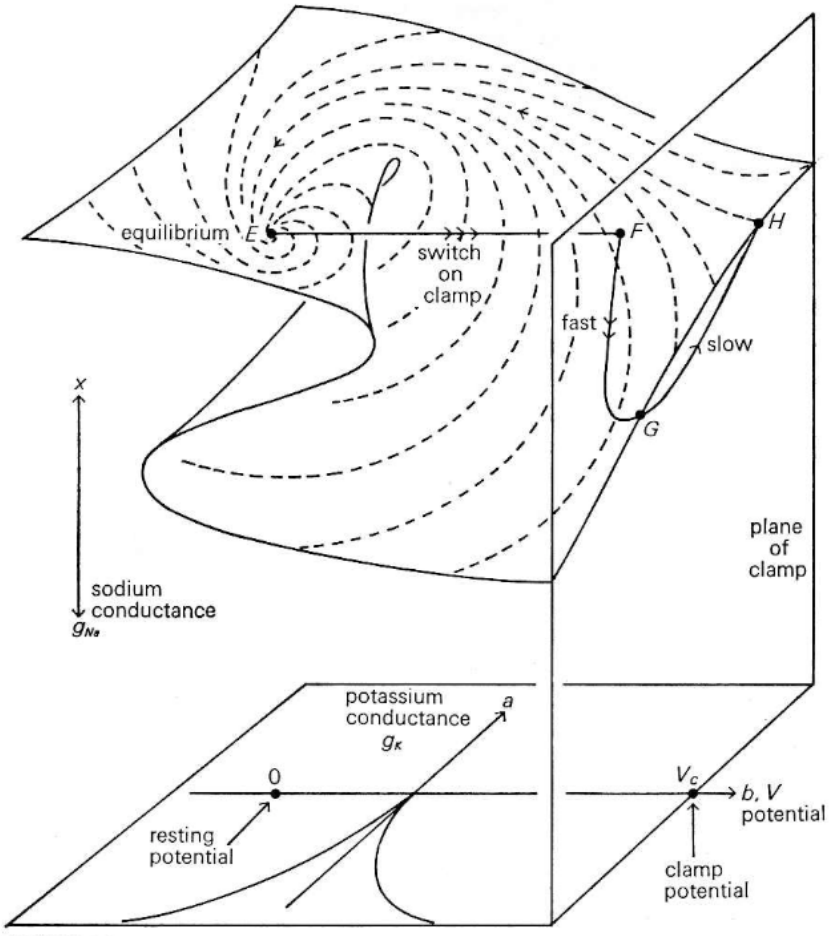

- Spikes and subthreshold membrane activity determine the neural coding.
  - Rate coding,
  - Sparse coding with robust temporal structure,
  - Rank coding (order of first spikes in neuronal assemblies).

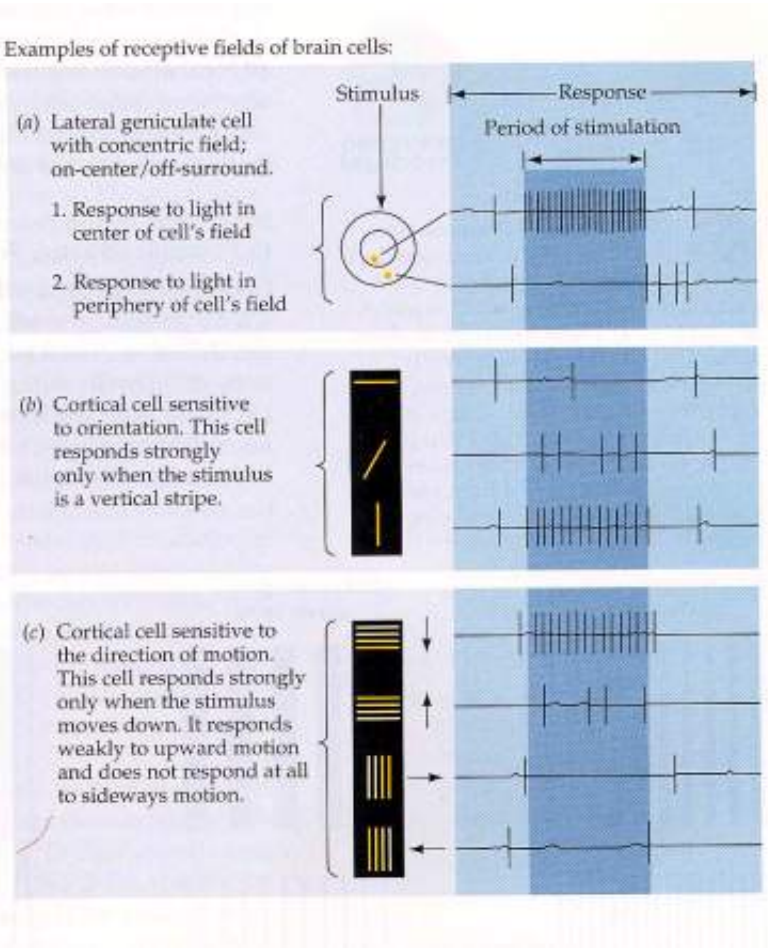
Examples of receptive fields of brain cells:
Stimulus
Response
Period of stimulation
(a) Lateral geniculate cell with concentric field; on-center/off-surround.
1. Response to light in center of cell's field
2. Response to light in periphery of cell's field
(b) Cortical cell sensitive to orientation. This cell responds strongly only when the stimulus is a vertical stripe.
(c) Cortical cell sensitive to the direction of motion. This cell responds strongly only when the stimulus moves down. It responds weakly to upward motion and does not respond at all to sideways motion.

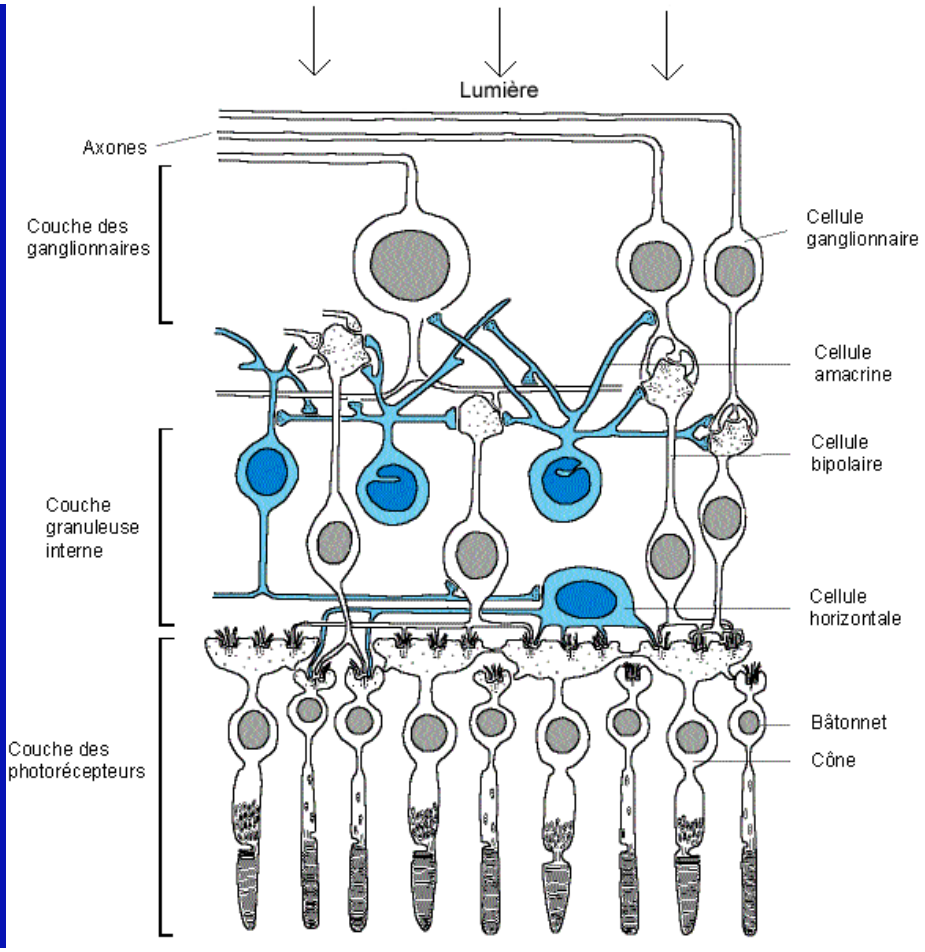
Lumière
Axones
Couche des ganglionnaires
Couche granuleuse interne
Couche des photorécepteurs
Cellule ganglionnaire
Cellule amacrine
Cellule bipolaire
Cellule horizontale
Bâtonnet
Cône

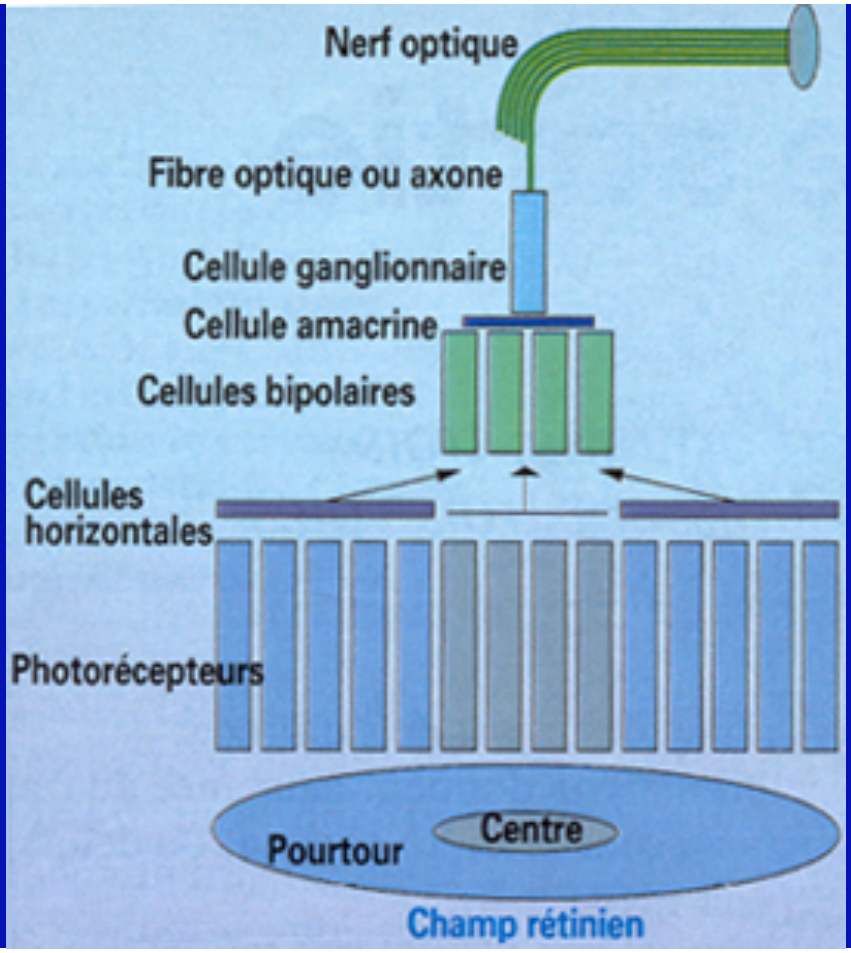

- In general the direction in V1 of an orientation ray of a pinwheel is not the orientation associated to it in the visual field.
- When the ray spins around the singular point with an angle θ the associated orientation rotates with an angle θ /2. Two diametrally opposed rays correspond to orthogonal orientations.

- If the orientation p_θ associated with the ray of angle θ is $p_\theta = \alpha + \theta/2$, the two orientations will be the same for

$$p_\theta = \alpha + \theta/2 = \theta$$

that is for $\theta = 2\alpha$.

- As α is defined modulo π, there is only one solution : end point.

- If the orientation p_θ associated with the ray of angle θ is $p_\theta = \alpha - \theta/2$, the two orientations will be the same for

$$p_\theta = \alpha - \theta/2 = \theta$$

that is for $\theta = 2\alpha/3$.

- As α is defined modulo π, there are three solutions : triple point.

- Other variables are “engrafted” in the pinwheel structure, in particular :
  - the variation of phase (De Angelis 1999) : in a column « spatial phase is the single parameter that accounts for most of the difference between receptive fields of nearby neurons ».
  - the spatial frequency distributed along the rays of the pinwheels (Bressloff, *J. of Phys*., 2003) .

- P. E. Maldonado, I. Gödecke, C. M. Gray, T. Bonhöffer (« Orientation Selectivity in Pinwheel Centers in Cat Striate Cortex », *Science*, 276 (1997) 1551-1555) have analyzed the fine-grained structure of orientation maps at the singularities. They found that
  - « orientation columns contain sharply tuned neurons of different orientation preference lying in close proximity ».
- The columnar redundancy vanishes at the singular points.

- James Schummers (*Neuron*, 36, 2002) has shown that
  - « neurons near pinwheel centers have subthreshold responses to all stimulus orientations but spike responses to only a narrow range of orientations ».
- Analyzing carefully the pattern of neural activity elicitated by a thin and long line stimulus, William Bosking (*Nature Neuroscience*, 5, 9, 2002) has shown the independance of position and orientation.

- The following picture (a) shows the population (stripe) of V1 neurons activated by a line stimulus located at a precise (vertical) position (scale bar = 1mm).
- (b) The stripe is embedded in the population of V1 neurons responding to the same vertical orientation but at different positions.

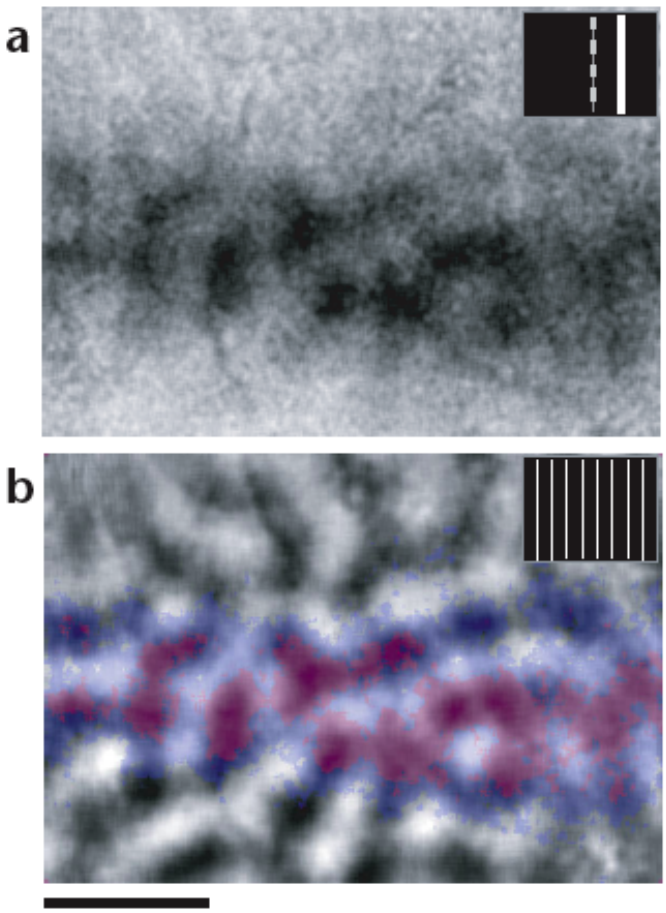

- When the position of the line moves in the visual field, the stripe moves in V1.
- The following picture shows that the position preference map (stripes, 0.5° intervals) and the orientation preference map (pinwheels) are essentially independent.

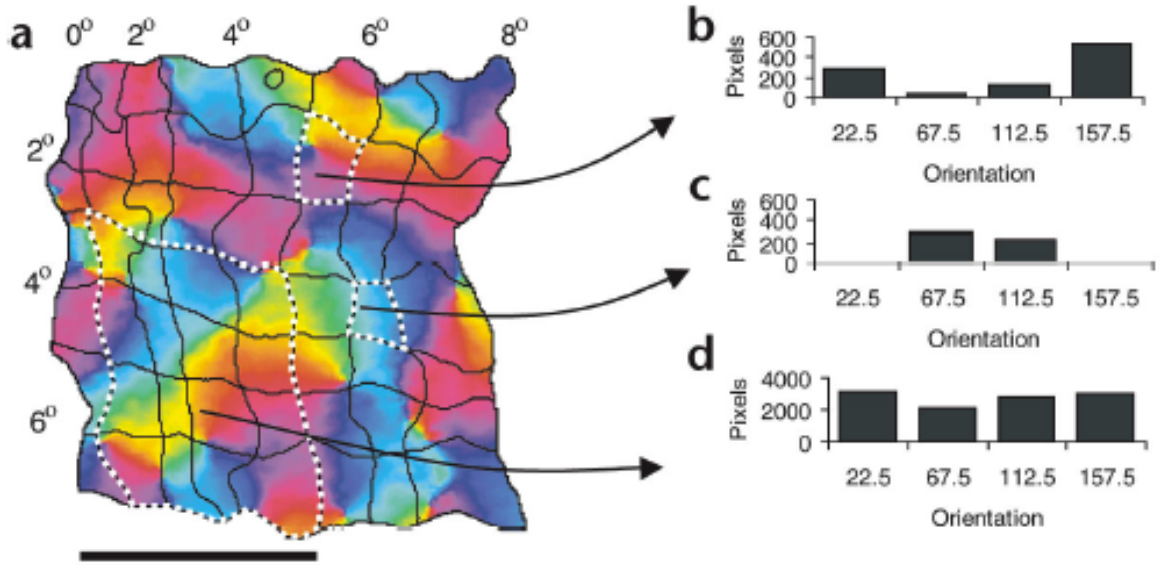

- So, Bosking has shown that

  « the map of visual space in V1 is orderly at a fine scale and has uniform coverage of position and orientation whithout local relationships in the mapping of these features. »

- This means that the local triviality of the fibration $\pi : R \times P \rightarrow R$ is neurally implemented.

- To select a direction θ and a scaling σ is the same thing as selecting a differential 1-form α such that
  - θ = kernel K of α,
  - σ codes the value $\alpha(v)$ where v is the unitary vector orthogonal to the kernel K (« characteristic » vector).
- As the set of filters is invariant under the action of the group G, we are therefore led to consider G- invariant 1-forms α.

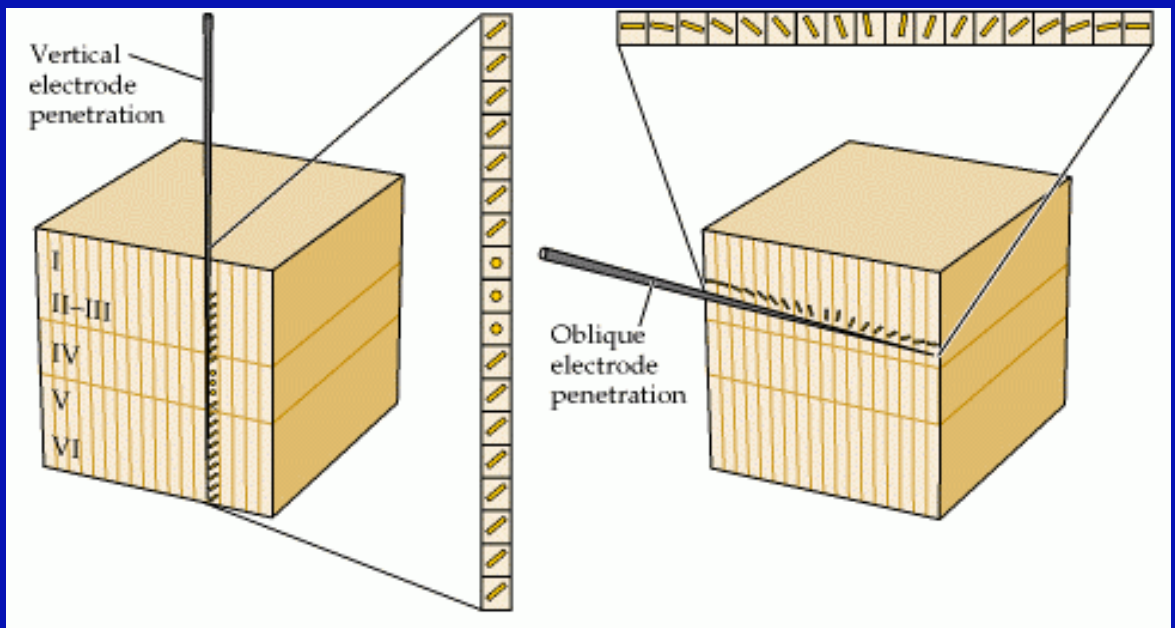

- Connectivity implementing the sharp orientation tuning near the centre.
- Dendritic tree near the centre C (few tens μ) in an iso-orientation domain *D* (yellow dots = excitatory synapses).
  - (a) d.t. biased towards *D*.
  - (b) d.t. symmetric, but excitatory inputs biased towards *D*.
  - (c) d.t. sym., excit. inputs sym. but local and therefore inside *D* (good segregation near *C*).
  - (d) d.t. sym., excit.inputs sym. and integrated uniformly over a large dendritic area.

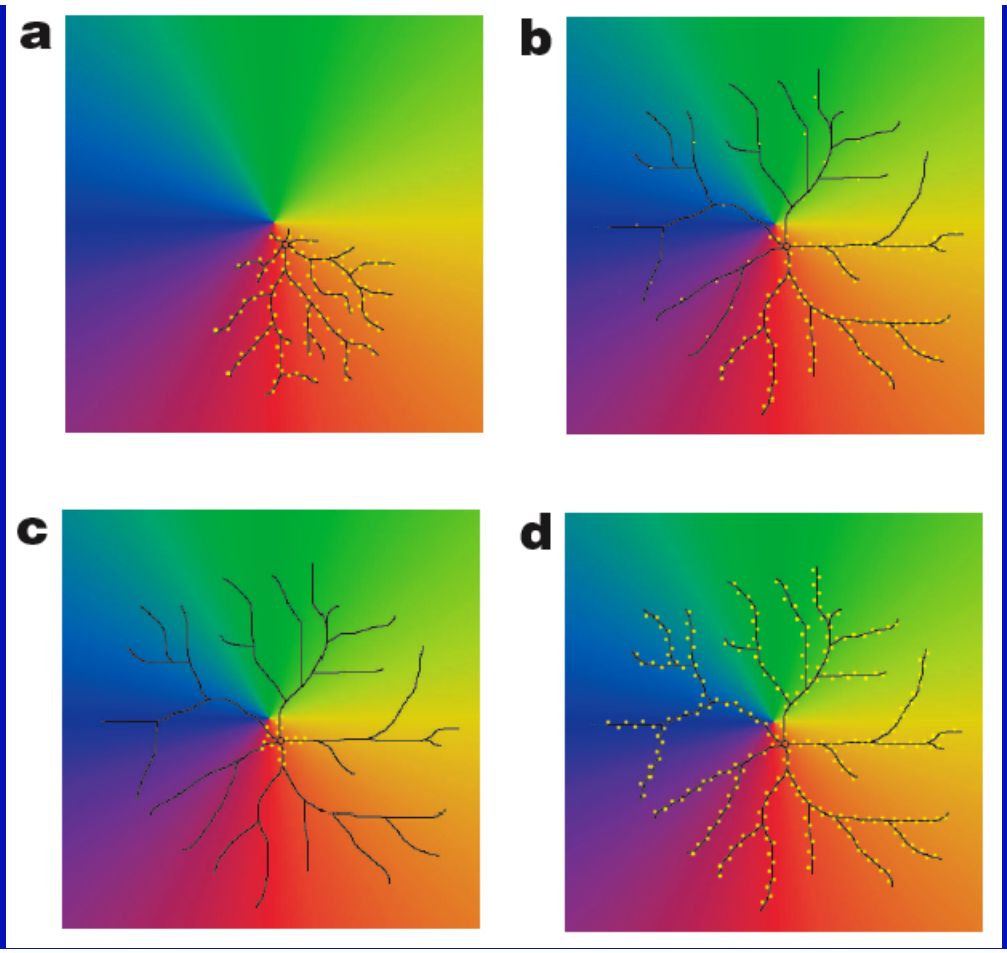

- Jan Koenderink (1987) strongly emphazised the importance of the concept of jet. Without jets, it is impossible to understand how the visual system could extract geometric features such as the tangent or the curvature of a curve.

– « geometrical features become *multilocal* objects, i.e. in order to compute boundary curvature the processor would have to look at different positions simultaneously, whereas in the case of jets it could establish a format that provides the information by addressing a *single location*. Routines accessing a single location may aptly be called *points processors*, those accessing multiple locations *array processors*. The difference is crucial in the sense that point processors need no geometrical expertise at all, whereas array processors do (e.g. they have to know the environment or neighbours of a given location). »

- Coherent states enable to represent a signal $f \in \mathcal{H}$ by its transform

$$T_f(g) = \langle f, \varphi_g \rangle \in L^2(G)$$

- It is what is done by V1, the $\langle f, \varphi_g \rangle$ being the measure of *f* by the receptive profiles φ_g.
- The covariance of the measures follow from the fact that the wavelets φ_g belong to a sub-representation of the (left) regular representation λ of *G* in $L^2(G)$.

- If *T* is the transform

$$\begin{array}{rccc} T: & \mathcal{H} & \rightarrow & L^2(G) \\ & f & \mapsto & T_f \end{array}$$

we have the intertwining

$$T \circ \pi = \lambda \circ T$$

The Weyl-Heisenberg affine group

- If we add a scale *s*, we get the Weyl-Heisenberg affine group *G*

$$(x, y, p, s).(x', y', p', s') = (q + sq', y + y' + spx', s^{-1}p', ss')$$

whose elements *g* can be represented by the matrices

$$g = \begin{pmatrix} 1 & sp & y \\ 0 & a & x \\ 0 & 0 & 1 \end{pmatrix}$$

- The elements of the Lie algebra are then represented by matrices

$$t = \begin{pmatrix} 0 & \pi & \eta \\ 0 & \sigma & \xi \\ 0 & 0 & 1 \end{pmatrix}$$

- Unitary irreducible representations are then deducible from the orbits of the co-adjoint representaion Ad*(*g*) (C. Kalisa, B. Torrésani).

- As the matrix of Ad*(g) operating on covectors is

$$\begin{pmatrix} s^{-1} & 0 & 0 & -p \\ 0 & s & 0 & x \\ s^{-1}x & -sp & 1 & -px \\ 0 & 0 & 0 & 1 \end{pmatrix}$$

these orbits are easily computed.

- F elliptic integral of the first kind of module k

$$F(\psi, k) = \int_0^{\psi} \frac{1}{\sqrt{1 - k\sin^2(\theta)}} d\theta$$

- E elliptic integral of the second kind

$$E(\psi, k) = \int_0^{\psi} \sqrt{1 - k\sin^2(\theta)} d\theta$$

- am Jacobi amplitude, inverse of F : $\psi = am(u, k)$ iff $u = F(\psi, k)$,
- Jacobi functions $sn(u) = \sin(\psi)$, $cn(u) = \cos(\psi)$, $dn(u) = (1 - k\sin^2(\psi))^{1/2}$.

- We get for t

$$t = \int_0^t dt = \frac{1}{\sqrt{c}} \int_{\varphi(0)}^{\varphi(t)} \frac{d\varphi}{\sqrt{1 - \frac{1}{c}\sin^2(\varphi)}}$$

$$= \frac{1}{\sqrt{c}} \left(F\left(\varphi(t), \frac{1}{c}\right) - F\left(\varphi(0), \frac{1}{c}\right) \right)$$

- For $\varphi(0) = 0$ ($\theta(0) = \pi/2$), and $c > 1$ (modulus $1/c < 1$), the pendulum makes complete turns.

$$\varphi(t) = \mathrm{am}\left(t\sqrt{c}, \frac{1}{c}\right) + k\pi$$

$$x(t) = ct - \sqrt{c}E\left(\varphi(t), \frac{1}{c}\right)$$

$$y(t) = \sqrt{c}\left(\mathrm{dn}\left(t\sqrt{c}, \frac{1}{c}\right) - 1\right)$$

- For $c < 1$ (modulus $1/c > 1$), the pendulum oscillates between two extremal values $-\varphi_{ex}$ and $+\varphi_{ex}$ where with $\varphi_{ex} = \operatorname{Arcsin}(\sqrt{c})$

$$\theta(t) = \operatorname{Arccos}(\sqrt{c}\,\mathrm{am}(t,c))$$
$$x(t) = t - E(\mathrm{am}(t,c),c)$$
$$y(t) = \sqrt{c}\,(\mathrm{cn}(t,c) - 1)$$

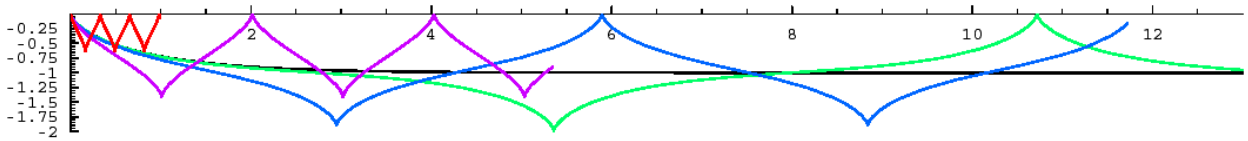

FIGURE 31. Différentes géodésiques sous-riemanniennes pour c croissant de 0.1 à 1 : $c = 0.1$ (rouge), $c = 0.5$ (violet), $c = 0.9$ (bleu), $c = 0.99$ (vert), $c = 1$ (noir). (D'après les calculs d'A. Agrachev).

- A way of describing the orientation maps (Wolf & Geisel) is to consider the activity pattern $E_k(x)$ for each orientation $\varphi_k = \theta_k/2$ and to construct the complex field

$$z(x) = \sum_k E_k(x) e^{i\theta_k}$$

- The development can then be described by a PDE of the type

$$\frac{\partial z(x,t)}{\partial t} = F\left(z(x,t)\right) + \eta(x,t)$$

where F is a non linear operator and η a random term.

- The pinwheels centers are the zeroes of $z(x)$.
- Such dynamics can be induced by an Hebbian learning process, $F(z(x))$ being the average of $z(x)$ under very rapidly changing stimuli A following a certain probability law.
- The characteristic bifurcations are fusions and splittings of pinwheels.